Accelerated Settling of Particulate Matter by 'Marine Snow' Aggregates

by

Vernon L. Asper

B.A., Messiah College (1978)

M.S., University of Hawaii (1981)

SUBMITTED IN PARTIAL FULFILLMENT OF THE

REQUIREMENTS FOR THE DEGREE OF

DOCTOR OF PHILOSOPHY

at the

WOODS HOLE OCEANOGRAPHIC INSTITUTION

and the

MASSACHUSETTS INSTITUTE OF TECHNOLOGY

December 1985

Signature of Author.....
Joint Program in Marine Geology and Geophysics, Woods Hole Oceanographic Institution / Massachusetts Institute of Technology, December 1985

Certified by.....
Thesis Supervisor

Accepted by.....
Chairman, Joint Committee of Marine Geology and Geophysics, Woods Hole Oceanographic Institution / Massachusetts Institute of Technology

This thesis is dedicated to my daughter,

Alicia Danielle Asper

TABLE OF CONTENTS

LIST OF FIGURES.....iv

LIST OF TABLES.....vii

ABSTRACT.....viii

ACKNOWLEDGMENTS.....xi

INTRODUCTION.....1

CHAPTER 1. TIME SERIES SEDIMENT TRAP EVIDENCE FOR RAPID SETTLING OF MARINE PARTICULATE MATTER BY AGGREGATES..... 5

CHAPTER 2. THE DISTRIBUTION AND TRANSPORT OF MARINE SNOW AGGREGATES IN THE PANAMA BASIN AND NORTHEAST ATLANTIC OCEAN.....51

CHAPTER 3. MEASURING THE FLUX AND SINKING SPEED OF MARINE SNOW AGGREGATES.....136

LIST OF FIGURES

Figure 1.1 Measured sediment flux at site PB_2 in the Panama Basin.....16

Figure 1.2 Measured sediment flux at Station Papa in the North Pacific..20

Figure 1.3 Cross correlation of the flux of particles in shallow vs. deep traps at station Papa.....22

Figure 1.4 Measured sediment flux in the Black Sea.....25

Figure 1.5 Cross correlation of the flux of particles in shallow vs. deep traps in the Black Sea.....29

Figure 1.6 Ratios of the flux of various particle type to total mass flux in the Panama Basin.....33

Figure 1.7 Ratios of the flux of combustible material to biogenic minerals (opal and carbonate) at Station Papa.....37

Figure 1.8 Ratios of the flux of various particle types to total mass flux in the Black Sea.....40

Figure 1.9 Ratio of the fluxes of several particle types in the Black Sea.....42

Figure 1.10 Diagram of the three flux signal types identified in this study.....46

Figure 2.1 Configuration of marine snow photography system.....59

Figure 2.2 Location map of marine snow profiles taken on R/V Knorr cruise #94 in the Northwest Atlantic Ocean.....63

Figure 2.3 Cruise track of R/V Columbus Iselin (cruise CI-83-13) showing marine snow profile stations.....66

Figure 2.4 Scanning electron microscope (SEM) micrographs of critical point dried marine snow aggregates.....70

Figure 2.5 Photographs of marine snow taken by photographic survey system in the Panama Basin.....72

Figure 2.6 Profile of marine snow abundance in the Panama Basin comparing unprocessed with filtered data.....75

Figure 2.7 Vertical profile of suspended matter taken from hydrocasts and large volume in situ pumps in the Panama Basin.....78

Figure 2.8 Transect of marine snow abundance profiles taken in the Panama Basin south of the Coiba Ridge.....81

Figure 2.9 Profiles of marine snow abundance taken offshore of Guayaquil, Ecuador.....86

Figure 2.10 Profile of marine snow abundance taking in the Western North Atlantic.....89

Figure 2.11 Contour plot of marine snow abundance in the Western North Atlantic and Panama Basin.....95

Figure 2.12 Profiles of marine snow abundance in the Panama Basin showing relative temporal stability of the observed signals.....100

Figure 2.13 Results of time series sediment traps deployed at the S.T.I.E. site in the Panama Basin.....108

Figure 2.14 Schematic of proposed flux model.....113

Figure 2.15 SEM images of samples of biogenic carbonate collected by a sediment trap at 3800m in the Panama Basin.....117

Figure 2.16 SEM images of sediment samples collected by DSRV Alvin at the sediment trap site.....119

Figure 3.1 Configuration of marine snow flux camera system.....143

Figure 3.2 Configuration of mooring system used to deploy the flux camera in 3900m of water in the Panama Basin.....146

Figure 3.3 Flux camera photographs showing the accumulation of material in the sediment trap.....151

Figure 3.4 Flux camera photographs showing resuspension events.....153

Figure 3.5 SEM images of material collected by the flux camera trap....156

Figure 3.6 Plot of the number of aggregates in the trap vs. time since deployment.....159

Figure 3.7 Plot of image area occupied by aggregates in the trap vs. time since deployment.....161

Figure 3.8 Flux camera photographs of particle motions associated with resuspension event at 23 hours.....164

Figure 3.9 Flux camera photographs of resuspension event at 26 hours...166

Figure 3.10 - 3.12 Plots of the arrival of aggregates in three size classes (1.0-2.5mm, 2.5-4.0mm, and 4.0-5.0mm) vs. time.....169

Figure 3.13 Plot of the average diameter of aggregates in the trap vs. time since deployment.....173

Figure 3.14 Vertical profiles of the abundance of marine snow aggregates in three size classes.....176

LIST OF TABLES

Table 1.1 Summary of PARFLUX sediment trap deployments and samples reviewed in this thesis.....12

Table 1.2 Correlation coefficients for components of the observed flux with lithogenic flux in the Panama Basin.....35

Table 2.1 Correlation of particle flux with marine snow abundance in the Panama Basin.....107

Table 2.2 Calculated contributions of surface and resuspended flux in sediment trap samples in the Panama Basin.....122

Table 3.1 Calculated bulk densities and mass flux contributions of marine snow aggregates.....182

ACCELERATED SETTLING OF MARINE PARTICULATE MATTER BY 'MARINE SNOW' AGGREGATES

by

VERNON L. ASPER

Submitted to the Woods Hole Oceanographic Institution
and Massachusetts Institute of Technology
in partial fulfillment of the requirements for the degree
of Doctor of Philosophy

ABSTRACT

Samples from time-series sediment traps deployed in three distinct oceanographic settings (North Pacific, Panama Basin, and Black Sea) provide strong evidence for rapid settling of marine particles by aggregates. Particle water column residence times were determined by measuring the time lag between the interception of a flux event in a shallow trap and the interception of the same event in a deeper trap at the same site. Effective sinking speeds were determined by dividing the vertical offset of the traps (meters) by the interception lag time (days). At station Papa in the North Pacific, all particles settle at 175 m day^{-1}, regardless of their composition, indicating that all types of material may be settling in common packages. Evidence from the other two sites (Panama Basin and Black

Sea) shows that particle transport may be vertical, lateral, or a combination of directions, with much of the Black Sea flux signal being dominated by lateral input.

In order to ascertain whether marine snow aggregates represent viable transport packages, surveys were conducted of the abundance of these aggregates at several stations in the eastern North Atlantic and Panama Basin using a photographic technique. Marine snow aggregates were found in concentrations ranging from ~1 $mm^3 liter^{-1}$ to more than 500 $mm^3 liter^{-1}$. In open ocean environments, abundances are higher near the surface (production) and decline with depth (decomposition). However, in areas near sources of deep input of resuspended material, concentrations reach mid-water maxima, reflecting lateral transport. A model is proposed to relate the observed aggregate abundances, time series sediment flux and inferred circulation. In this model, depthwise variations in sediment flux and aggregate abundance result from suspension from the sea floor and lateral transport of suspended aggregates which were produced or modified on the sea floor. Temporal changes in sediment flux result from variations in the input of fast-sinking material which falls from the surface, intercepts the suspended aggregates, and transports them to the sea floor.

A new combination sediment trap and camera system was built and deployed in the Panama Basin with the intent of measuring the flux of marine snow aggregates. This device consists of a cylindrical tube which is open at the top and sealed at the bottom by a clear plate. Material lying on the bottom plate is illuminated by strobe lights mounted in the wall of the cylinder and photographed by a camera which is positioned below

the bottom plate. Flux is determined as the number of aggregates arriving during the time interval between photographic frames (# $area^{-1}time^{-1}$). Results show that essentially all material arrives in the form of aggregates with minor contributions of fecal pellets and solitary particles. Sinking speeds (m day^{-1}), calculated by dividing the flux of aggregates (# $m^{-2}day^{-1}$) by their abundance (# m^{-3}), indicate that the larger (4-5mm) aggregates are flocculent and sink slowly (~1m day^{-1}) while the smaller aggregates (1-2.5mm) are more compact and sink more quickly (~36m day^{-1}). These large, slow-sinking aggregates may have been re-suspended from the sediment water interface at nearby basin margins.

ACKNOWLEDGMENTS

The single most important person in my life, and the one most responsible for my continued enthusiasm is my wife, Lindell. Over the course of my graduate studies, she has been alone almost one full year, yet she remains supportive of my career and is a constant and vital source of loving encouragement.

Without the advice, encouragement and generosity of Sus Honjo, I might be repairing microscopes today. Sus not only provided all of the financial and logistic support for my data collection, but he also pointed me in the direction of marine snow research, provided me with his one-of-a-kind camera system, and, in essence, turned over to me an area of research which has been very special to him for many years. In addition, Sus generously provided unlimited access to all of his sediment trap samples and unpublished data for inclusion in my thesis. Sus has provided uncommon opportunities to gain valuable experience, not the least of which is the fulfillment of a lifelong ambition to dive in the Alvin.

Discussions with Kozo Takahashi have been a great influence over the last six years. On many occasions Kozo's unique perspective helped to clear my thinking and focus my concentration.

Steve Manganini has been a good friend and companion on several cruises. He taught me everything I know about deploying, finding, and recovering deep-sea moorings and was responsible for all of the sample analyses included in this thesis. Abby Spencer provided cheerful

encouragement, helped perform the analyses, and was a pleasure to be with on cruises.

In addition to their role as advisor, each member of my thesis committee contributed uniquely to the success of my efforts. Bill Curry's point of view was instrumental in making many career decisions and scientific discussions with him helped me sort out the importance of my data. Mike Bacon provided unpublished hydrocasting and large volume pump data. Larry Madin supplied ship time for the Atlantic marine snow survey. Recommendations by Ed Boyle at critical times helped prevent my efforts from becoming diverted from important subject areas. John Milliman provided useful input and chaired the thesis defense.

Dave Aubrey was my longsuffering tutor in differential equations and time series analysis and provided useful criticisms of my thesis proposal and finished thesis. Hans Schouten and Charles Denham patiently taught me geophysics and provided the subject matter for one of my general examination papers. Discussions with Bernward Hay led to a deeper understanding of the Black Sea environment. Rindy Osterman was an invaluable co-worker on several sediment trapping cruises and provided endless entertainment and encouragement.

I would like to thank the officers and crews of all the ships used to deploy the marine snow camera and sediment traps, including the Polarstern, Atlantis II, Columbus Iselin, Knorr, C.F.A.V. Endeavor, Piri Reis, Cayuse, and Kaimalino. A special thanks to the Alvin group for their cooperation and for making those cruises so pleasant.

Skip Pelletier helped design and build the various electronic gadgets and freely loaned any piece of equipment I needed. On numerous occasions, Earl Young generously loaned his valuable deep-sea cameras, without which most of the data could not have been collected. Ken Doherty refined the design of the flux camera, assisted on several cruises, and supplied unlimited engineering expertise. Cindy Pilskaln, Jon Trent, Peter Sachs, and Terry Hammer helped out on cruises and Amy Karowe helped with laboratory analyses of sediment trap samples. Emily Evans helped with many aspects of the preparation of this manuscript.

This research was supported by ONR contract numbers N00014-82-C-0019 and N00014-85-C-0001, NSF grant numbers OCE-83-09024, OCE-84-17106, and DPP-85-01152 and the WHOI education office.

INTRODUCTION

Ever since the existence of life on the deep-sea floor was confirmed by the Challenger expedition, scientists have speculated over the source and transport mechanism of energy to this environment. Early ideas focused on a slow, continuous rain of particles which delivered to the benthos material which had spent considerable time in the water column and was mostly decomposed.

Several sources of evidence have emerged over the past 30 years which indicate that marine particles may settle very quickly from the surface to the sea floor. For example, the distribution of clay minerals and coccolithophorids at the sea surface is reflected in their respective distributions on the sea floor (Berger, 1976; Honjo, 1976). If these particles settled at their expected low Stokesian rates, dispersal by ocean currents would prevent any such correspondence. Material collected in deep-sea sediment traps was found to be remarkably well preserved and often intact, indicating short water column residence times.

Perhaps the strongest support of rapid settling was reported by Honjo (1982) from the first time-series sediment trap deployment. Honjo found that the flux vs. time signal observed in a near surface trap was repeated in several deeper traps over the same sampling intervals. This could only happen if particles were settling faster than 40 m day^{-1} and indicates that the benthic community is being supplied with a time-varying source of energy and nutrients.

Honjo (1980) proposed that transport by fecal pellets could, in some cases, explain this rapid transfer of particles to the sea floor. However, later evidence showed that insufficient quantities of fecal pellets are found in most sediment trap samples to account for the observed flux (Honjo, 1982a). Further, scanning electron microscopy of these samples showed most particles to be unfragmented, indicating that passage through a grazer's gut was unlikely.

"Marine snow" has been proposed as a possible alternative transport mechanism (Honjo, 1982b; Shanks and Trent, 1978). These large, amorphous, organic aggregates have been studied intensively by biologists interested in their potential role in marine ecosystems. However, relatively few studies have been published regarding their potential role in sediment flux, and deep-sea measurements of their existence and settling characteristics are rare (see Shanks and Trent, 1980; Silver and Alldredge, 1981).

The research described in this thesis is aimed at investigating the potential role of marine snow aggregates in the transport of particulate matter. In order for marine snow to be important in the settling of particles, three criteria must be met: 1) sufficient evidence must be produced to show that particles do, indeed, settle at accelerated rates (ie. faster than expected based on assumptions of solitary sinking), 2) marine snow aggregates must exist in sufficient quantities at all ocean depths, and 3) these aggregates must settle at sufficiently high rates. This thesis is divided into three chapters, each aimed at addressing these criteria.

The first chapter presents a review of largely unpublished PARFLUX sediment trap data provided by Susumu Honjo. Data from depth-paired sediment traps exist for three environments: Station Papa in the North Pacific, the Panama Basin, and the Black Sea. These data allow the determination of effective particle sinking speeds (using the depth interval / interception time lag method) and also provide indications of particle packaging and transport pathways.

Marine snow distributions and abundances in two geographic areas are presented in chapter two. Vertical profiles of abundance reveal the locations of sources; comparison of several profiles taken at the same position but hours, days, weeks, or months apart reveal the relative temporal stability of these sources. Finally, transects of several vertical abundance profiles show whether the aggregates are moving laterally and also indicate the spatial scale of variations.

Chapter three presents the results of an attempt to directly measure the flux of marine snow aggregates using a combination sediment trap and camera. The camera records the successive addition of particles which fall into the trap between film exposures. Aggregate sinking speeds (m day^{-1}) can be calculated by dividing the flux (# $m^{-2}day^{-1}$) by the observed aggregate abundance (# m^{-3}). This method also allows observation of scavenging organisms feeding on the collected sample, as well as possible post-collection decomposition or break-up of the aggregates.

REFERENCES

Berger, W.H. (1976) Biogenous deep sea sediments: production, preservation and interpretation. In: J.P. Riley and R. Chester (eds.), Chemical Oceanography, 5, 265-388.

Honjo, S. (1976) Coccoliths: production, transportation and sedimentation. Mar. Micropaleo., 1, 65-79.

Honjo, S., (1980) Material fluxes and modes of sedimentation in the mesopelagic and bathypelagic zones. J. Mar. Res., 38(1), 53-97.

Honjo, S., (1982) Seasonality and interaction of biogenic and lithogenic particulate flux at the Panama Basin. Science, 218, 883-884.

Honjo, S., S.J. Manganini, and J.J. Cole (1982a) Sedimentation of biogenic matter in the deep ocean, Deep-Sea Res., 29(5A), 609-625.

Honjo, S., S.J. Manganini, L.J. Poppe (1982b) Sedimentation of lithogenic particles in the deep ocean. Mar. Geol., 50, 199-220.

Shanks, A.L. and J.D. Trent (1980) Marine snow: sinking rates and potential role in vertical flux. Deep-Sea Res., 27, 137-143.

Silver, M.W. and A.L. Alldredge (1981) Bathypelagic marine snow; deep-sea algal and detrital community. J. Mar. Res., 39, 501-530..

Chapter 1

TIME SERIES SEDIMENT TRAP EVIDENCE FOR RAPID SETTLING OF MARINE PARTICULATE MATTER BY MARINE SNOW AGGREGATES

Abstract

In addition to their usefulness as recorders of particle production events, time series sediment traps also provide indications of particle transport pathways and mechanisms. A review of recent PARFLUX sediment trap data reveals evidence supporting rapid settling via aggregates. Cross-correlation of the signals from shallow and deep time-series flux (mg $m^{-2}day^{-1}$) signals indicates that: a) all particles settle at similar speeds regardless of their composition, b) the observed sinking speeds are significantly higher than expected for particles settling as individuals, and c) combustible (organic) material correlates best in shallow and deep traps and is indicated as a controlling factor in the settling of other particles. Three classes of flux signals are identified: a) Vertical settling (Mid-North Pacific) where flux peaks appearing in shallow traps also appear in deep traps with equal or diminished amplitude, b) lateral transport (Black Sea) where many flux peaks appear only in the deep trap, and c) a combination of vertical settling and lateral input (Panama Basin) where peaks occur in both shallow and deep signals but with higher amplitude in the deep trap.

INTRODUCTION

Particles sinking through the oceanic water column transfer energy and nutrients from the surface mixed layer to the deeper aphotic layers and the sea floor. The speed and rate at which this transfer takes place will affect the degree of coupling between surface and deep processes as well as the site of deposition or dissolution. Before the era of wide spread sediment trap experiments, it was assumed that most particles settled individually, resulting in a slow, continuous rain of particles to the sea floor and a complete spatial and temporal decoupling of surface and bathyl environments. Recent evidence, however, indicates that when particles settle, their sinking speeds are generally quite high and that the flux of various types of material collected in traps is correlated. Fine particles settle only when they become part of some type of larger faster-sinking particles such as fecal pellets or marine snow aggregates (Honjo 1982, Honjo et al. 1982a,b), requiring that a distinction be made between "suspended" and "settling" particles (Honjo, 1982, 1984).

While sediment traps provide the means of collecting the settling particles, the integrity of the sedimenting package has not been shown to be preserved in the recovered samples. Most sediment trap samples not only contain insignificant numbers of recognizable fecal pellets (Pilskaln,

1985), they are also dominated by intact phyto- and zooplankton which apparently have not been consumed or digested by feeding organisms (K. Takahashi, pers. comm., 1985). Marine snow aggregates are extremely fragile and unlikely to survive sample analyses (sieving and splitting), making dependable evaluation of aggregate size and abundance impossible in sediment trap samples. Therefore, knowledge of the sedimentation mechanisms, indications of particle packaging, and sinking speed information must be derived from less direct evidence using sediment trap material.

Modern, time-sequencing sediment traps are capable of providing this information in several ways. In situ particle transit times can be determined by placing synchronized traps at several depths along a mooring. The time offset between the arrival of a flux event ("peak" or "valley" in the flux vs. time curve) at near-surface and near-bottom traps will be a measure of the transit time. This lag time divided by the vertical separation of the traps yields the effective sinking speed. This calculation assumes that the events can be identified in both traps and that the flux signal measured in this way is produced by vertical sedimentation and is not an artifact of trap efficiency. This method can be applied to all types of settling particles. If sinking speeds appear to correlate with particle size, then individual sinking is inferred. However, if similar sinking speeds are observed for many sizes and weights of particles, then aggregated settling is indicated for the non-fecal pellet material.

A second type of evidence for aggregate sedimentation can be obtained by examining the correlations (ratios) of the fluxes of various

components. As they settle through the water column, marine snow aggregates are thought to intercept and scavenge fine, suspended particles and incorporate them into the settling package. If this is, in fact, the case, then the flux of these fine particles (eg. clays, individual coccoliths, small diatoms) should correspond with the flux of organic matter and biogenic minerals. Examination of the ratios and degree of correlation of fine particle fluxes to various components should indicate which components (if any) control the sedimentation of fine particles.

Lithogenic material, defined by Honjo et al., (1982b) as the portion of the flux which is neither combustible, acid soluble, nor Na_2CO_3 leachable, represents a useful tracer of the flux pathway of fine particles. This lithogenic matter is generally conservative in the deep sea and would remain essentially suspended due to its small particle size, unless incorporated in settling aggregates. (Honjo 1985).

Investigation of these correlations can be applied to time series flux samples and to samples collected in different environments and depths. Each environment will be characterized by a specific seasonal cycle of primary and secondary production as well as input of lithogenic material. By looking at several environments and seasons, it should be possible to determine the relative importance of each factor. For example, lithogenic material may be transported with carbonate particles in one environment (or season) and with siliceous particles in another.

In this paper, the results of several PARFLUX sediment trap deployments will be reviewed with the intent of examining sedimentation trends in several environments. Three of these deployments included

multi-depth time series traps, allowing direct estimation of particle sinking speeds. At each location, the correlation of lithogenic flux to other components will be examined in order to evaluate similarities and differences in particle packaging and transport.

METHODS

Sample collection and analysis

Since its inception in 1975, the PARFLUX sediment trap has evolved from single receptacle, 1.5m^2 opening, polyvinyl-chloride cones (1976-80) to the present, multi-receptacle designs (1982-present, Honjo et al., 1980). These new traps are smaller (0.5-1.2m^2 opening), constructed of lighter, more durable polypropylene, controlled by sophisticated microprocessors, and collect up to 25 samples per deployment (Honjo 1985). Table 1.1 lists a summary of sediment trap samples collected and analyzed by the PARFLUX group over the past 10 years and partially reviewed in this paper. All traps deployed along a single mooring were programmed to take synchronous samples.

In the laboratory, these samples are treated according to the method of Honjo (1982). The samples are first sieved into 3 size fractions (<63μmm 63μm-1mm, and >1mm) and then split into smaller aliquots for the individual chemical analyses. Total mass flux (mg $m^{-2}day^{-1}$) is determined by weighing a dried aliquot of material and normalizing the result for the size of the trap opening and the duration of the deployment. Carbonate flux is determined by weight loss on addition of a weak acid, and combustible material flux as weight loss after ashing (4 hours at 500°C) a carbonate free sample. Biogenic silica is determined by leaching a carbonate free sample in 1M Na_2CO_3 at 90°C for three hours. Lithogenic flux is defined as the difference between the non-combustible and biogenic silica fluxes. This method works well where the ratio of lithogenic to biogenic opal flux is ca. 0.3 or greater. However, if this

Table 1.1 Summary of PARFLUX sediment trap samples reviewed in this manuscript.

Station Name	Panama Basin PB_2	Station Papa PP_{1-3}	Black Sea BS_{1-4}
Location	5°22'N 85°35'W	50°0'N 145°0'W	42°10'N 32°32'E
Dates	12/79-12/80	10/82-4/84	10/82-10/84
Depth(m)/ # of samples	890/6 2590/6 3560/6	1000/18 3800/59	250/59 1200/47
Total samples	18	77	106
Water Depth	3850	4200	2200

ratio is low (< ca. 0.3), small errors in silica leaching, opal weight estimation (grams of opal from moles of Si), or sample weighing will result in errors which overwhelm the lithogenic flux signal. At station Papa in the North Pacific, lithogenic flux is very small relative to biogenic opal (ratio <0.2) so that no accurate assessment of lithogenic flux is available using the described methodology.

Deployment Site Description

Three principal sites will be discussed: Panama Basin, North Pacific (weather station Papa), and the Black Sea. Each location is characterized by a unique set of environmental and oceanic features which influence the nature of the samples collected.

The Panama Basin is a semi-enclosed, equatorial basin characterized by seasonal upwelling and high primary production. The deployment site (Honjo 1982) is located in the Coiba Gap between the Malpelo and Coiba ridges in 3900m of water. This location is well within the influence of material which is re-suspended from the Coiba ridge and transported offshore at midwater depths, resulting in the observed depthwise flux changes reported by Honjo et al. (1982a,b).

In contrast to this proximity to sources of deep terrigenous input, station Papa is located over 2000 km from any potential source of lateral input. Primary production is moderately high with major peaks in sediment flux occurring in May and August (Honjo, 1985). These peaks in flux correspond in part to seasonal succession of various phyto- and micro-zooplankton species (Takahashi, 1985) and help to prove that both shallow and deep traps are intercepting the same material as it settles from the euphotic zone.

While the Black Sea deployment site is most noted for its anoxic water chemistry, this condition has little effect on the collection of settling particles. Restricted circulation in the Black Sea has resulted in the depletion of oxygen below 100-250m throughout the 2200m deep Basin (Deuser, 1974). These conditions favor the accumulation of particles due to reduced decomposition in the sediments, but have little effect on the overall delivery of material to the sea floor. In the 'typical" oceanic environment, most (~90%) recycling of organic matter occurs in the surface water with lesser amounts occurring in the sediment and almost insignificant loss occurring as the particles settle (Honjo et al., 1982a,b) due to their short water column residence times. From the viewpoint of settling particle collection, and for the components examined here, the two important environmental characteristics of this site are its proximity to the continental shelf (<40 km) and the relatively warm water temperature (~9°C). Proximity to sources of deep lateral input (shelf and slope) will result in a similar situation to the Panama Basin where flux increases with depth. In the Black Sea, this deep input will be more seasonal than in the Panama Basin due to the effects of storm-induced resuspension on the shelf (B. Hay, pers. comm., 1985). Warmer deep water enhances preservation of carbonate and dissolution of silica, in spite of low pH which would favor opposite tendencies. Anoxic conditions may enhance post-depositional preservation of labile organic material in the trap samples, although this effect will be similar to the addition of a chemical preservative at oxygen rich deployment sites.

RESULTS AND DISCUSSION

Sinking Speed

Honjo (1982) published the results of a multiple time series sediment trap experiment in the Panama Basin (fig. 1.1). These plots of flux vs. time and depth indicate first, that fluxes of all components increase with depth due to deep lateral input, and second that the fluxes of all components are well correlated. That is, the primary bimodal signal observed in total mass flux also appears in organic carbon (combustible material), carbonate, biogenic opal, and lithogenic particle flux. The large summer peak in flux is the result of a bloom of a single coccolithophorid species (Umbellicosphaera sibogae). As nutrients were depleted, the coccolithophorids entered a palmelloid stage (Smayda 1971, Honjo 1982) and settled very quickly. During the resulting flux event, the receiving cup (#4) in the 890m trap was completely full and material from this time interval may have been carried into the subsequent cup (#5); no compensation has been attempted for this effect. Carbonate flux during this period (and consequently total mass flux) decreased slightly with depth, in contrast to all other samples where flux increased. This singular decrease is interpreted as indicating that the bloom covered only a limited geographic area, the decrease resulting from dispersal of the coccolith remains as they settled. In order for this material to intercept both the 890m and 3560m traps in a single two-month sampling interval, the particles must have settled through the 2670m of water in no more than 61 days. This results in a minimum sinking speed of 44 m day^{-1} although the speed could have been much higher.

Figure 1.1 Measured sediment flux at site PB_2 in the Panama Basin (Honjo, 1982). Numbers designate sequential samples over a period of one year; only 4 usable samples were obtained at 890m and 2590m. a) Total mass flux. b) Biogenic carbonate flux. c) Biogenic opal flux. d) Lithogenic material flux. e) Combustible material flux.

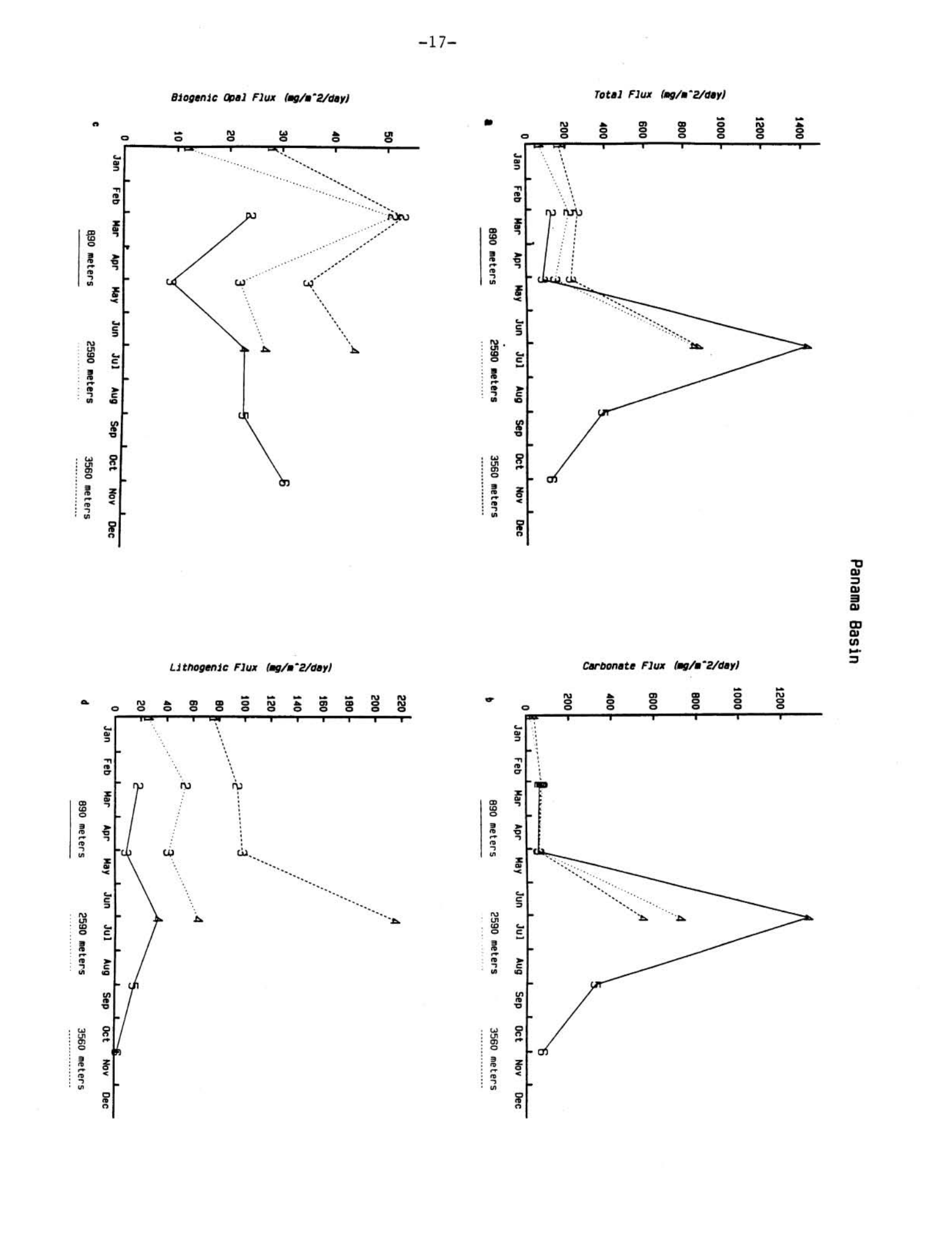
Panama Basin
Total Flux (mg/m^2/day)
Carbonate Flux (mg/m^2/day)
Biogenic Opal Flux (mg/m^2/day)
Lithogenic Flux (mg/m^2/day)
Jan Feb Mar Apr May Jun Jul Aug Sep Oct Nov Dec
890 meters
2590 meters
3560 meters
a
b
c
d

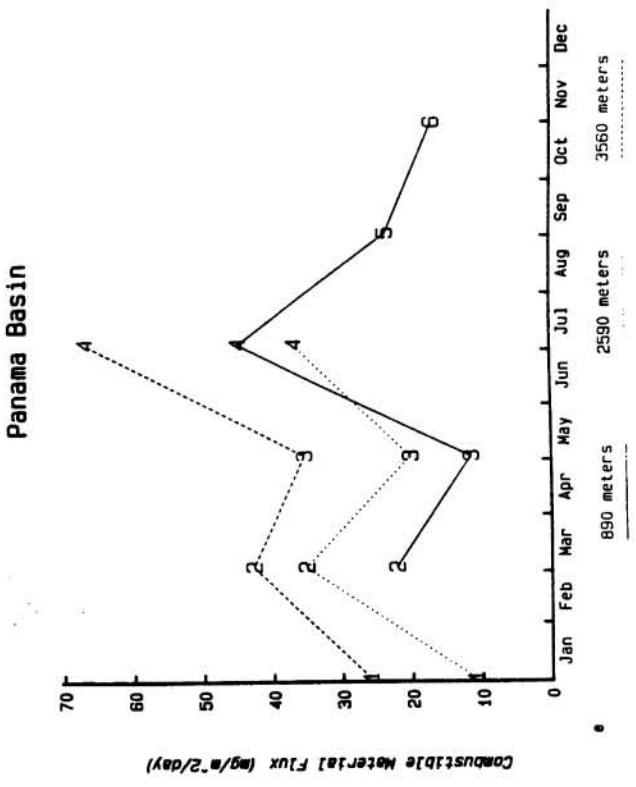
Panama Basin
Combustible Material Flux (mg/m^2/day)
70
60
50
40
30
20
10
0
Jan
Feb
Mar
Apr
May
Jun
Jul
Aug
Sep
Oct
Nov
Dec
890 meters
2590 meters
3560 meters

The findings of this experiment (Honjo, 1982) pointed to the need for a similar experiment with shorter sampling intervals to provide higher temporal resolution. Deployments of improved (12 samples/deployment) sediment traps were initiated in the Black Sea and at the former site of weather Station Papa in the North-Central Pacific (50°N 145°W) in the fall of 1982 (Honjo, 1985). Logistic constraints limited depth-paired observations at station Papa to one set of twelve samples plotted in figure 1.2. In this case, the flux peaks are offset one sampling interval (ca. 16 days) over the 2800 m vertical displacement, indicating an average sinking speed of 175 m day^{-1} for all particles. This lag interval is confirmed by cross-correlation of the results of the first 36 deep (3800m) samples and the middle 12 shallow (1000m) samples (fig. 1.3a). These values were obtained by first linearly interpolating both sets of data to an even sampling interval (16 days). Best correlation (0.88) is obtained at an offset of one sampling interval (lag one), confirming the subjective observation that the same signal appears in both shallow and deep traps, and that, within the limits of confidence, the offset is one sampling interval (16 days).

The same pattern is also observed in each of the particle types evaluated. Figures 1.2b-d show plots of carbonate, opal and combustible flux as well as the cross-correlations of these fluxes in shallow and deep traps (fig. 1.3b-d). As in the total mass flux, each constituent correlates best at a lag of one sampling interval, with correlations ranging from 0.79 for carbonate to 0.96 for combustible material. The sinking speeds are similar for all components regardless of their composition, indicating that settling most likely occurs in the form of a common package such as marine snow aggregates.

Figure 1.2 Measured sediment flux at the former site of weather station Papa at 50°N, 145°W in the North Pacific. Numbers designate sequential samples over a period of 6 months in the shallow (1000 meters below the surface) trap and 18 months in the deep trap (3800 meters below the surface, water depth is 4200 meters). a) Total mass flux. b) Biogenic carbonate flux. c) Biogenic opal flux. d) Combustible material flux. Because of the sample composition, determination of the flux of lithogenic particles was not possible at this site.

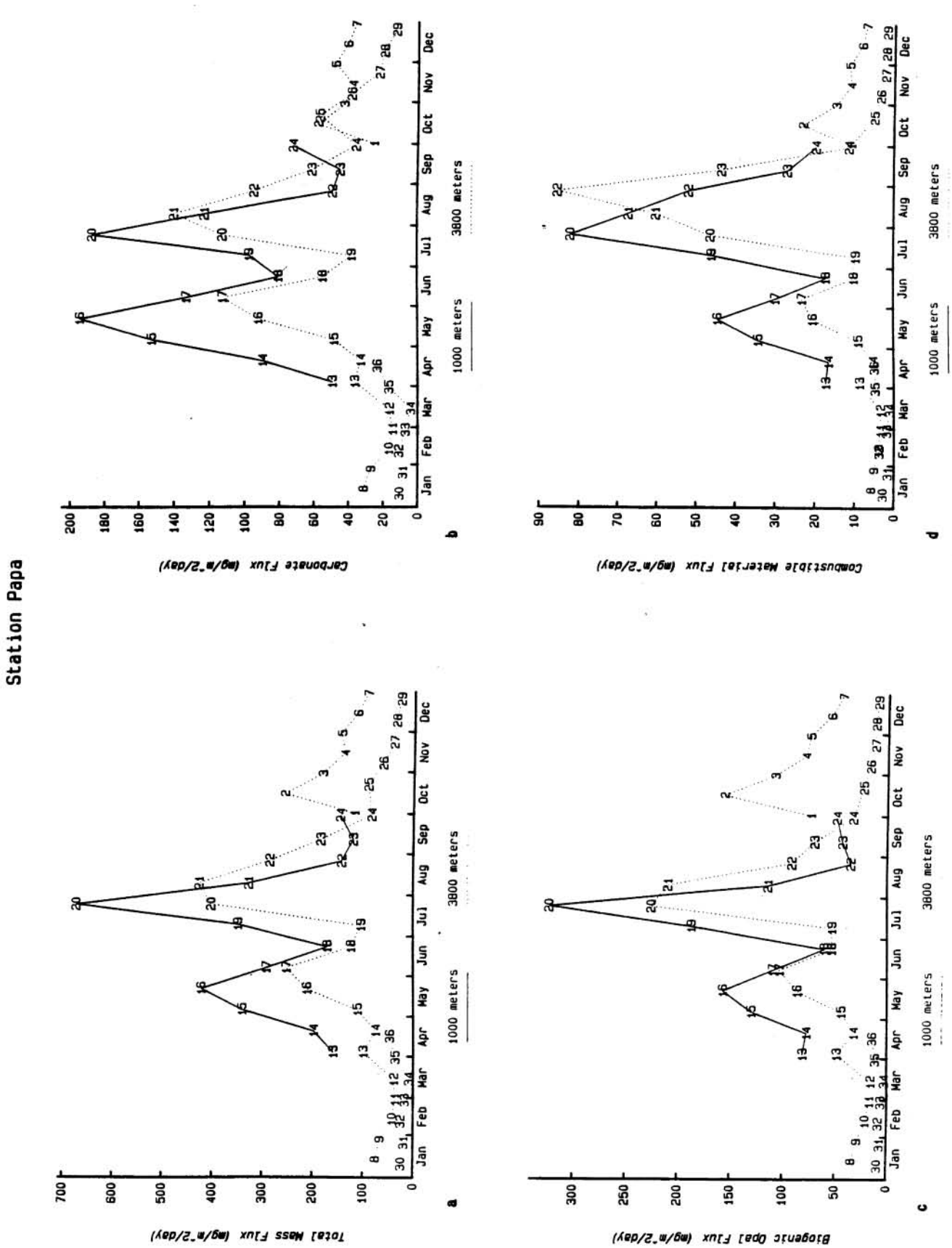
Station Papa
Carbonate Flux (mg/m^2/day)
Combustible Material Flux (mg/m^2/day)
Total Mass Flux (mg/m^2/day)
Biogenic Opal Flux (mg/m^2/day)
1000 meters
3800 meters
a
b
c
d
Jan Feb Mar Apr May Jun Jul Aug Sep Oct Nov Dec

Figure 1.3 Cross-correlations of the flux of a given particle type in shallow (1000m) vs. deep (3800m) traps at Station Papa in the North Pacific. Flux values (mg $m^{-2}day^{-1}$) were first linearly interpolated to an even sampling interval (16 days). The shallow series, consisting of 12 samples, was correlated with the longer deep series which consisted of 36 samples. Only the central 27 correlation values are plotted (0±13) to eliminate edge effects. Correlations greater than 0.708 are significant at the 99% confidence level (N=12). a) Total mass flux. b) Biogenic carbonate flux. c) Biogenic opal flux. d) Combustible material flux.

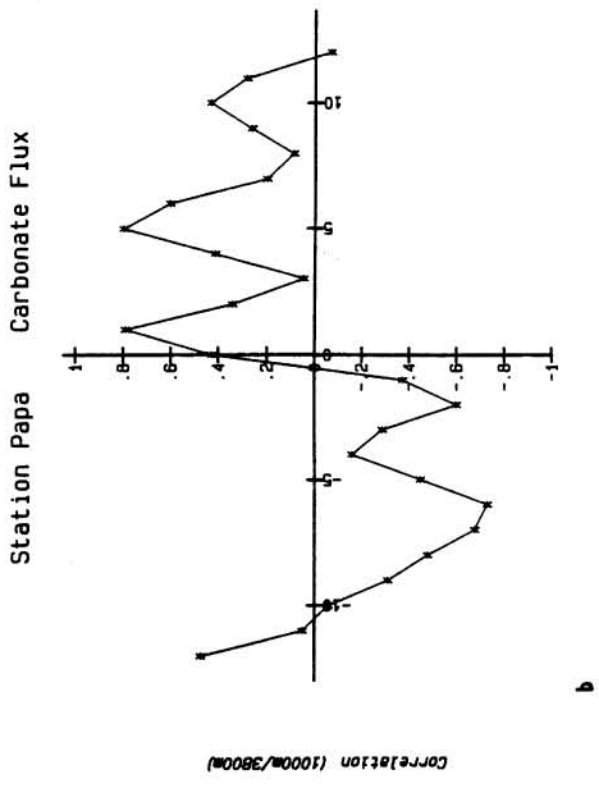
Station Papa Carbonate Flux
Correlation (1000m/3800m)
Lags (interval is 16 days)
b

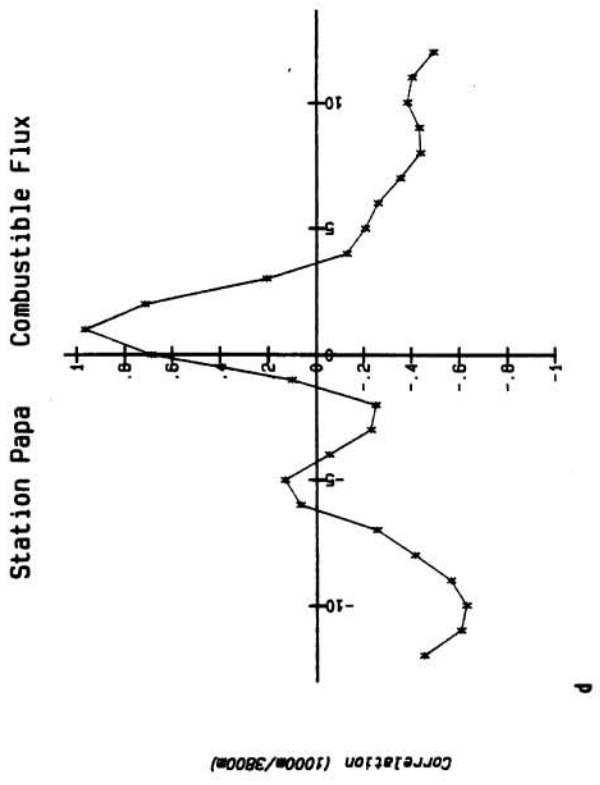
Station Papa Combustible Flux
Correlation (1000m/3800m)
Lags (interval is 16 days)
d

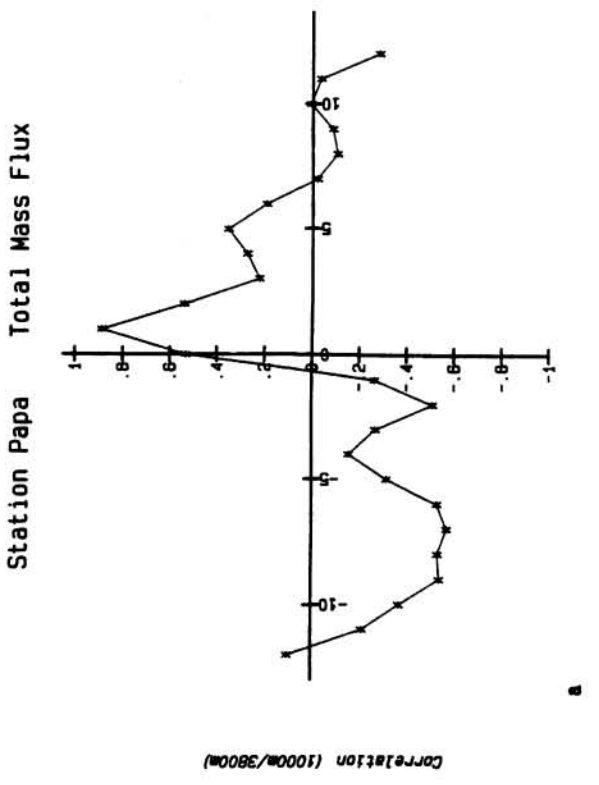
Station Papa Total Mass Flux
Correlation (1000m/3800m)
Lags (interval is 16 days)
a

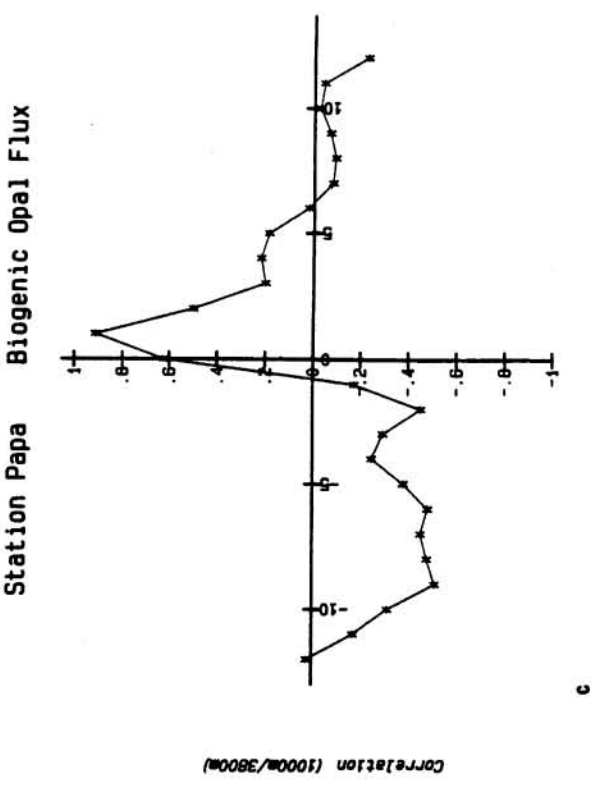
Station Papa Biogenic Opal Flux
Correlation (1000m/3800m)
Lags (interval is 16 days)
c

The pattern in the Black Sea is different than at Station Papa in several respects due to the domination of the deep trap samples by deep lateral input (fig. 1.4). First, flux in the deeper (1200m) trap is generally higher than flux in the shallow (250m) trap for all constituents. Second, the total flux vs. time signal is less systematic and less regular from year to year, especially in the deep trap. Comparison of shallow and deep signals reveals that all flux peaks occurring in the shallow trap are also observed in the deep trap, while the converse is not the case. For example, several of the carbonate peaks (fig. 1.4b) and most of the biogenic silica peaks (fig. 1.4c) found in the deep trap samples are not found in the shallow samples. Any particles sinking directly from the surface must intercept both the shallow and deep traps. However, material which arrives in the deep trap but which is not sampled by the shallow trap must have been delivered as particles which were re-suspended (perhaps from the shelf and slope) and then delivered at depth to the central basin.

Lithogenic flux follows a pattern similar to that of carbonate and opal particles with the exception of a large peak in November/December in the shallow trap. This flux was most likely produced by localized addition of concentrated suspended matter to the surface water; dispersal with settling results in lower values in the deep trap in this sample.

Fluxes of combustible material are more similar in deep and shallow traps than fluxes of other components (fig. 1.4e). In this case, nearly all peaks observed in the deep trap are present in the shallow trap as well, indicating increased importance of direct vertical transport over

Figure 1.4 Measured sediment flux at a site in the Black Sea. a) Total mass flux. Numbers designate sequential samples over a period of 12 months in the shallow (250 meters below the surface) and 24 months in the deep trap (1200 meters below the surface, water depth is 2200 meters). Sampling interval is variable from 11 to 15 days. b) Biogenic carbonate flux. c) Biogenic opal flux. d) Lithogenic material flux. e) Combustible material flux.

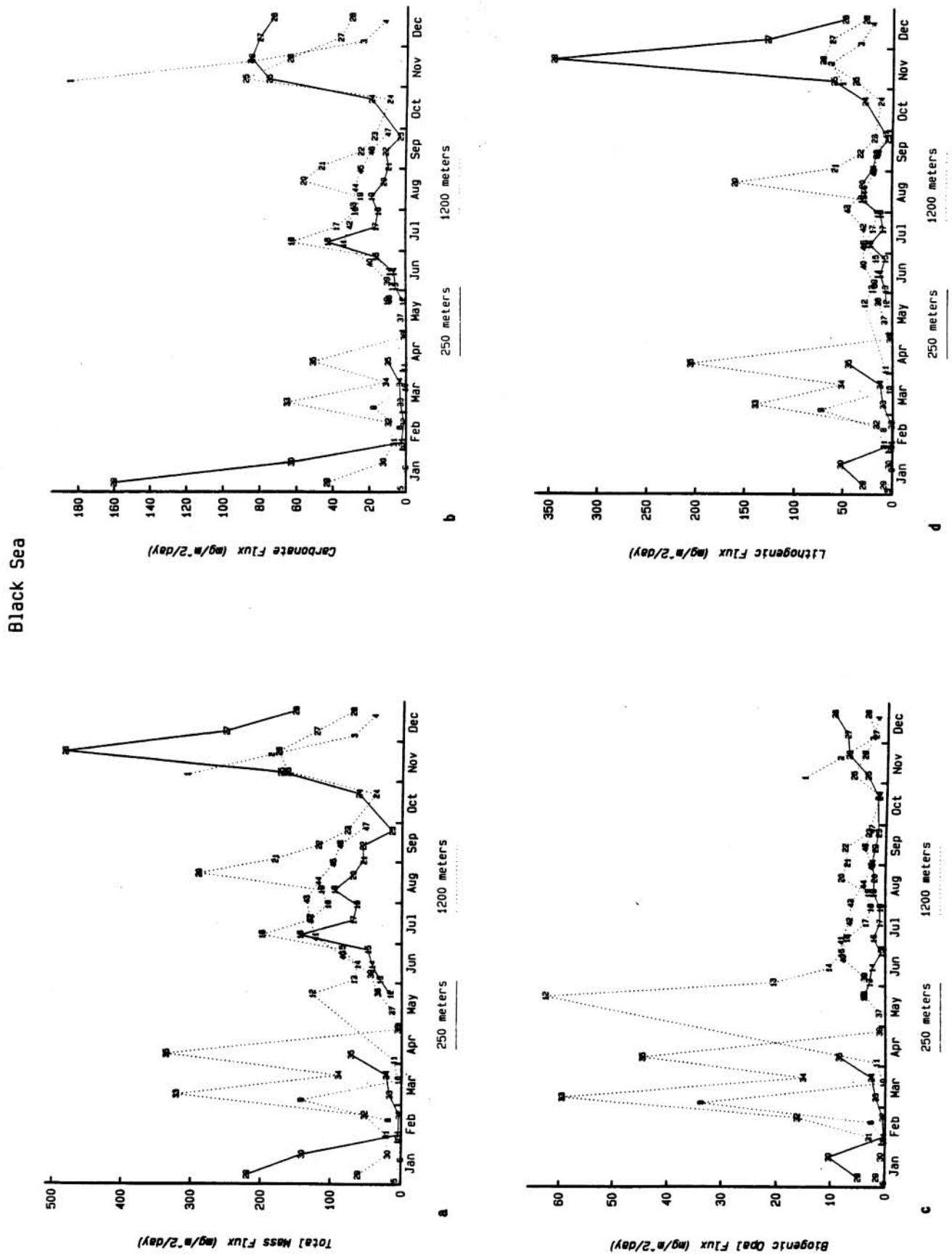
Black Sea
Total Mass Flux (mg/m^2/day)
Carbonate Flux (mg/m^2/day)
Biogenic Opal Flux (mg/m^2/day)
Lithogenic Flux (mg/m^2/day)
Jan Feb Mar Apr May Jun Jul Aug Sep Oct Nov Dec
250 meters
1200 meters
a
b
c
d

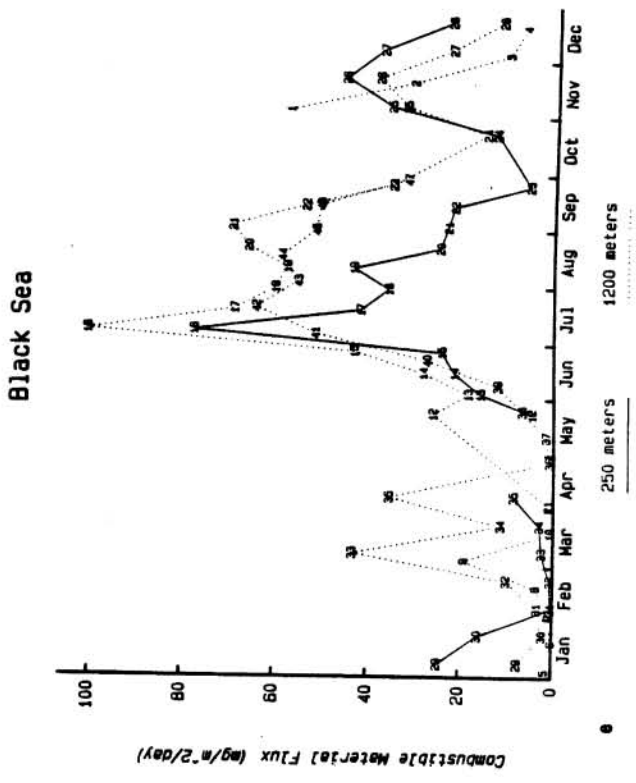
Black Sea
Combustible Material Flux (mg/m^2/day)
0
20
40
60
80
100
Jan
Feb
Mar
Apr
May
Jun
Jul
Aug
Sep
Oct
Nov
Dec
250 meters
1200 meters

deep lateral input. In places where flux peaks correspond in shallow and deep traps, the lag is either zero or one sampling interval (15 days). These trends are confirmed by cross-correlation of the shallow and deep trap records (fig. 1.5a-e). Correlation of biogenic opal and lithogenic are poor at lag one (0.03 and 0.21 respectively), indicating predominantly deep lateral input, while correlations of combustible and carbonate material are good (0.64 and 0.44 respectively) indicating increasing dominance vertical settling.

Because of the deep input of re-suspended material, sinking speeds determined by the vertical offset/time lag method are less certain than those observed at Station Papa. Combustible flux correlates best at lag 1 while carbonate flux correlates equally well at lag zero or one (0.46 and 0.44 respectively). These lags result in sinking speeds of 63 m day^{-1} for lag one (950 m/15 days) and an unknown but higher (>63 m day^{-1}) sinking speed for lag zero.

Flux Ratios

In addition to examining the correlations of the flux in shallow and deep traps, it is also useful to look at ratios of various components in the flux at a single depth. These ratios and the degree to which the fluxes of the components correlate help to indicate which components influence the total mass flux. Seasonal changes in the ratios are also expected as more or less of a given component is produced and settles into the traps. Geographic variations in these ratios provide evidence of environmental factors influencing the sediment flux. In the three areas studied, these ratios reveal both seasonal changes and regional trends in the sedimentation processes.

Figure 1.5 Cross-correlation of the flux of a given particle type in shallow (250m) vs deep (1200m) traps the Black Sea. Flux values (mg $m^{-2}day^{-1}$) were first linearly interpolated to an even sampling interval (16 days). The shallow series, consisting of 24 samples, was correlated with the longer deep series which consisted of 36 samples. Only the central 27 correlation values are plotted (0±13) to eliminate edge effects. Correlations greater than 0.515 are significant at the 99% confidence level (N=24). a) Total mass flux. b) Biogenic carbonate flux. c) Biogenic opal flux. d) Lithogenic material flux. e) Combustible material flux.

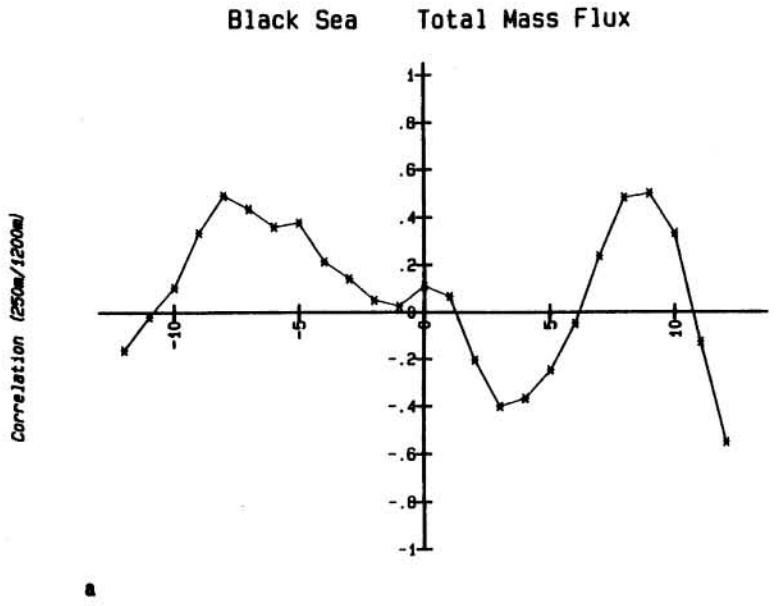
Black Sea Total Mass Flux
Correlation (250m/1200m)
Lags (interval is 15 days)
a

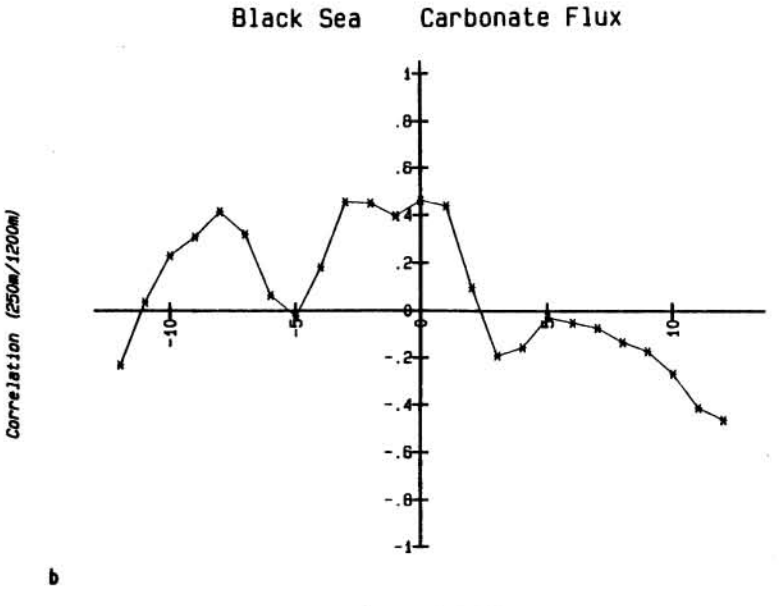
Black Sea Carbonate Flux
Correlation (250m/1200m)
Lags (interval is 15 days)
b

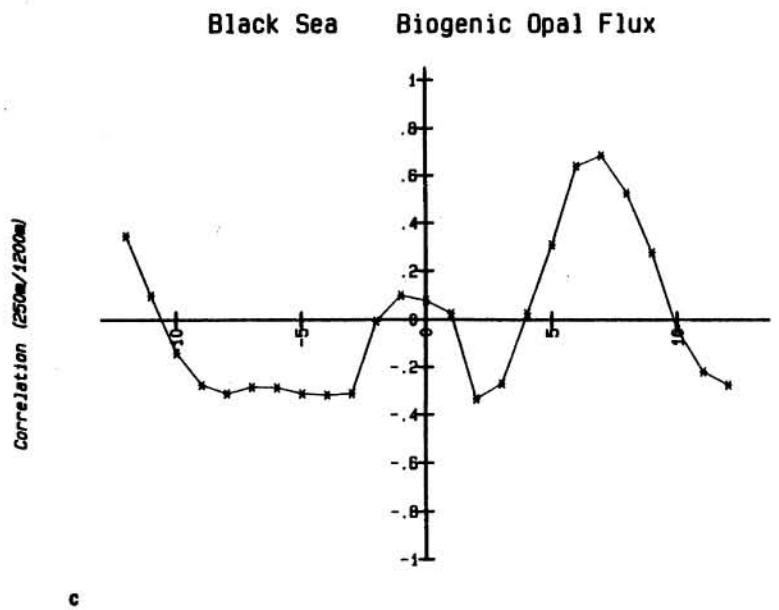
Black Sea Biogenic Opal Flux
Correlation (250m/1200m)
Lags (interval is 15 days)
c

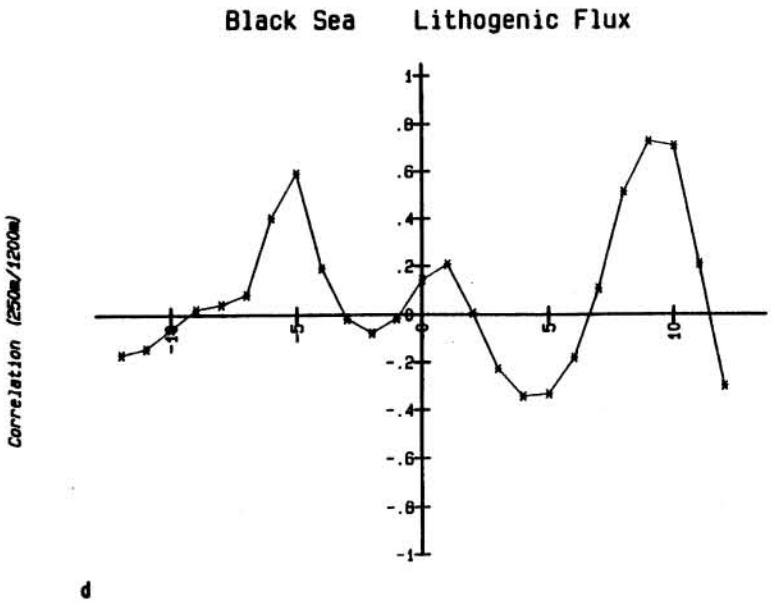
Black Sea Lithogenic Flux
Correlation (250m/1200m)
Lags (interval is 15 days)
d

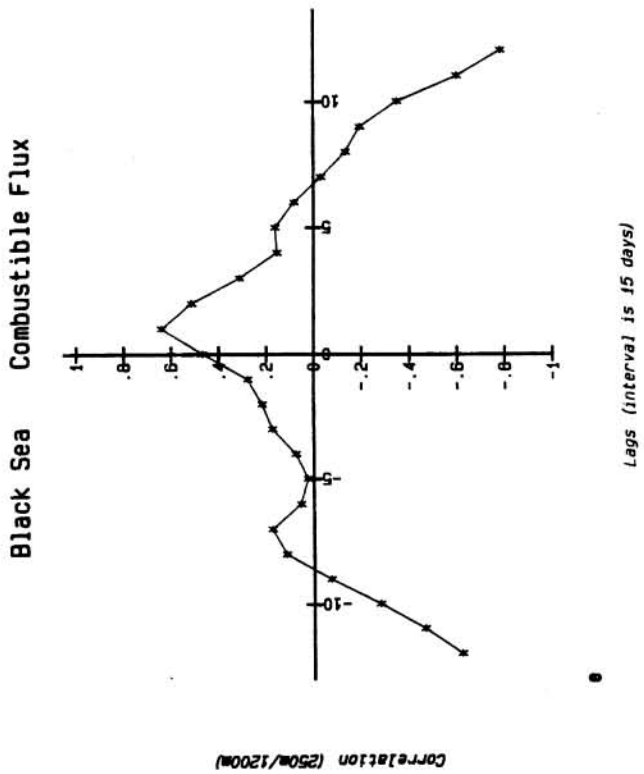
Black Sea Combustible Flux
Correlation (250m/1200m)
Lags (interval is 15 days)
1
.8
.6
.4
.2
0
-.2
-.4
-.6
-.8
-1
10
5
-5
-10

Panama Basin. Flux ratios in the Panama Basin samples reflect the large summer coccolithophorid bloom as well as the effect of deep lateral input (fig. 1.6). Although their total mass flux increases with depth, ratios of combustible or biogenic opal to total flux (percent/100) remain relatively constant with depth. In contrast, carbonate flux changes little or decreases slightly with depth, while the percent of total flux decreases. In the case of lithogenic particles, both mass flux and percent of total flux increase with depth. All of the observed effects are due to dilution of the vertical flux of sediment particles by deep input of resuspended material. This material is low in carbonate, high in opal and combustible material, and very high in lithogenic particles (see chapter 2 of this thesis). The resulting sediment flux reflects increasing amounts of this resuspended material in successively deeper traps.

If sedimentation of fine particles is by aggregates, then correlation of the flux of lithogenic particles to fluxes of other material should reveal which substances are controlling the flux. Table 1.2 lists values of correlation coefficients of lithogenic to other materials. The strongest and most depthwise consistent correlation results from correlation of lithogenic with combustible material (>0.91). This strong correlation indicates that the flux of lithogenic material will increase (or decrease) in proportion to the amount of settling organic material regardless of the the type or amount of biogenic mineral (carbonate or opal) associated with it. Although this ratio increases with depth due to additional input of lithogenic relative to combustible material in the resuspended particles, the seasonal constancy of the ratio at a given depth results in the good observed correlation.

Figure 1.6 Ratio of the flux of a given particle type to the total mass flux in the Panama Basin. a) Ratio of carbonate material to total flux. b) Ratio of biogenic opal to total flux. c) Ratio of combustible material to total flux. d) Ratio of lithogenic material to total flux.

Panama Basin

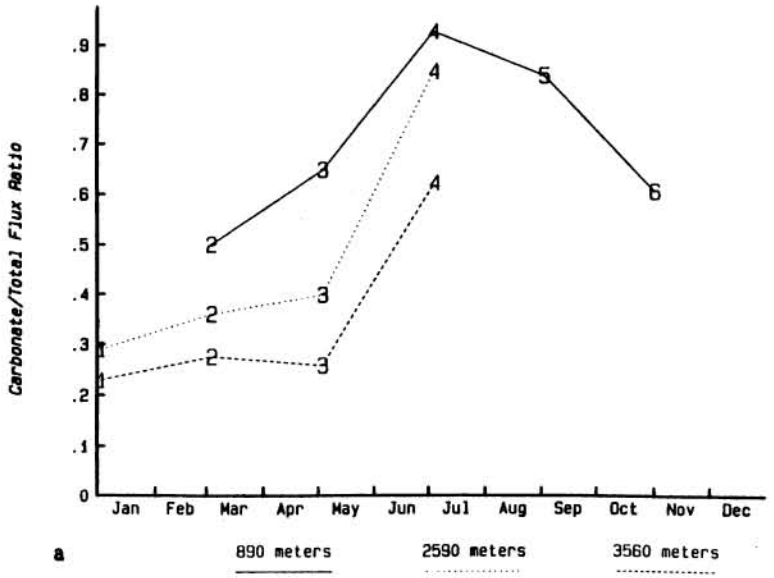

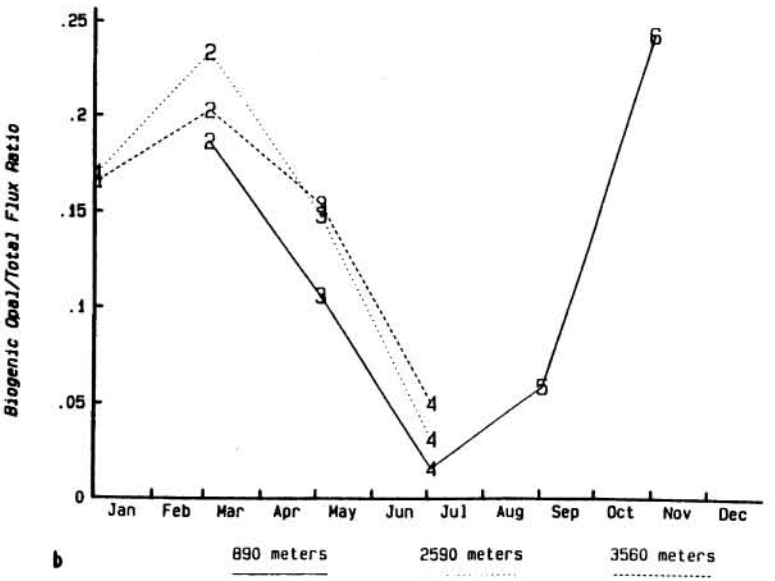

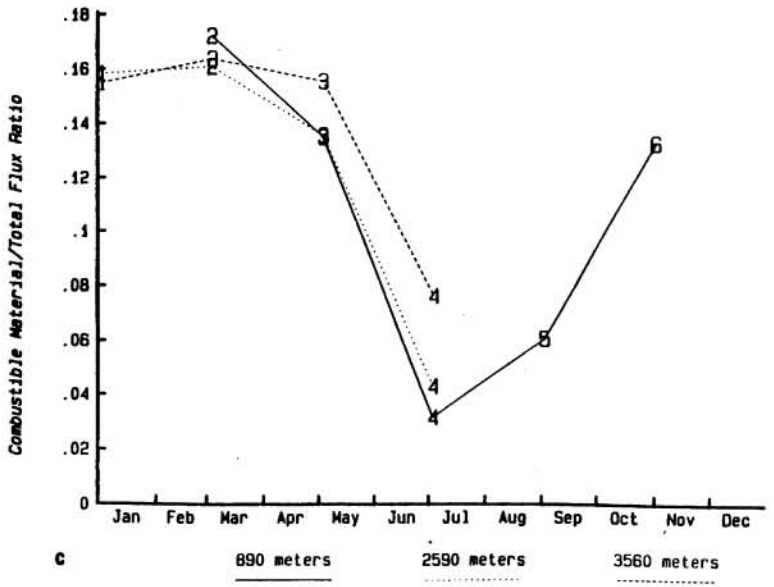

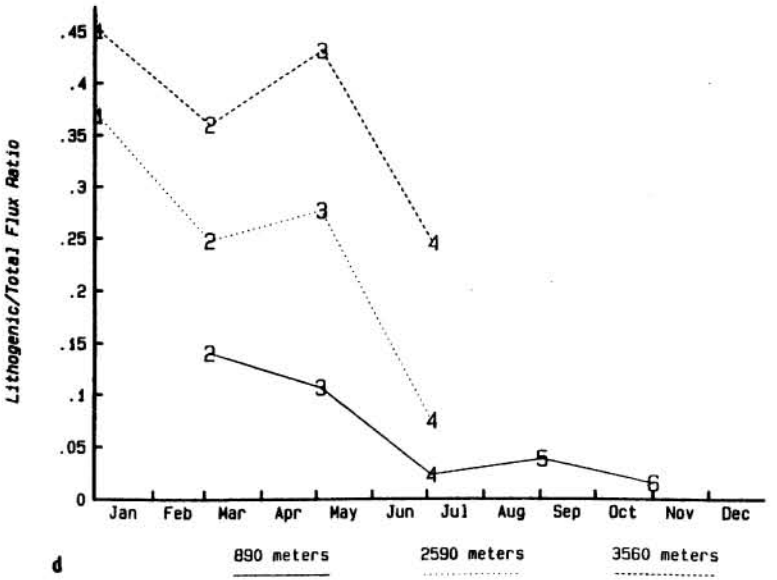

Table 1.2 Correlation coefficients for components of the observed flux with the lithogenic flux in the Panama Basin. At 890m and 2590m, N=4; at 3560m N=6. Results are given as slope of the best fit straight line / correlation coefficient.

Depth	890 meters	2590 meters	3560 meters
Lithogenic / Total	0.018 / 0.87	0.038 / 0.83	0.19 / 0.99
Lithogenic / Carbonate	0.018 / 0.87	0.037 / 0.77	0.26 / 0.99
Lithogenic / Combustible	0.83 / 0.91	1.30 / 0.98	3.50 / 0.96
Lithogenic / Opal	-0.059 /-0.004	0.63 / 0.63	1.90 / 0.33

Station Papa. Honjo (1985) described the seasonal cycle of physical and chemical changes which influence the production of biogenic material in the surface ocean at this site. Although further discussion of the causes of these cycles is beyond the scope of this paper, it is useful to examine the seasonal changes in the flux ratios as they reflect modes of sedimentation. Without a reliable estimate of the flux of lithogenic material, however (see above), it is not possible to evaluate the sedimentation mechanisms of these small particles.

Examination of the ratios of combustible to opal or carbonate flux in the late summer production peak reveals that significant combustible material settles which is not associated with either opal or carbonate (fig. 1.7a,b). Both minerals peak synchronously in sample 20 in the shallow trap and 21 in the deep trap. In contrast, the flux of combustible material peaks later (sample 22) in the deep trap and has a broader flux peak in the shallow trap. This difference is exhibited as ratios of combustible to opal and carbonate fluxes which are constant throughout the year except for the large peak in sample 22 in both the shallow and deep traps. This combustible material is most likely the result of a salp population, the remains of which were found in sample 22 in both traps. The observation that this material arrives at both depths within the same sampling interval indicates that these gelatinous zooplankton remains settle at more than 175 m day^{-1}.

Black Sea While in some respects the Black Sea environment is similar to the Panama Basin (eg. proximity to a margin), the flux record is markedly

Figure 1.7 Ratios of the flux combustible material to the flux of biogenic minerals at Station Papa in the North Pacific. a) Ratio of combustible material to biogenic opal flux. b) Ratio of Combustible material to biogenic carbonate flux.

Station Papa

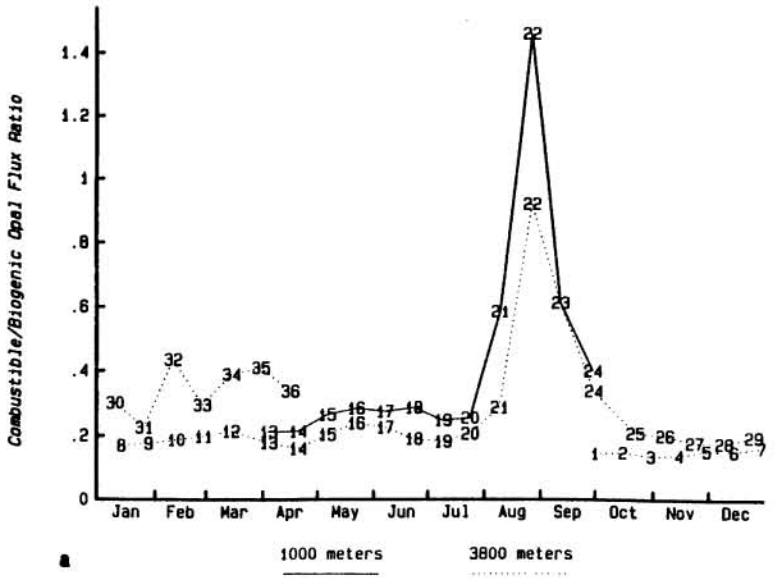

a

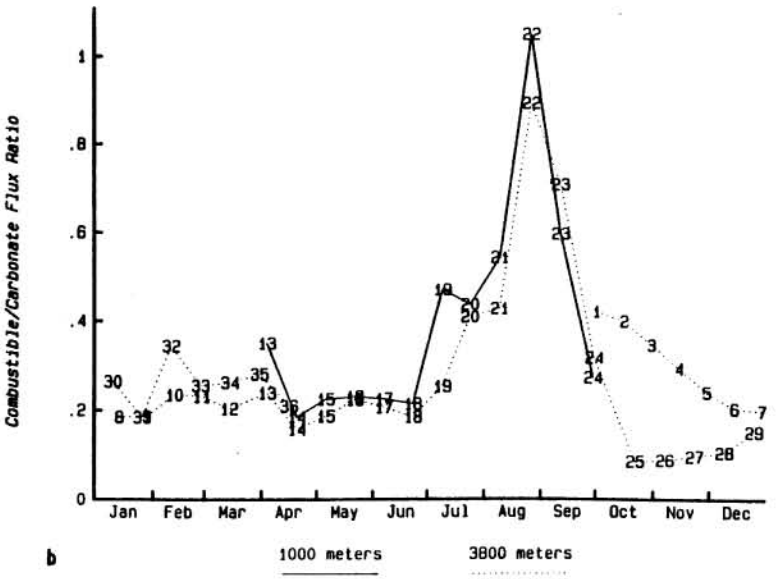

b

different. Ratios of carbonate to total flux, for example, are highest in the summer in Panama and in the winter in the Black Sea. Further, while the ratio of a given constituent to total flux generally changes with depth in Panama, they remain constant over the two depths sampled in the Black Sea (fig. 1.8). This result is due to the enhanced preservation of sediments in the Black Sea, leading to increased similarity of resuspended (deep lateral) and direct vertical flux.

As at station Papa, a large peak in combustible flux occurs in the summer which is not associated with either opal or carbonate. This is again reflected in the total combustible flux as well as the ratio of combustible to either opal (fig. 1.9a) or carbonate (fig. 1.9b) material. The ratio of lithogenic to combustible flux (fig. 1.9c) reaches a minimum during the period of high combustible flux, indicating that little lithogenic material is transported with this combustible matter.

In contrast, the ratio of lithogenic to opal flux is relatively constant throughout the year except for the peaks in samples 26 (shallow) and 27 (deep). This good correlation of opal and lithogenic flux from January to October is due to resuspension and lateral input of both. In the early winter (November and December), lithogenic material is delivered directly to the surface water and sinks independent of the opal.

The overall picture which emerges for the Black Sea is one in which deep lateral input generally dominates direct vertical settling. Only the flux of combustible material (and to a limited extent carbonate) reflects the expected cycles of production and subsequent sedimentation of biogenic matter in both traps. For these particle types, most flux peaks appear in

Figure 1.8 Ratio of the flux of a given particle type to the total mass flux in the Black Sea. a) Ratio of carbonate material to total flux. b) Ratio of biogenic opal to total flux. c) Ratio of combustible material to total flux. d) Ratio of lithogenic material to total flux.

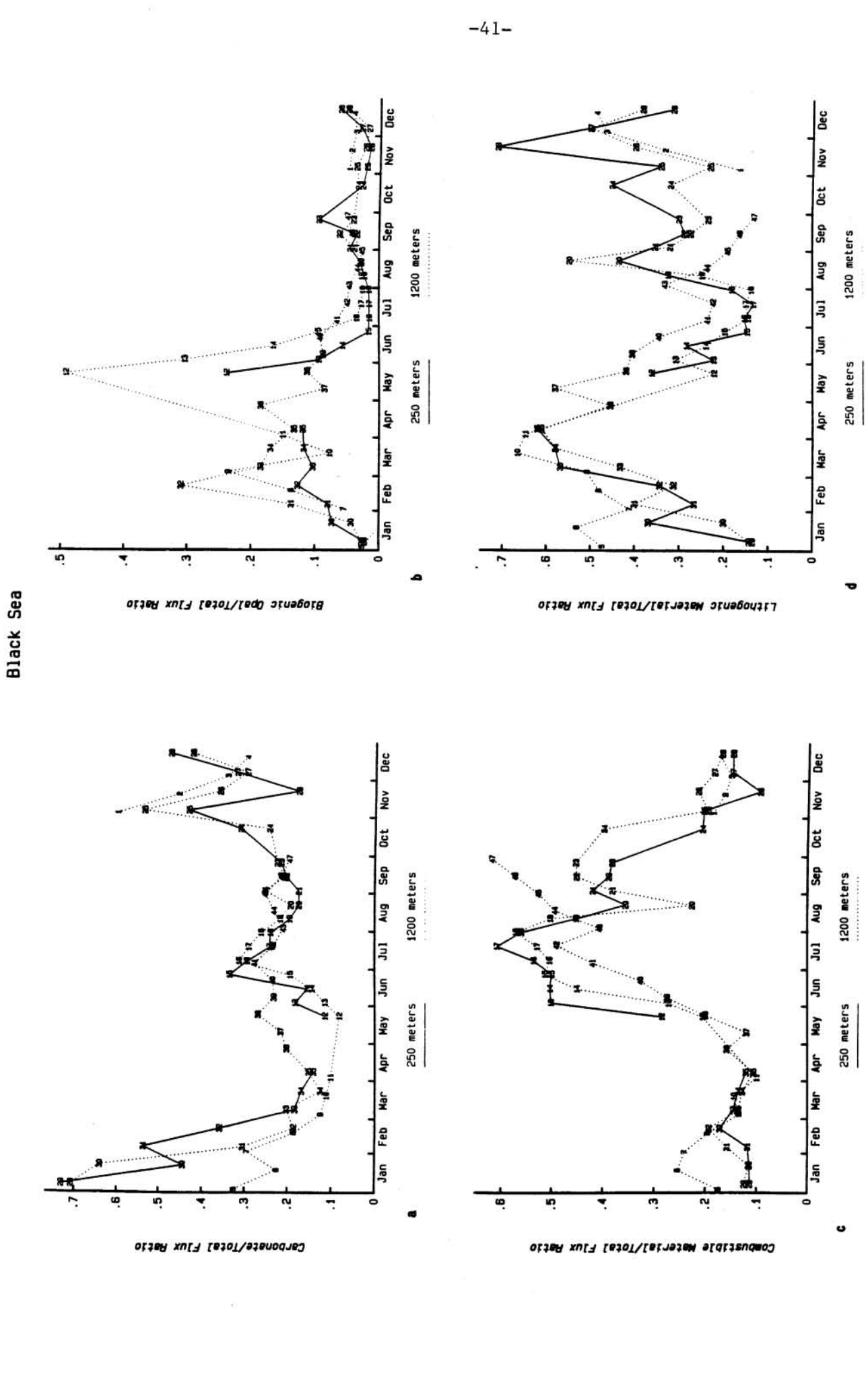
Black Sea
Biogenic Opal/Total Flux Ratio
Lithogenic Material/Total Flux Ratio
Carbonate/Total Flux Ratio
Combustible Material/Total Flux Ratio
Jan Feb Mar Apr May Jun Jul Aug Sep Oct Nov Dec
250 meters
1200 meters
a
b
c
d

Figure 1.9 Ratio of the fluxes of several particle types in the Black Sea. a) Ratio of combustible material to biogenic opal. b) Ratio of combustible material to biogenic carbonate. c) Ratio of lithogenic material to combustible material.

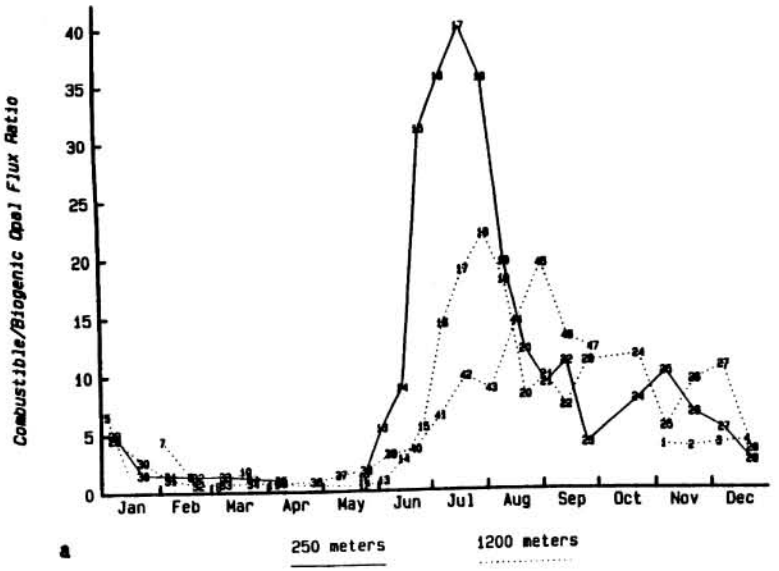
Combustible/Biogenic Opal Flux Ratio
0
5
10
15
20
25
30
35
40
Jan
Feb
Mar
Apr
May
Jun
Jul
Aug
Sep
Oct
Nov
Dec
250 meters
1200 meters

a

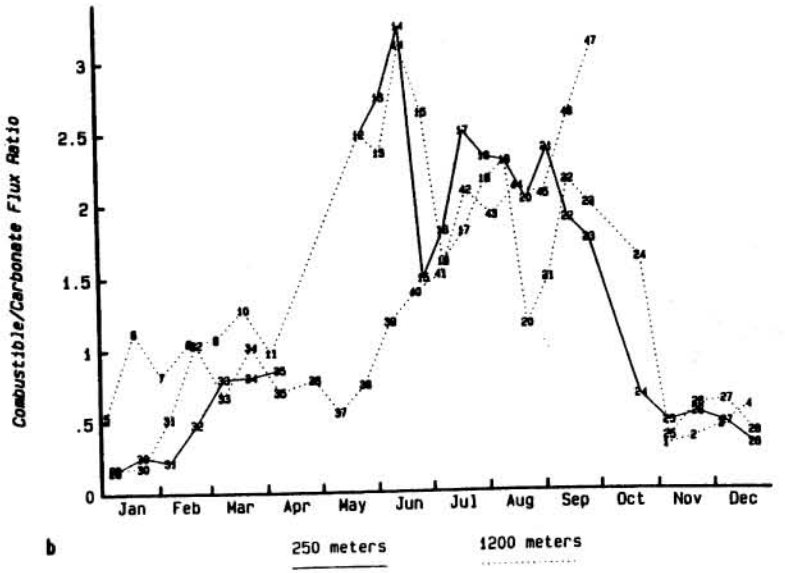
Combustible/Carbonate Flux Ratio
0
.5
1
1.5
2
2.5
3
Jan
Feb
Mar
Apr
May
Jun
Jul
Aug
Sep
Oct
Nov
Dec
250 meters
1200 meters

b

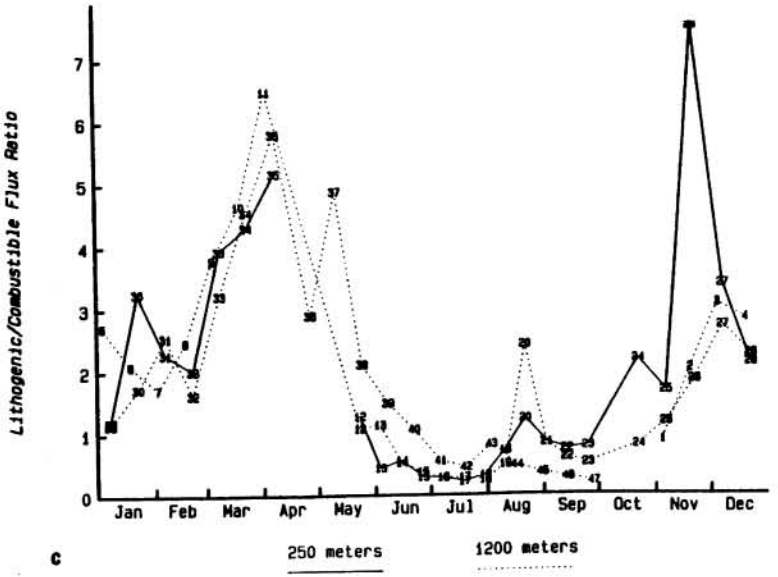
Lithogenic/Combustible Flux Ratio
0
1
2
3
4
5
6
7
Jan
Feb
Mar
Apr
May
Jun
Jul
Aug
Sep
Oct
Nov
Dec
250 meters
1200 meters

c

both traps, indicating vertical settling with blooms of coccolithophorids occurring in November and December. However, in both cases and especially for carbonate particles, several events occur in which the flux is greater in the deep trap, indicating the input of laterally advected particles. The flux of opal increases in the spring and summer in both traps due to vertical settling of diatoms. However, much larger flux values are observed many months later in the deep trap due to lateral input of resuspended opal. These resuspension events influence the flux signal in the shallow trap, but completely dominate the signal in the deep trap.

The Black Sea samples are composed of between 15% and 72% lithogenic particles due to the proximity of the station to the continental shelf and to the extremely steep continental slope (7° to 18° at this site). In a typical open oceanic environment, only a small and constant number of lithogenic particles are available for incorporation into settling aggregates (Deuser, 1981, 1983). In this situation, lithogenic flux is controlled by the availability of settling aggregates which can incorporate the lithogenics and transport them to the sea floor. In contrast, in the Black Sea the flux of lithogenic particles is controlled by their supply (resuspension and river input) rather than the availability of settling aggregates.

CONCLUSIONS

Time series sediment trap samples can be used to determine particle flux pathways as depicted in figure 10. Flux peaks appearing in both shallow and deep signals with similar amplitudes or with slightly diminished amplitude in the deeper traps, indicate predominantly vertical settling as in the case of Station Papa. Peaks appearing only in the deep trap indicate lateral input, as observed for opal and most lithogenic flux in the Black Sea. In cases such as the Panama Basin, where peaks occur in both shallow and deep samples but with higher amplitudes in the deep trap, a mixture of vertical and lateral inputs is indicated.

Evidence from time series sediment trap samples supports the concept of rapid settling of fine particles by aggregates. The sinking speeds resulting from this method are considerably higher than those predicted for settling of individual particles. Where available, data for lithogenic materials indicates that these fine particles in particular are settling at a greatly enhanced rate.

Sediment trap data also indicate that, not only do most particles settle quickly and at similar speeds, but the fluxes of the individual particle types also correlate well with fluxes of all other particles. Settling in the form of aggregates is again indicated, as these packages collect suspended particles and transport them to the abyss. Organic matter associated with aggregates appears to be the major controlling factor in the sedimentation of other material, since the flux of combustible material corresponds most closely in shallow and deep traps and also correlates best with the flux of fine particles.

Figure 1.10 Diagram of the three types of flux signals identified in this review. a) Vertical settling, where the peak in the flux signal observed in the shallow trap also occurs in the deep trap with equal or diminished amplitude. b) Lateral transport, where the flux peak observed in the deep trap does not occur in the shallow signal. c) Combination of vertical settling and lateral input, where flux peaks occur in both shallow and deep traps but with higher amplitude in the deep trap.

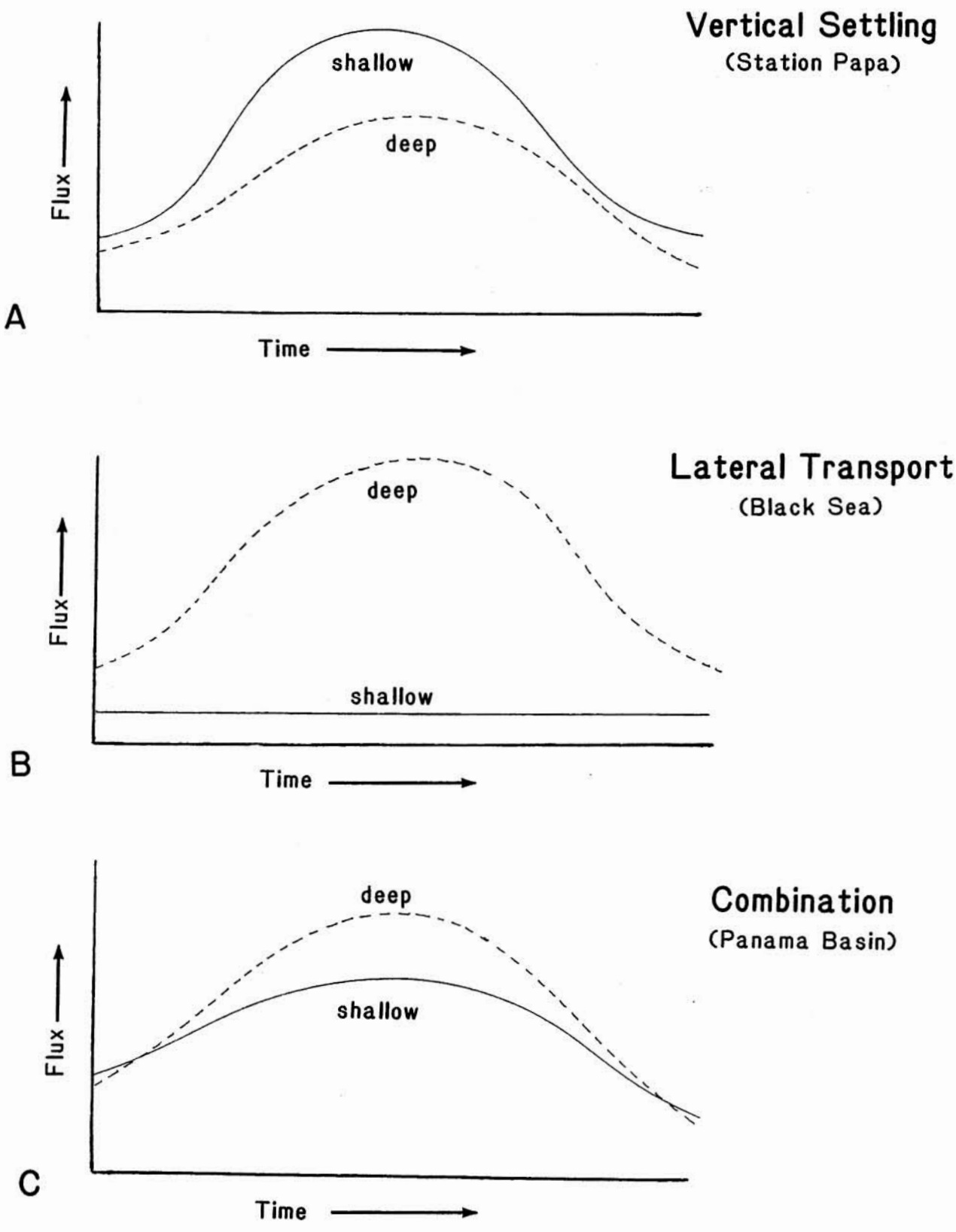
Vertical Settling
(Station Papa)
shallow
deep
Flux
A
Time
Lateral Transport
(Black Sea)
deep
shallow
Flux
B
Time
Combination
(Panama Basin)
deep
shallow
Flux
C
Time

In areas such as the Black Sea or the Panama Basin where deep lateral input is important, sediment traps can provide information relating to the timing and nature of these deep inputs. In the Panama Basin, deep input is constant throughout the year and, while it influences the total flux signal, vertical input is dominant. At the station in the Black Sea, however, this deep input varies considerably throughout the year and often overwhelms and obscures the direct vertical input.

REFERENCES

Deuser, W.G., (1974) Evolution of anoxic conditions in the Black Sea during Holocene. in The Black Sea-geology, chemistry and biology A.A.P.G. Memoir 20, Tulsa Ok.

Deuser, W.G., P.G. Brewer, T.D. Jickells and R.F. Commeau (1983) Biological control of the removal of abiogenic particles from the surface ocean. Science vol. 219, 388-391.

Deuser, W.G., E.H. Ross and R.F. Anderson (1981) Seasonality in the supply of sediment to the deep Sargasso Sea and implications for the rapid transfer of matter to the deep ocean. Deep-Sea Res. vol. 28A(5), 495-505.

Honjo, S. (1982) Seasonality and interaction of biogenic and lithogenic particulate flux at the Panama Basin. Science vol. 218, 883-884.

Honjo, S. (1985) Study of ocean fluxes in time and space by bottom-tethered sediment trap arrays: a recommendation. in Global ocean flux study; proceedings of a workshop, National Academy Press, Washington, D.C., 306-324.

Honjo, S., K.W. Doherty, Y.C. Agrawal and V.L. Asper (1984) Direct optical assessment of large amorphous aggregates (marine snow) in the deep ocean. Deep-Sea Res. vol. 31(1), 67-76.

Honjo, S., S.J. Manganini, and L.J. Poppe (1982a) Sedimentation of lithogenic particles in the deep ocean. Mar. Geol. vol. 50, 199-220.

Honjo, S., S.J. Manganini, and J.J. Cole (1982b) Sedimentation of biogenic matter in the deep ocean. Deep-Sea Res. vol. 29(9A), 609-625.

Pilskaln, C.H., (1985) The fecal pellet fraction of oceanic particle flux, unpublished Ph.D. thesis at Harvard University, Cambridge, MA.

Smayda, T.J., (1971) Normal and accelerated sinking of phytoplankton in the sea. Mar. Geol. vol. 11, 105-122.

Takahashi, K.,(1985) Seasonal biogenic silica flux in the subarctic Pacific, Geol. Soc. Amer., Abstracts with Programs, 17(7), 732.

Chapter 2

THE DISTRIBUTION AND TRANSPORT OF MARINE SNOW AGGREGATES IN THE PANAMA BASIN AND NORTHEAST ATLANTIC OCEAN

ABSTRACT

Depth profiles of marine snow aggregate abundance were acquired in the Panama Basin and Western North Atlantic. Concentrations are generally highest in the surface water with maximum abundances varying from 30 to 90 $mm^3 l^{-1}$. In areas removed from deep sources of resuspended material, aggregate concentrations decrease with depth to a minimum value several hundred meters above the sea floor; concentrations increase again near the bottom. When deep sources of resuspended material are present, sub-surface maxima in aggregate concentration are observed. Samples from time series sediment traps deployed during the marine snow survey in the Panama Basin reveal that sediment flux (mg $m^{-2} day^{-1}$) varied by a factor of six over the 28 day deployment. Aggregate abundance, however, varied only by a factor of three with depth and varied little over time scales of hours to weeks.

In the proposed particle transport model, large, resuspended aggregates are lighter and more flocculent than fresh material due to partial remineralization in the benthic transition layer. These modified aggregates remain suspended and are transported offshore, producing the signal in the abundance profiles. As the resuspended aggregates are transported away from their sources, fresh, fast-sinking material falling directly from the surface collides with them, scavenges them from the water column, increases their sinking speed, and produces the time-varying flux signal.

INTRODUCTION

Although it has been established that most marine particulate material is produced at the sea surface, a clear understanding of the processes involved in the transport of this material to the benthos is lacking. Recent investigations (Bishop, et al. 1977; Deuser et al., 1983; Gardner et al., 1984; Honjo, 1978, 1980, 1982; Honjo et al., 1982a, b; Lal, 1980; McCave, 1975; Suess, 1980; Tanoue and Handa, 1980; Tsunogai and Mingawa, 1978; Wakeham et al., 1980) have proposed that most sedimentation occurs in the form of large, fast-sinking particles which are not adequately sampled by standard hydrocasting techniques. This evidence includes: seasonality of particulate flux (Billett et al., 1983; Deuser et al., 1981, 1982, 1983; Honjo, 1982), excellent preservation of sediment trap material (Honjo, 1980), empirical models (McCave, 1975), isotopic evidence (Osterberg et al., 1963), and the close correspondence (allowing for dissolution) of surface coccolithophore assemblages with those found in surface sediments, indicating minimal influence of water motion on distribution patterns (Honjo, 1976).

In some regions of close coupling between primary and secondary production, fecal pellets can play an important role in the vertical transport process (Knauer et al., 1979; Urrere and Knauer, 1981), but in

most of the world's oceans, other mechanisms must be invoked because of the observed scarcity of fecal pellets in sediment trap samples. One such mechanism, marine snow aggregates, has recently received a great deal of attention not only for its potential role in vertical flux (Alldredge, 1979; Honjo et al., 1982b, 1984; Shanks and Trent, 1980; Silver and Alldredge, 1981) but also as an important site for primary production (Alldredge and Cox, 1982; Knauer et al., 1982), microbial growth (Caron and Madin, 1982; Paerl, 1975), microzooplankton habitat (Alldredge and Cox, 1982; Silver et al., 1978, 1984; Silver and Trent, 1978; Silver and Alldredge, 1981), and as a food source for filter feeding zooplankton which could not otherwise access the constituent particles because of their small size (Alldredge, 1976; Lenz, 1977; Prezelin and Alldredge, 1983; Riley et al., 1965; Trent et al., 1978).

Like the aggregates themselves, definitions of marine snow seem to be amorphous and quite variable. Suzuki and Kato (1953) define marine snow as "aggregates of the remains of plankton, sinking in some stages of disintegration..." For the purpose of this paper, flocs, flakes, fecal matter, aggregates, large amorphous aggregates, macroscopic organic aggregates, marine snow and marine snow aggregates all refer to the larger than 1.0mm, fragile, amorphous aggregates commonly found in all environments. Smaller particles populating the flocculent organic matrix of these aggregates include bacteria, microzooplankton (flagellates, protozoan), fecal pellets, diatoms and other algae, clay particles, crustacean moults and significant amounts of unidentifiable organic matter (Alldredge, 1979; Kajihara, 1971, 1974; Silver et al., 1978).

The origins of marine snow are still poorly understood. As listed by Alldredge (1984), several likely formation mechanisms include: zooplankton byproducts (feeding nets, mucous, remains) (Gilmer, 1972; Hamner et al., 1975; Pomeroy et al., 1980), phytoplankton (Kane, 1967), bubble dissolution (Barber, 1966; Baylor, 1963; Johnson, 1976), bacterial aggregation, terrigenous sources (Suzuki ant Kato, 1953), and sheet layering at interfaces (Wheeler, 1975). Many of these and other mechanisms are the focus of current research.

Most marine snow research has been aimed at understanding the role of these aggregates in marine ecosystems; relatively few studies have speculated on the potential role of these aggregates in sediment transportation either in the vertical or horizontal dimensions (Alldredge, 1979; Honjo et al., 1982b, 1984; Shanks and Trent, 1980). This is partly due to the extremely delicate nature of the aggregates and the resulting difficulties associated with collecting unaltered specimens (Trent et al., 1978; Jannasch, 1973; Riley, 1963).

Kajihara (1971) collected marine snow from a submersible in an attempt to measure settling speeds. The sampling procedure produced disaggregated material which was returned to the laboratory and allowed to re-aggregate. Measured settling rates of this re-aggregated marine snow were in the range of 17-260m day^{-1} (mean ca. 70m day^{-1}). The authors speculated that the porous aggregates (99.3% porosity) collected near the sea floor in shallow water may act as 'parachutes', slowing the settling of component material.

Shanks and Trent (1980) measured in situ marine snow sinking speeds in Monterey Bay using open water SCUBA techniques by enclosing aggregates in clear tubes and timing their fall over a measured distance. They reported

speeds of between 43 and 95 m day^{-1} (mean 68 m day^{-1}) and calculated that 3-5% of the POC standing stock would be exported each day by these aggregates.

Using time lapse photography, Lampitt and Burnham (1983) and Lampitt (in press) observed seasonal deposition of large aggregates. Based on the delay between production at the surface and deposition on the sea floor, Lampitt estimates the sinking speeds of 100-150m day^{-1}. Billet et al. (1983) also notes that these aggregates are easily resuspended in weak (ca. less than 7 cm sec^{-1}) currents and are likely to be transported with the bottom flow, but also degrade and break up within 2 days of their arrival on the sea floor.

In order to be important in the flux of particulate matter on a global scale, marine snow aggregates must be ubiquitous in all environments and depths, sink at significant speeds, and contain material known to eventually reach the sea floor. Of all the studies conducted to date however, only one has included samples from the environment below 200m. Silver and Alldredge (1981) obtained the first intact deep (1000m and 1650m) marine snow samples using the research submersible DSRV Alvin. Using histological procedures, they found that the aggregates found at depth are not significantly different from those found in the euphotic zone, and contained intact algae and living protozoans. They conclude that these aggregates settle faster than their constituent parts (including clay and small fecal pellets) and thus contribute significantly to the vertical flux of these particles.

Alldredge (1984) reviewed the importance of these aggregates in particulate flux and recommended that, among other things, it is important

to investigate the abundance, distribution, and flux of these particles. If marine snow aggregates are sinking, then the abundance of aggregates should correlate with measured flux at a given location. Because of the delicacy of the aggregates, however, sampling them at depth is difficult and expensive (Alldredge and Silver, 1981) and no published measurements of aggregate flux are available.

Honjo et al. (1984) proposed a new photographic method of assessing the size and spatial distribution of marine snow aggregates. Their system uses light scattered at approximately 90° to image the aggregates in a defined volume of water. This non-disruptive method overcomes the problems of disaggregation and particle alteration which are inherent in any technique which requires recovery of intact aggregates.

In the present study, this photographic method is used to assess the distribution of aggregates in the Panama Basin and Western North Atlantic. Simultaneous deployments of time series sediment traps are used to assess spatial and temporal correlations of marine snow abundance to measured vertical particulate flux. Regional aggregate distribution patterns can be examined within the framework of previous sediment transport and vertical flux models to establish the role of aggregates in these processes. In the Panama Basin, sediment redistribution by subsurface currents has been proposed to explain depthwise increases in the vertical flux of both biogenic and lithogenic material (Honjo et al., 1982b). If marine snow distribution patterns reflect this advective transport, then an active role in horizontal as well as vertical transport is indicated for these aggregates.

MATERIALS AND METHODS

Marine snow abundance profiles

Profiles of marine snow abundance were acquired using the photographic method described by Honjo et al. (1984). The camera system (fig. 2.1a) consists of one or two Benthos model 392 underwater strobe lights mounted at the focal point of a compound Fresnel lens, producing a collimated 'slab' of illumination (fig. 2.1b). Mounted at approximately 90° from this slab, a Benthos model 372 underwater camera using either Kodak Tri-X or Plus-X film photographs an intersecting volume of water (600 liters). Objects above or below the slab are not illuminated and thus will not appear in photographs. The system is lowered slowly (10-20 m min^{-1}) through the water column on a trawl wire, exposing frames at a time interval (7-20 sec.) calculated to yield 700 frames between the surface and the sea floor (1.2-5.6 m $frame^{-1}$). Depth is monitored and recorded using an O.R.E. model 261 pinger and the ship's precision depth recorder. Lowering is halted when the frame is within 2-10 meters of the sea floor, when the ship's wire is exhausted, or occasionally when scheduling constraints require an abbreviated lowering.

Films were generally returned to shore and processed professionally to assure consistent film densities and minimal contamination on the negatives. Images were analyzed directly from the film negatives using a Luzex^{R} model 450 image digitizer and Hewlett Packard^{R} 87XM micro-computer for control and data storage. Total image area occupied by aggregates, average diameter, and the number of particles in four size classes (1-2.5mm, 2.5-4mm, 4-5mm, and larger than 5mm) were counted in representative portions of each image.

Figure 2.1 a) Configuration of marine snow photography system. Benthos model 292 strobes (200 watt seconds each) are mounted at the focal point of a pair of compound Fresnel lenses. The Camera, Benthos model 372, is mounted at 90° to the "slab" of light produced by the strobes. b) Diagram showing the dimensions of slab. 600 liters of water are included in the photograph.

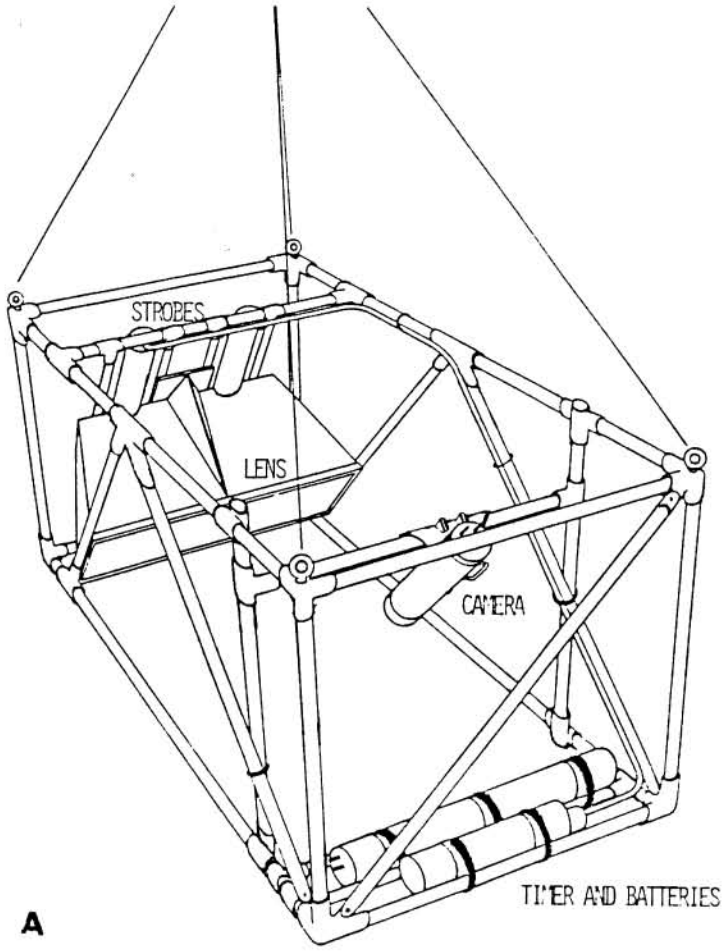
STROBES
LENS
CAMERA
TIMER AND BATTERIES

A

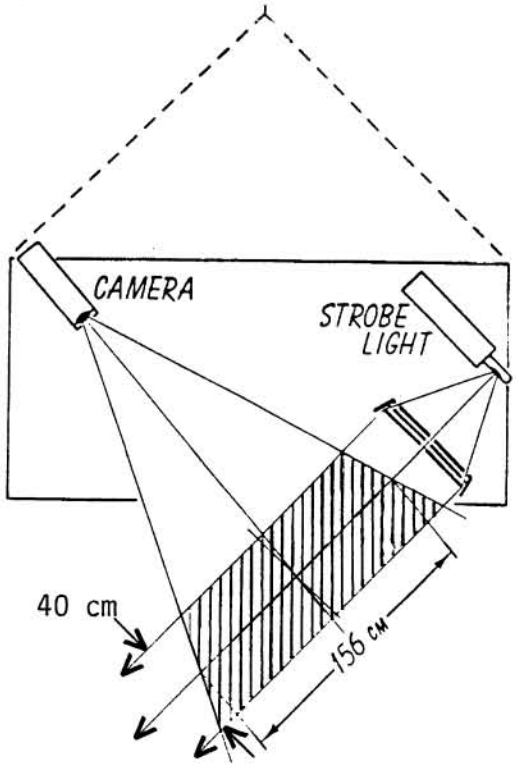
CAMERA
STROBE LIGHT
40 cm
156 cm

B

Images with large zooplankton or nekton were excluded. Because this method relies on optical contrast between large aggregates and relatively clear water, photographs taken in the upper 50-100m should be regarded with caution. At these depths, ambient light levels and phytoplankton abundances substantially reduce contrast levels and introduce uncertainties into the measurements.

Uncertainties in the method

No rigorous error analysis will be attempted for this method; however several considerations should be discussed. Images represent volumes which are trapezoidal in thickness cross section (fig. 2.1b), but which are analyzed (in two dimensions) as if they were rectangular. This leads to a perspective error of approximately 15% if objects are not in the center of the slab. This error however, should almost cancel if particles are randomly distributed within the volume since equal numbers will be above and below center. Absolute size of photographed objects is determined using calibration factors obtained by photographing objects of known dimensions.

The image analyzer interprets an analog (many shades of gray) signal as a digital (black and white) image. During this digitizing process, the operator must specify a darkness threshold level. Any portions of the image which are lighter than this level will be interpreted as white (not counted) and those which are darker as black (counted). This level is critical; small changes in threshold level result in up to a factor of two difference in the counted result. This difference is due to the machine including random noise in its digitized image if the threshold is set too low. Because of slight changes in overall exposure and contrast,

background suspended material, and instrument drift, minute adjustments must be made to this level during the course of digitizing the 200-800 exposures which constitute a single profile. Although a single operator (VLA) analyzed all images, this process adds a small element of subjectivity to the result which is not felt to be significant.

The optical resolution of the technique is on the order of 0.1mm to 0.2mm. However identification of small (1mm-3mm size) objects on 35mm film format, even when projected on a high resolution monitor, is impractical. For this reason we assume that all unrecognizable objects in the images are marine snow. Based on in situ observations from DSRV Alvin, this assumption is sustained, as marine snow is by far the most common macroscopic particle observed at all depths. Calibration experiments performed in Monterey Bay comparing abundance measured using the SCUBA method of Shanks and Trent (1980) with the photographic method showed similar results in surface waters. Also, abundances measured in deep water agree with estimates of Silver and Alldredge (1981) obtained during Alvin dives.

Study area

Reported here are the results of three cruises totaling 36 profiles. In May 1982, 9 profiles were completed from R/V Knorr (cruise 94) in various locations in the northeast Atlantic (Figure 2.2). A total of 27 profiles were obtained during two cruises in the Panama Basin (Figure 3); the first was aboard R/V Columbus Iselin (cruise CI-83-13, January 1984) and the second aboard R/V Atlantis II (cruise 112 leg 23, April 1985). The Panama Basin was chosen as the major study site because of the wealth of

Figure 2.2 Location map of marine snow profiles taken on Knorr cruise 94 in 1982. Stations 1-3 are Sargasso Sea, 4-6 are Gulf Stream, and 7 and 8 are in a warm core ring.

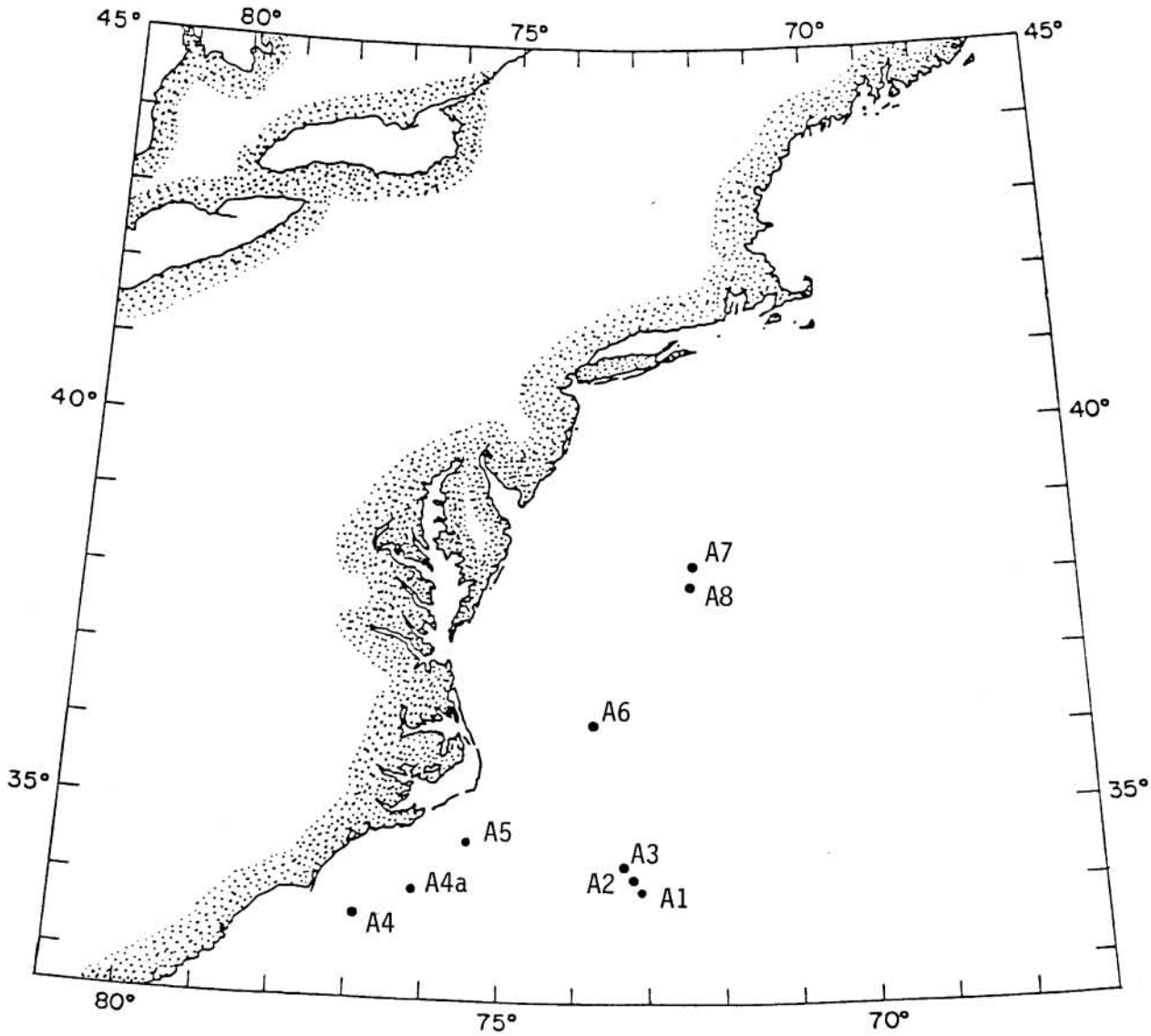
45°
80°
75°
70°
45°
40°
40°
35°
35°
80°
75°
70°
A7
A8
A6
A5
A3
A2
A1
A4a
A4

supporting data available, including several sediment trap experiments (Honjo, 1980b, 1982; Honjo et al., 1982a, b), nephelometer profiles (Gardner et al., 1984), and sediment distribution maps and models (Heath et al., 1974; Moore et al., 1973; Van Andel, 1973).

Vertical flux measurements

Sediment flux samples were collected using two consecutive deployments of PARFLUX Mk VI sediment traps at the PB site (Honjo 1982) in the Coiba Gap of the Panama Basin (fig 2.3). Each trap consists of a polyethylene cone ($0.5m^2$ opening), 13 sample receiving cups, and a timing mechanism which rotates an empty cup into position at the base of the cone at pre-selected times. Filled cups are completely sealed so that essentially no exchange between the cup contents and ambient sea water occurs between the time of cup closure and sample recovery. This allows determination of and correction for in situ decomposition by measuring the amount of particulate material in the cup and the concentration of dissolved species in the supernatant. No poisons or preservatives were used. Traps were deployed from R/V Columbus Iselin at 2 depths along a subsurface mooring. The first deployment (PB 3) lasted from January 7 to January 27, 1984 (20 days) with traps at 1930 and 3030m (sample duration 36 hours). The second deployment (PB 4) lasted from January 28 to March 24, 1984 with traps at 2430 and 3530m (sample duration 4.33 days) and was recovered from R/V Atlantis II.

In situ samples

Marine snow aggregates were collected in surface water in the Sargasso Sea and Monterey Bay using the SCUBA method of Shanks and Trent (1979). These samples were fixed immediately in glutaraldehyde and osmium

Figure 2.3 Cruise track of Columbus Iselin cruise CI-83-13. Marine snow profiles were taken at each station with major emphasis at station 1 (later re-occupied as station 17) which was also the location of the PB mooring site (Honjo 1982), several Alvin dives, and profiles E3-E5 (figure 2.12).

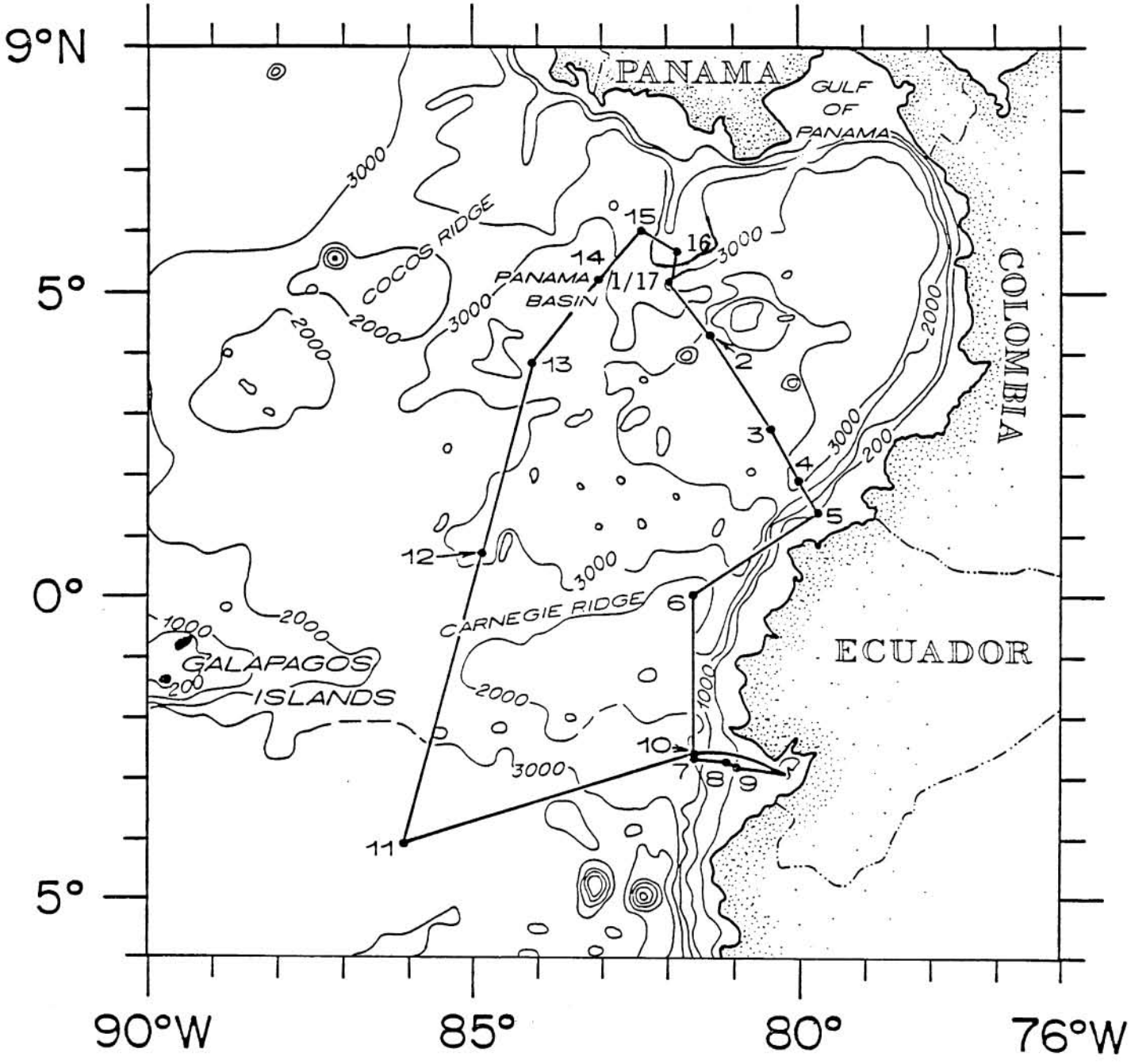
9°N
5°
0°
5°
90°W
85°
80°
76°W
PANAMA
GULF OF PANAMA
COLOMBIA
ECUADOR
COCOS RIDGE
PANAMA BASIN
CARNEGIE RIDGE
GALAPAGOS ISLANDS
3000
2000
1000
200
1/17
2
3
4
5
6
7
8
9
10
11
12
13
14
15
16

tetroxide, dehydrated in ethanol, returned to shore, and critical point dried from Freon® 13. Samples were examined and photographed using a JEOL JSM-U3 SEM.

Water samples were collected for suspended particle analysis using standard hydrocasting techniques and 30 liter Niskin^{R} bottles. Water (5-10 liters) was filtered through pre-weighed Nuclepore® filters which were air-dried and re-weighed to obtain sample weights. Large volume filtration system (LVFS) suspended particle samples were acquired using the in situ pumping method of Bacon and Anderson (1982). Pumps were suspended at 6 depths where 250 gallons (950 liters) of water were filtered through a pre-weighed filter.

RESULTS AND DISCUSSION

Microscopic observation

SEM photographs of surface collected aggregate contents are shown in Figures 2.4a-c. Material found on these aggregates is typical of what may be collected by conventional hydrocasting methods in surface waters. Considerable variability is observed in the particles. Some aggregates were apparently free of bacteria while others contained numerous bacteria. Fecal pellets associated with the aggregates were generally well preserved with intact membranes. Masses of mucoid material appear as webs of fibers in the SEM and are present in all aggregates but were more apparent in critical point dried samples than in air-dried material. Intact diatom chains and colonies were the most common component and appeared to be the source of some of the mucous.

In situ images

Examples of images produced by the photographic system taken at 500m from profiles PBMS17 and PBMS15 appear in Figures 2.5a and 2.5b respectively. Aggregates such as these have appeared in every photograph taken to date, including all depths in the Sargasso Sea. Abundances have ranged from one or two aggregates in 120 liters (0.01 liter^{-1}) to occasionally more than 1000 (8 liter^{-1}). However at concentrations greater than about 600 per photograph (~5 liter^{-1} or ~80 mm^{3}liter^{-3}) accuracy is compromised due to overlapping of images. Because of the relatively small size and large numbers of the aggregates in the images, an objective digitizing technique is mandatory in order to obtain reliable results.

Figure 2.4 Scanning electron microscope (SEM) micrographs of critical point dried marine snow which was hand collected in Monterey Bay. a) Overview of aggregate showing numerous centric diatoms embedded in a mucous matrix (scale bar is 50 μm). b) enlargement of diatoms indicates that they may be producing the mucous web (scale bar is 5μm). c) Well preserved diatom chain found attached to aggregate (scale bar is 20 μm). d) Fecal pellets associated with aggregates often contain intact membranes. This pellet contains small diatom fragments (scale bar is 50 μm).

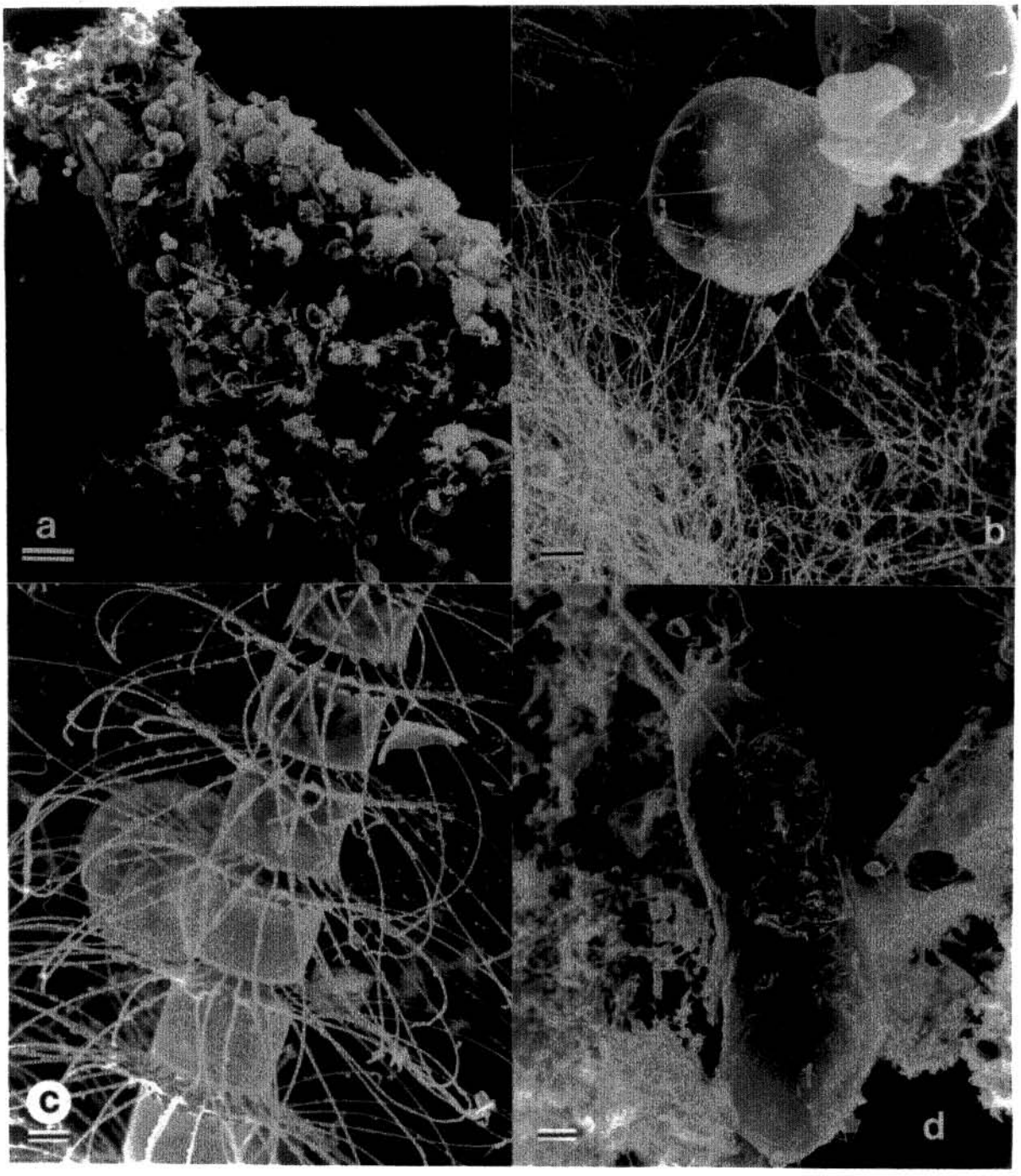
a
b
c
d

Figure 2.5 Photographs of marine snow aggregates at 500m taken by the photographic system in the Panama Basin. a) Photograph from profile PBMS17; estimated abundance = 12 aggregates liter^{-1}. b) photograph from profile PBMS15; estimated abundance = 50 aggregates liter^{-1}. Clearly an objective digitizing process is required to count the particles because of their small size and large numbers. Scale bar is 5 cm; volume of water included in this photograph is 210 liters. The dark vertical streak is caused by the gap between lenses and indicates that the illumination is well collimated. Variation in exposure from top to bottom is caused by absorbtion and scattering of light and is compensated for electronically during analysis.

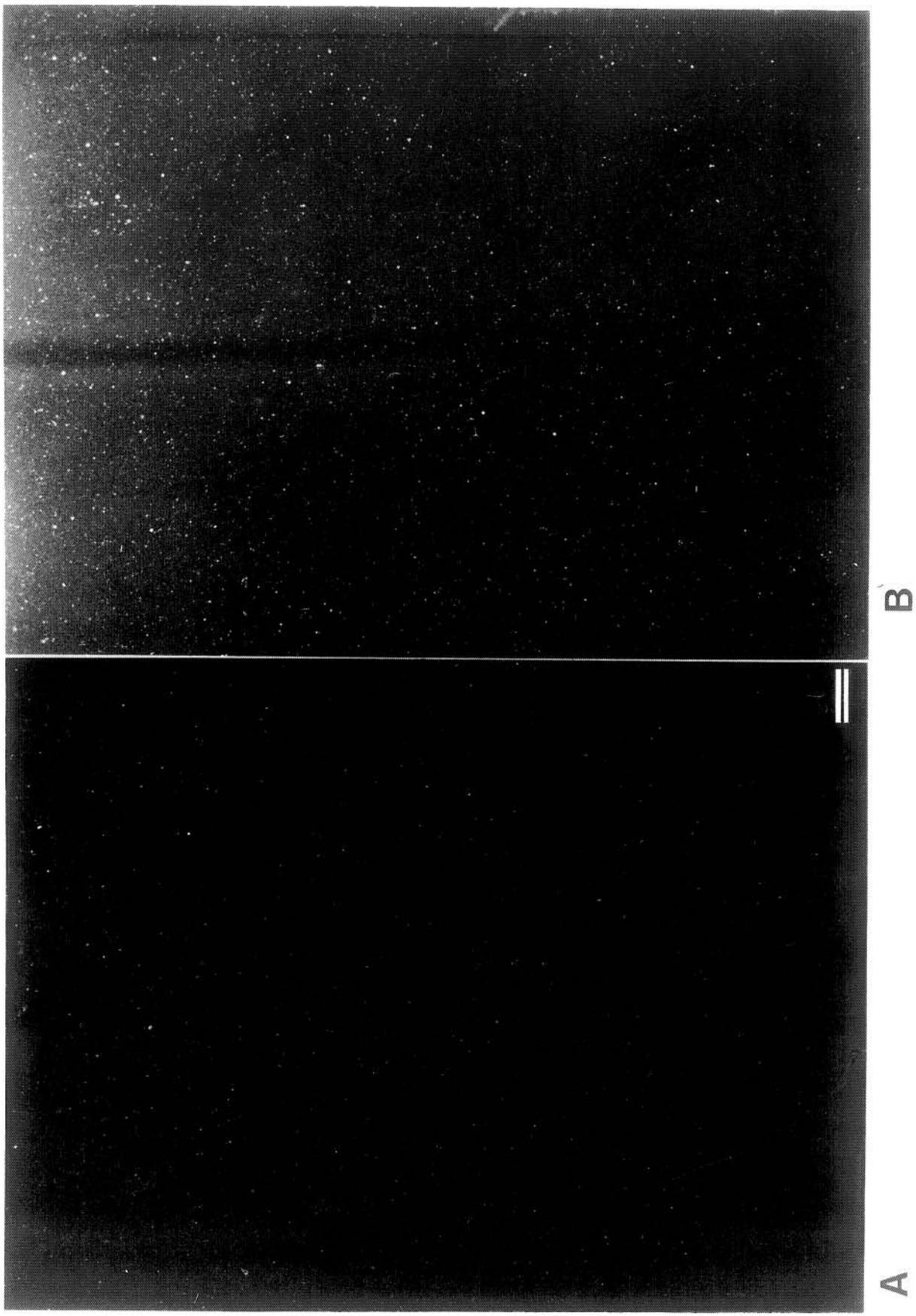
A
B

Marine snow abundance profiles

Short wavelength variability

Unprocessed concentration numbers (# of aggregates liter^{-1}) are plotted against depth for a profile in the Panama Basin in figure 2.6a. Superimposed on the large scale trend is a low amplitude, short (ca. 100m) wavelength variability indicating patchiness similar to that observed in nephelometer profiles by Gardner (1984). Small scale patchiness (scatter in the data points) resulting from the relatively low abundance of these large aggregates (Eppley et al. 1983, Knauer et al. 1982) is also observed in depth profiles of suspended matter produced by Niskin bottle samples (fig. 2.7). These relatively small volume samples show considerable scatter relative to in situ pump (LVFS) samples, which average concentrations over much larger volumes (up to 1000 liters). It should be emphasized that only broad generalizations are appropriate when comparing hydrocasting results with those of the new photographic technique. The former technique collects particles as small as the filter pore size (as small as 1μm) while only particles larger than 1mm are counted by the marine snow camera.

To remove some of the high frequency variability, a nine-point running mean filter was passed over all data. In addition, numbers of aggregates in each size class (1mm-2.5mm, 2.5mm-4mm, 4mm-5mm, >5mm) were converted into volume estimates using the arithmetic mean diameter for the size class and assuming spherical particles. For example, the volume of each aggregate in the 1mm-2.5mm size class ($V_{1.75}=4*]*(1.75)^3/3$ mm^3) was assumed to be 2.81mm^3. Total volume (V_t) of aggregates is the sum of volume in each class:

Figure 2.6 Profiles of marine snow abundance in the Panama Basin. a) Unprocessed concentration profile (number of aggregates larger than 1mm liter^{-1}) containing considerable scatter due to small scale patchiness. b) Same profile as (a), except that a nine point running mean filter has been passed over the data and abundance numbers have been converted to volume concentrations (mm^3 liter^{-1}).

Panama Basin #14

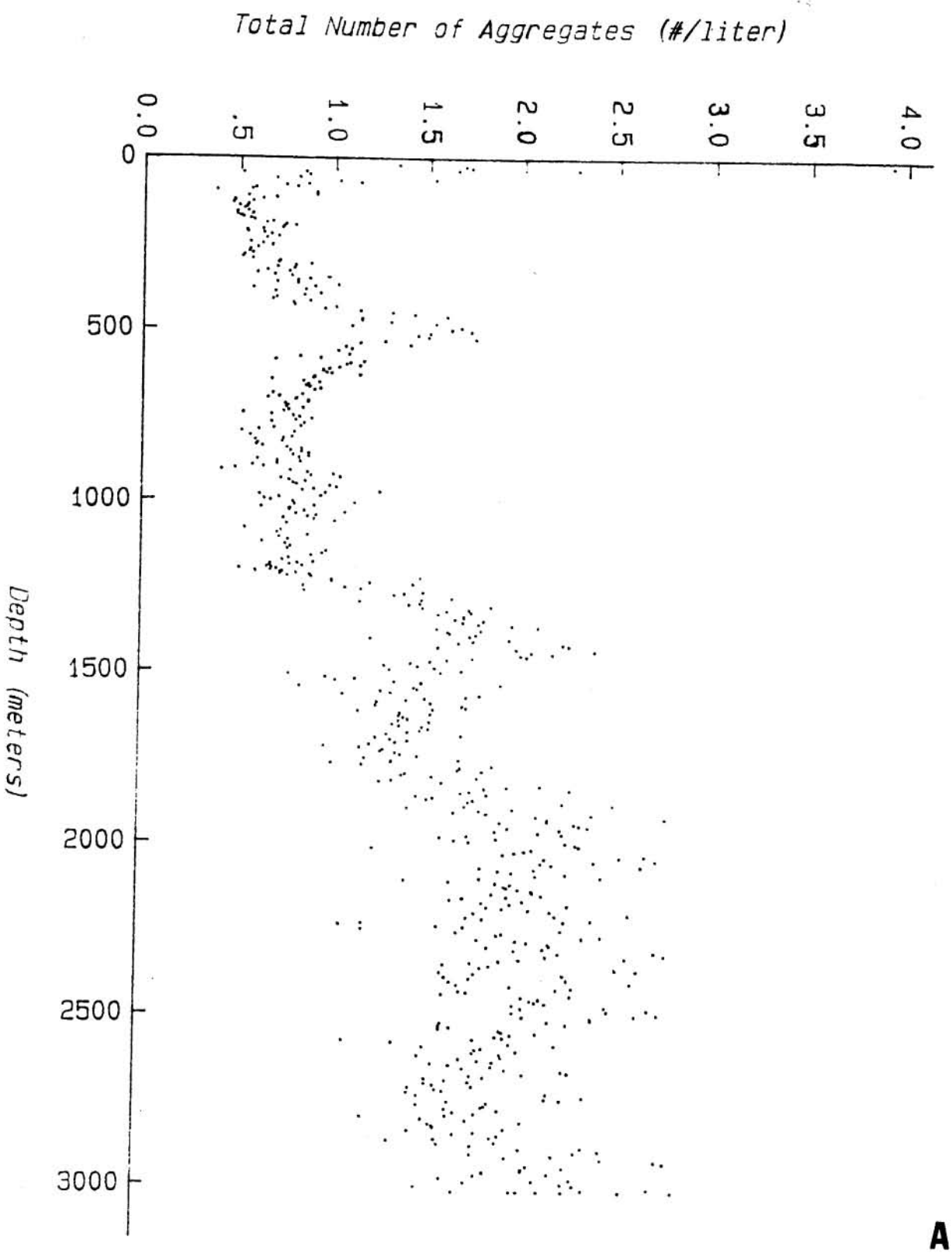

A

Panama Basin #14

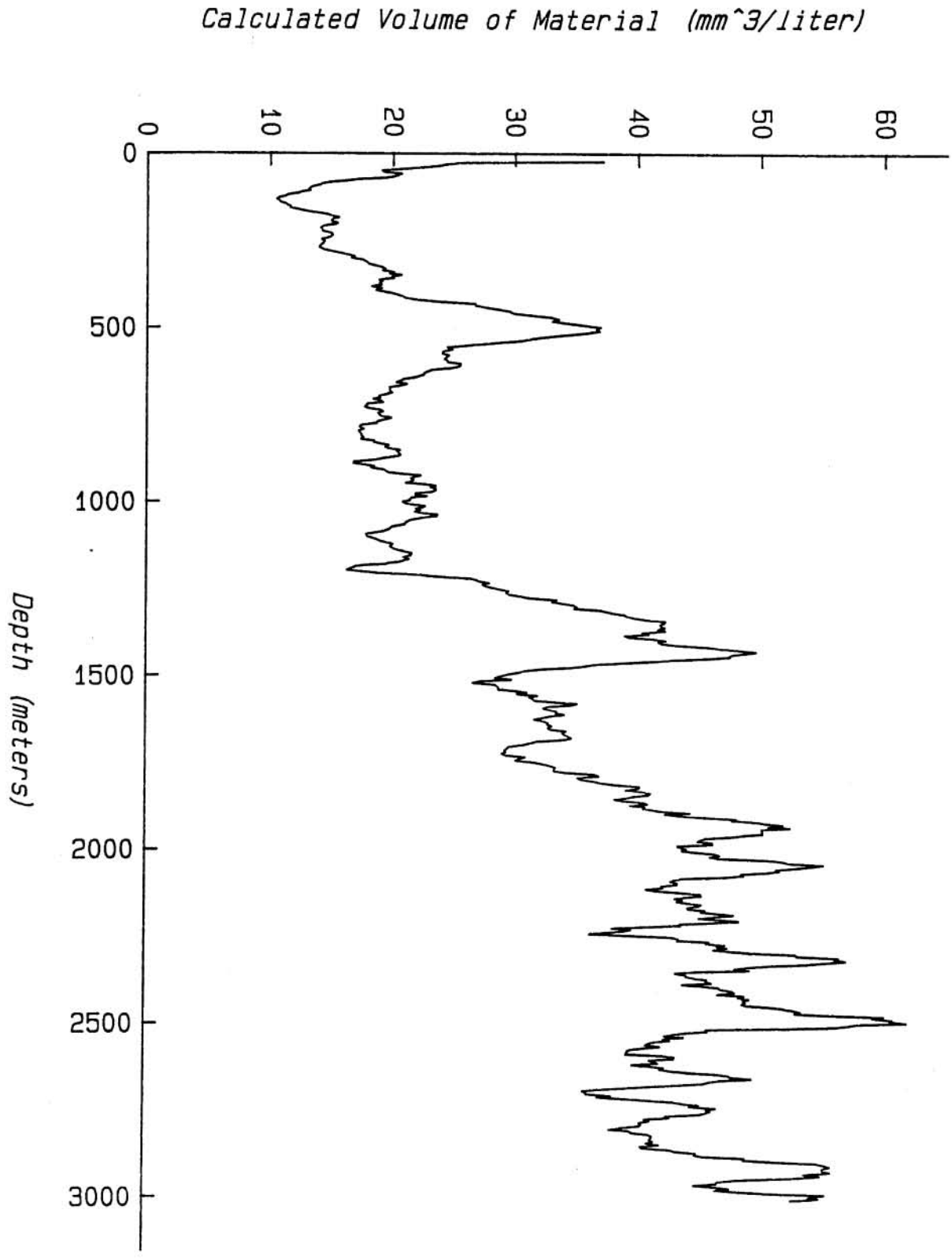

B

Figure 2.7 Vertical profile of suspended matter concentration taken from hydrocasts of 2-10 liter Niskin bottle samples (*) and 200-300 gallon in situ pump samples (o). Patchiness in the distribution of aggregates (and possible analytic error) causes scatter in the smaller bottle samples, but is reduced in the large volume pump samples.

Panama Basin Station 17

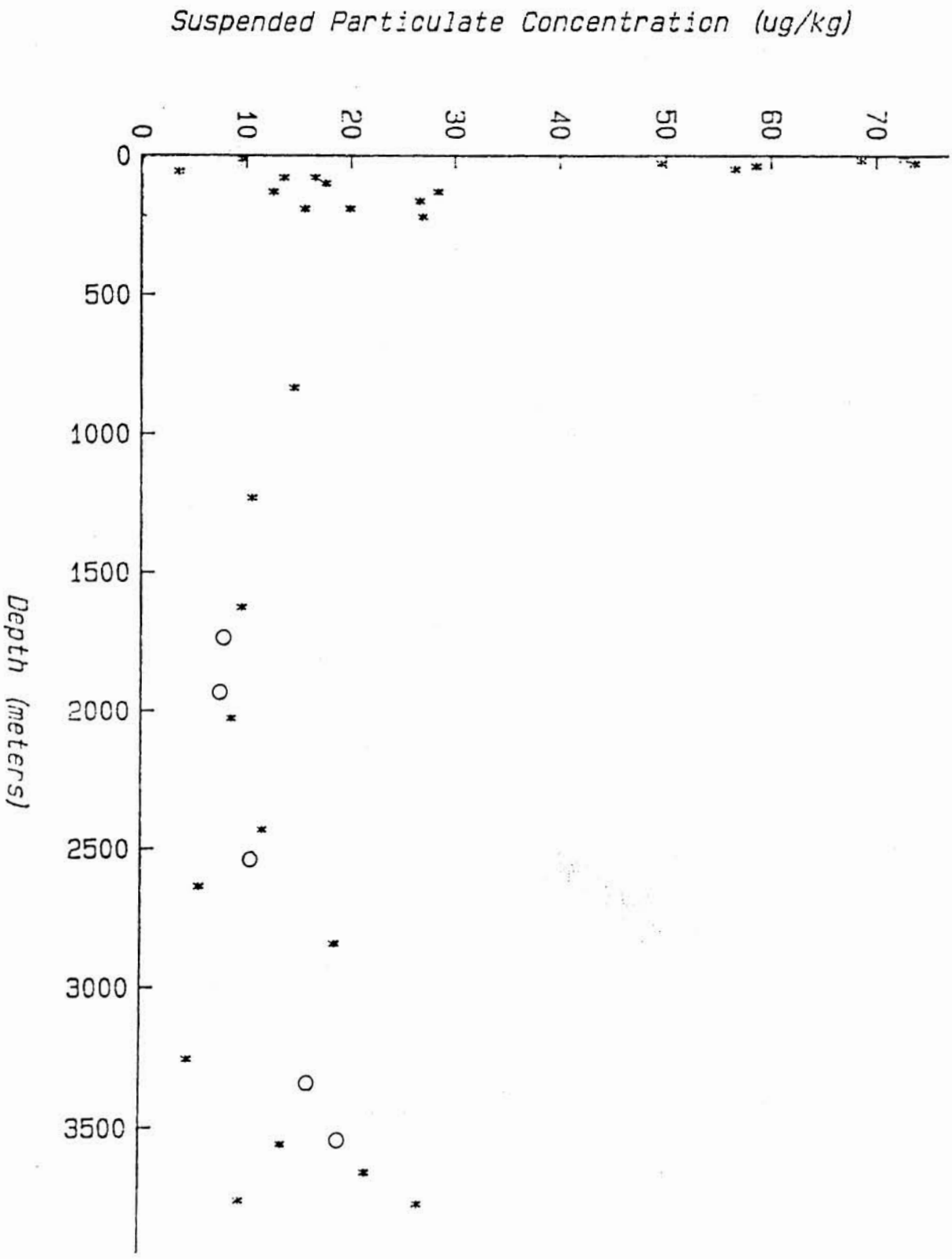

$$V_t = \sum_{n=1}^{4} N_n V_n$$

where N_n is the number of aggregates in size class n. These estimates give the most useful representations of the data when relating them to other measurements. Figure 2.6b shows the same profile as 2.6a except that the data have been converted to volume estimates and smoothed with the running mean filter.

Long wavelength signal

A variety of shapes are apparent in the depth/abundance profiles (figures 2.8-11). While surface concentrations are generally high (30-100 ml liter^{-1}), midwater abundances may remain constant (fig. 2.8d), decrease (fig. 2.10d), or increase (fig. 2.8b) with depth. They may also show maximum abundances just above the sea floor (fig. 2.10c), in midwater (fig. 2.10a), or contain some combination of several of these characteristics. (fig. 2.8a). Abundances were generally higher near continental margins in the Panama Basin and Gulf Stream areas than in the more oligotrophic Sargasso Sea.

The overall shape of a marine snow volume/depth profile is related to the balance of input and removal of aggregates. Marine snow aggregates found in the water column appear to arise from at least three sources: direct biologically mediated formation in the water column, resuspension from the sea floor at the site of the profile, and transportation from resuspension sites at the ocean margins. Most profiles show high abundances in surface water due to recent production by phyto- and zooplankton. As mentioned above, however, values above 100m should be

Figure 2.8 Transect of marine snow abundance profiles taken in the Panama Basin. All profiles show input of material from the surface. a) Profile 15 was taken near the shelf break and shows a sharp sub-surface minimum underlain by midwater and deep concentration maxima. b) Profile 14, taken further offshore, shows the same pattern as in profile 15 except that in this case the numbers are generally lower. c) Still further from the margin, profile 13 shows only relatively small amounts of resuspended material adjacent to the sea floor. d) Profile 12 is far enough from the margin to show no evidence of midwater maxima, and insignificant direct resuspension.

Panama Basin #15

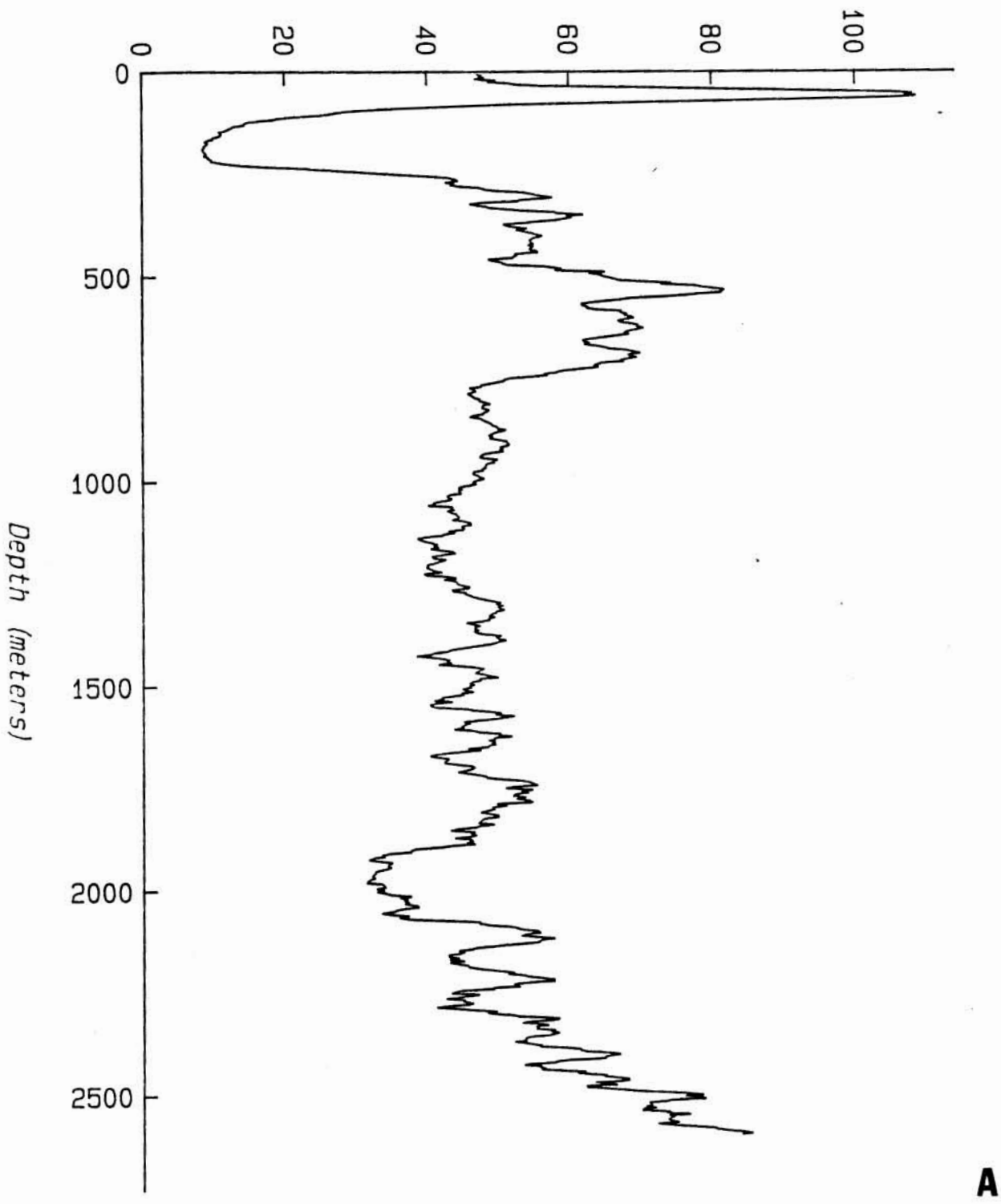

A

Panama Basin #14

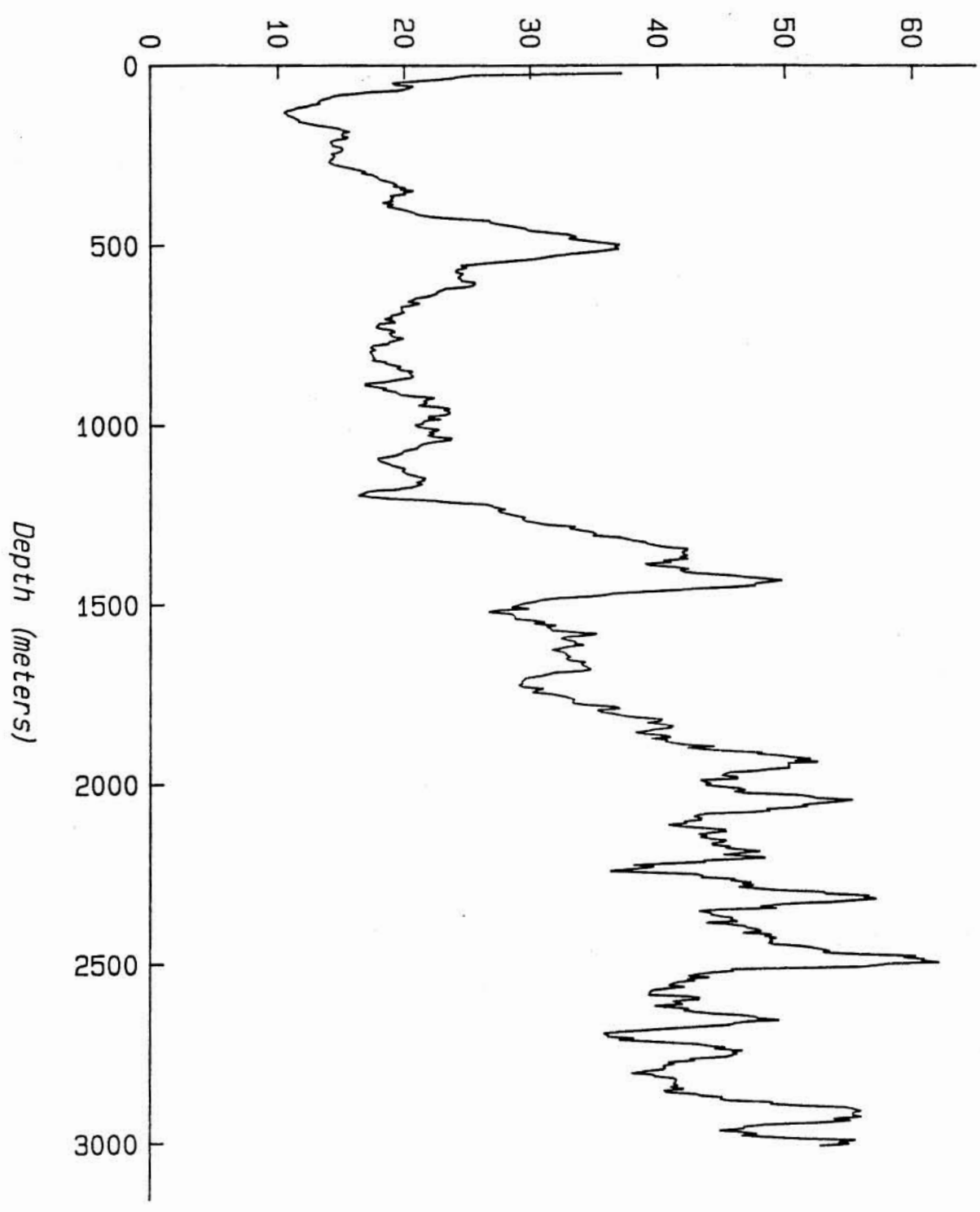

B

Panama Basin #13

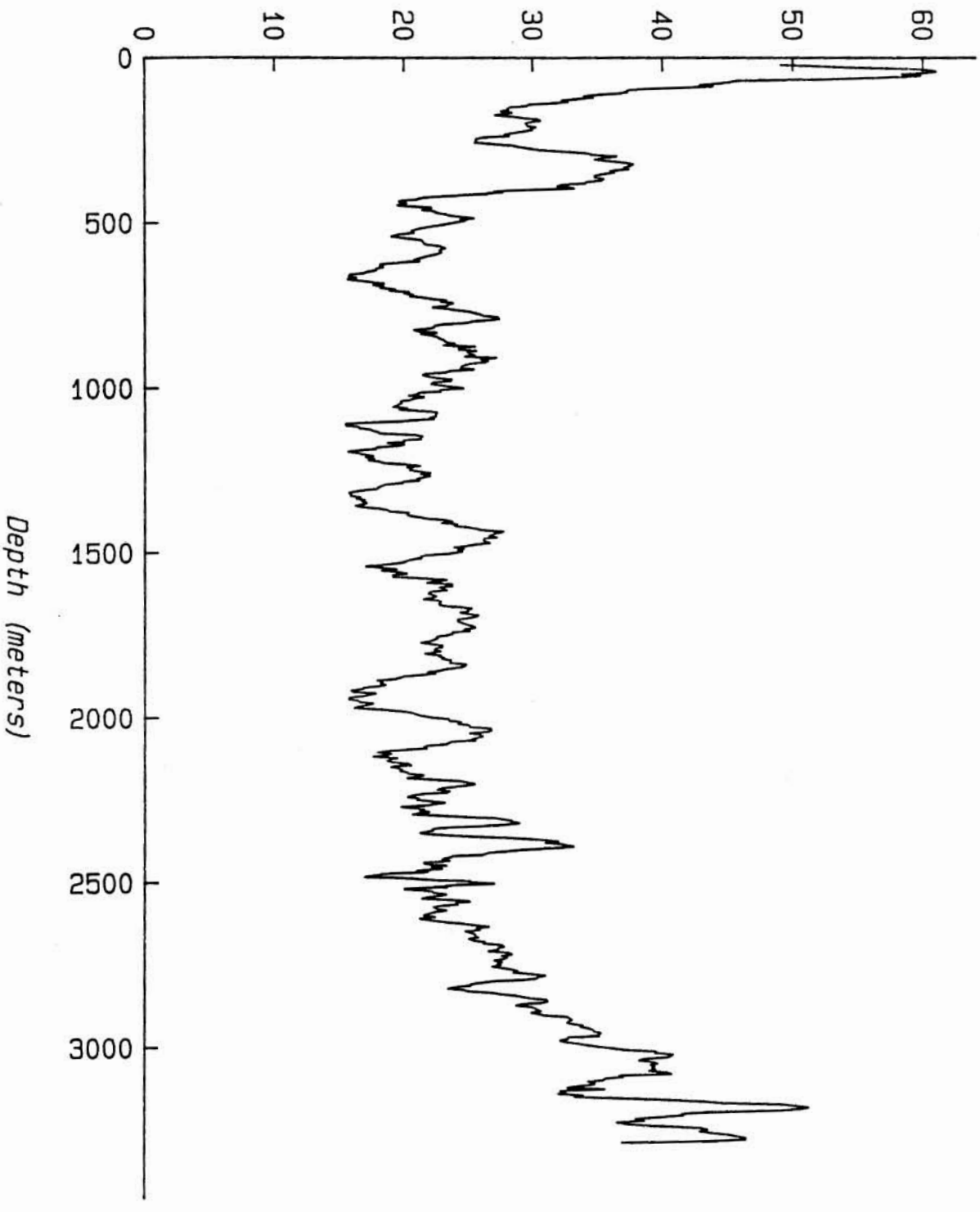

C

Panama Basin #12

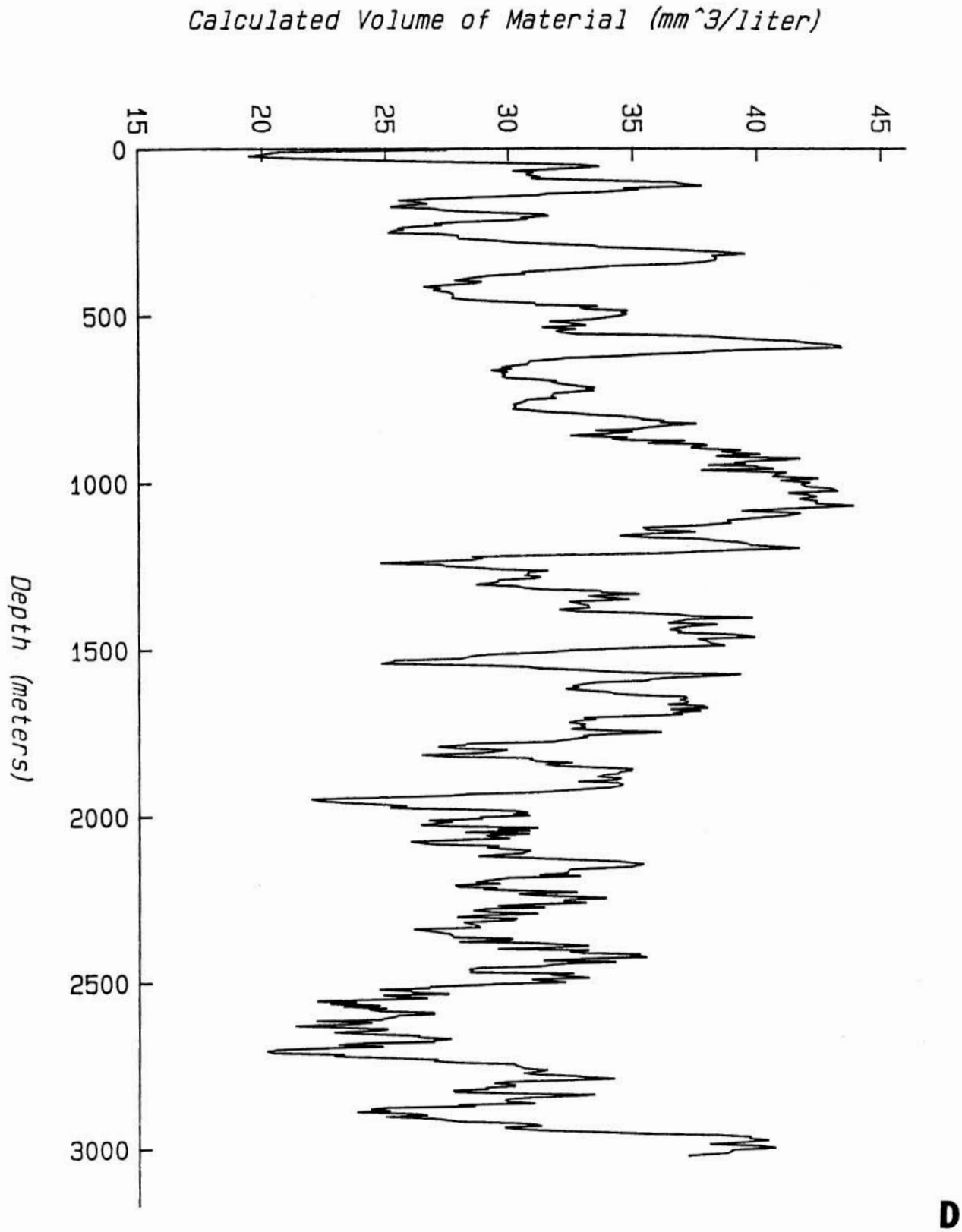

D

Figure 2.9 Two profiles of marine snow abundance taken offshore from Guyaquil Ecuador (see fig. 2.3). a) Profile PBMS7, taken just offshore from the shelf break, containing several midwater concentration maxima. b) Profile PBMS11, taken 400 km offshore, shows generally lower numbers, less pronounced midwater maxima, but significant near-bottom resuspension.

Panama Basin #7

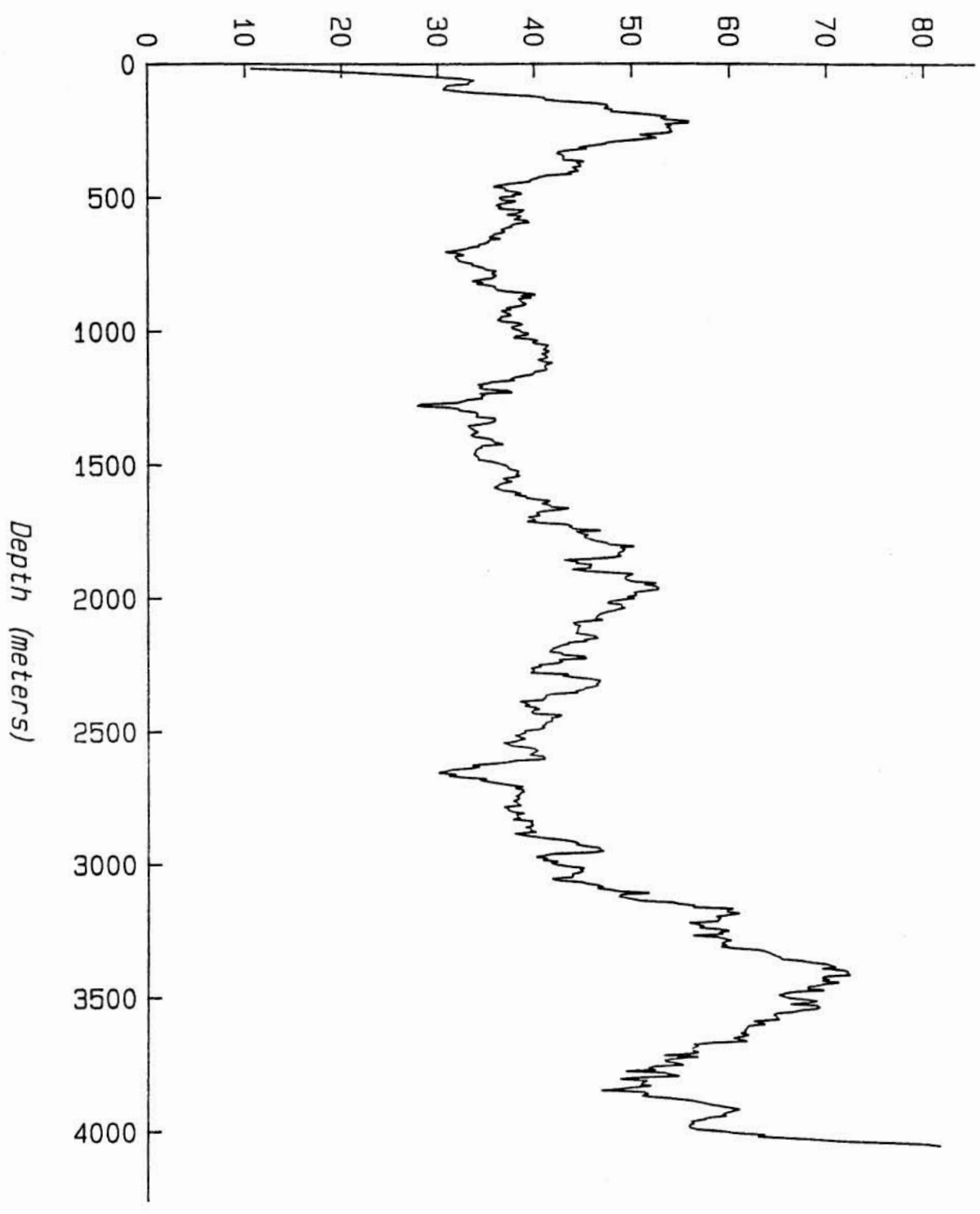

A

Panama Basin #11

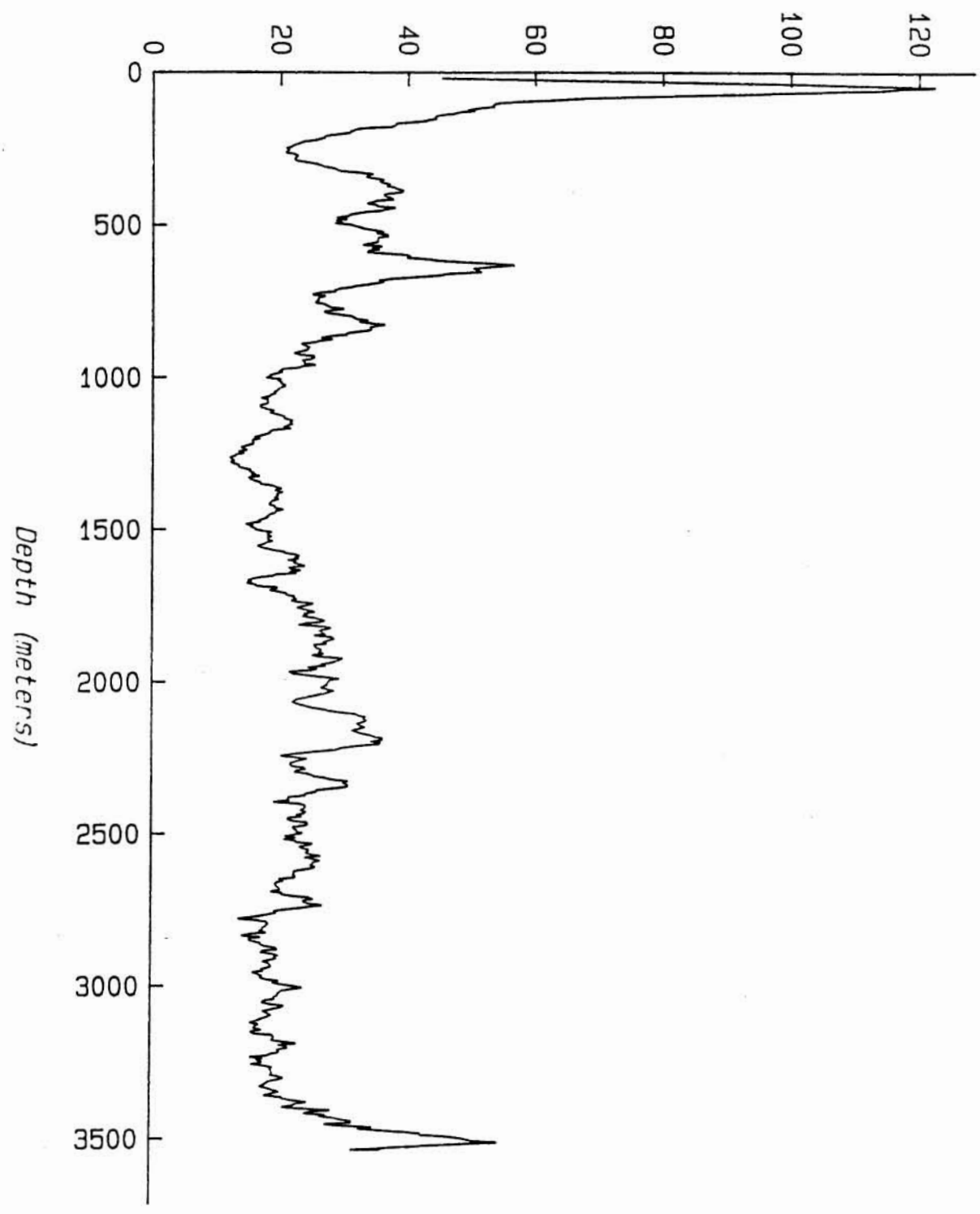

B

Figure 2.10 Profiles of marine snow abundance taken in the western North Atlantic. a) Profile A-5 show that considerable material is resuspended as the Gulf Stream impinges on the shelf and slope. b) Downstream, profile A-6 shows that much of this material is transported by the current; notice the scale change from a). c) This material remains in warm core ring #82B, as evidenced by the peak in abundance at 700 meters. Notice also the resuspension occurring at the sea floor. d) At station A-3 in the Sargasso Sea, biogenic production in the euphotic zone is the only source of material.

Atlantic #A-5

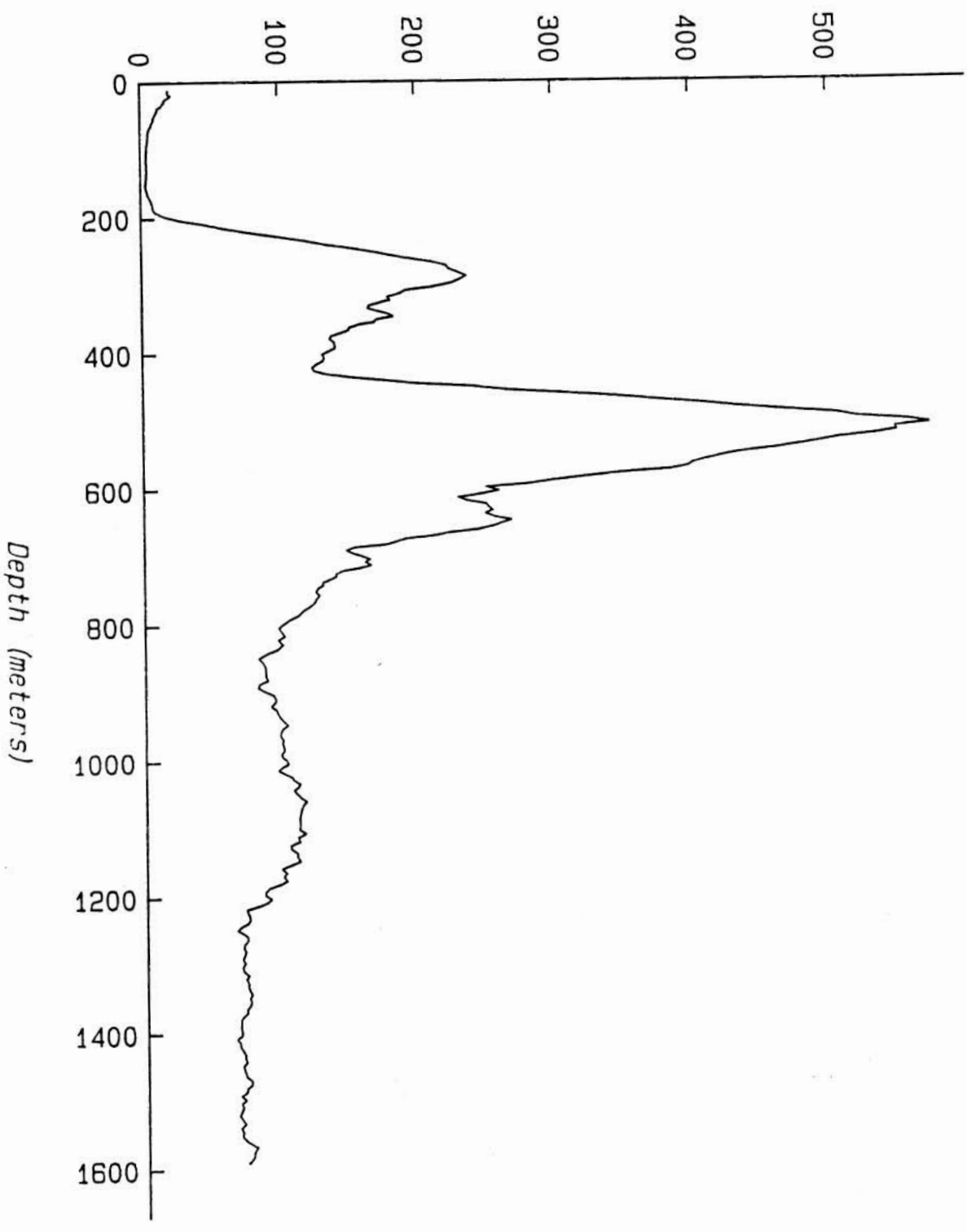

A

Atlantic #A-6

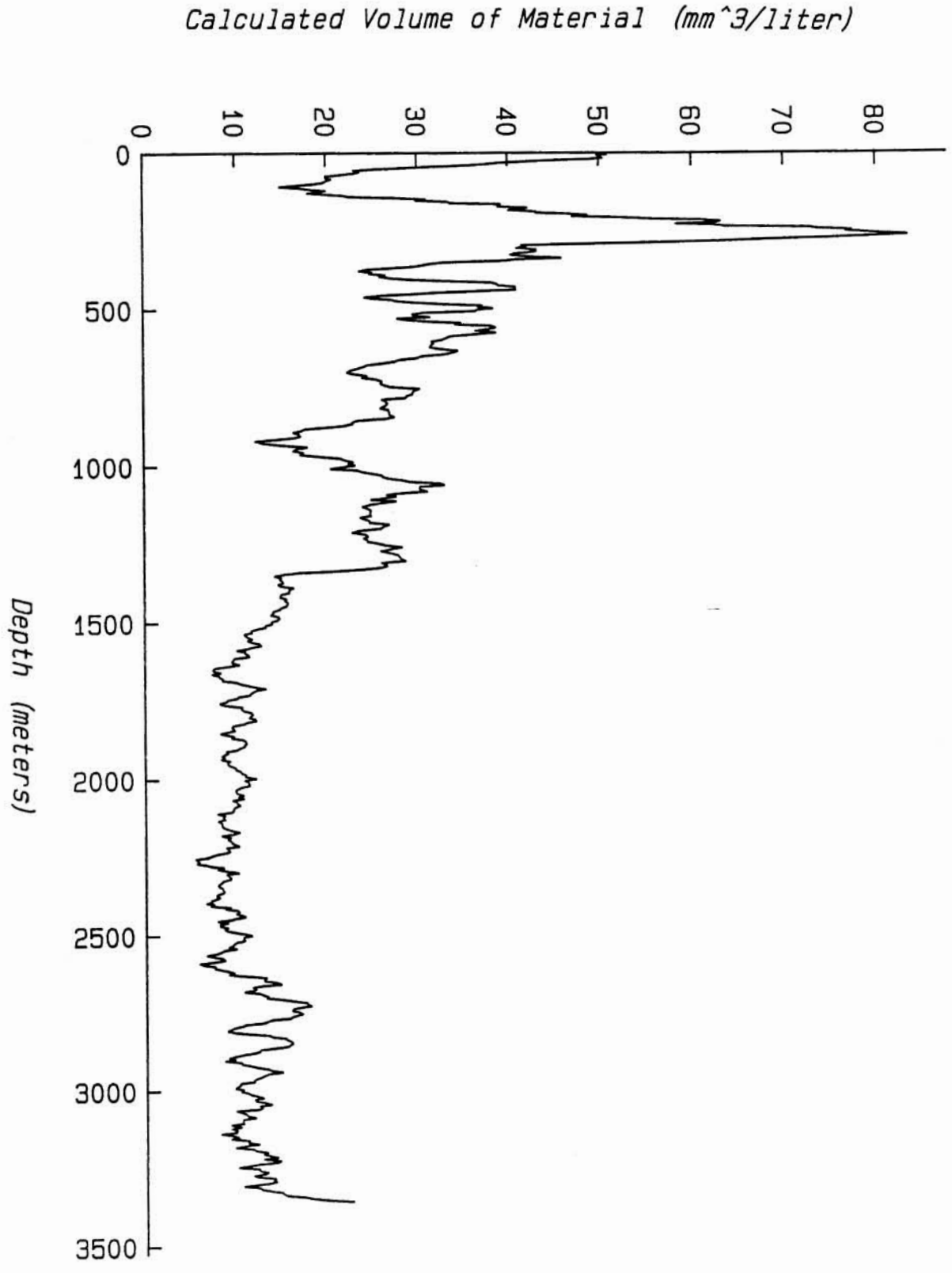

B

Atlantic #A-7

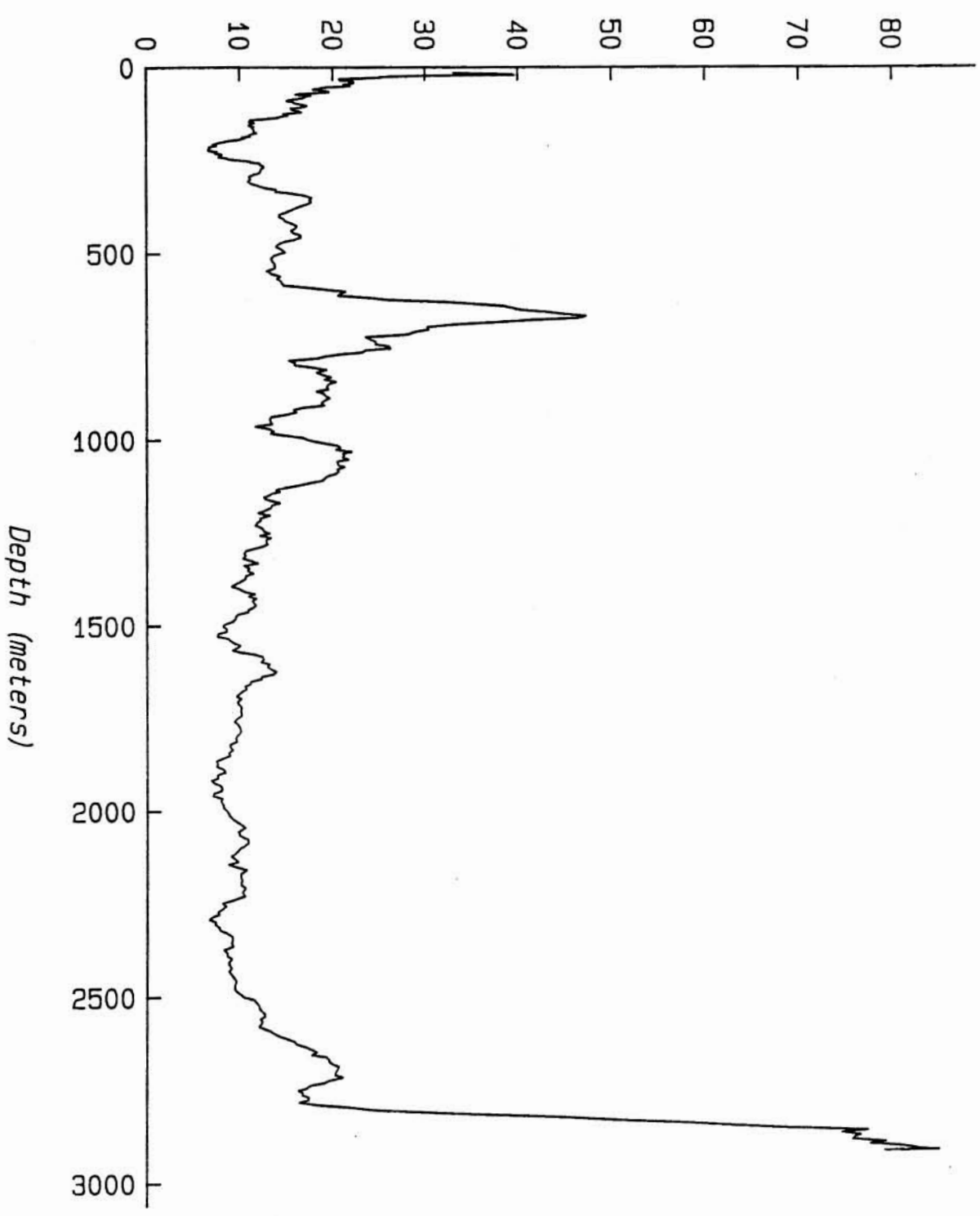

C

Atlantic #A-3

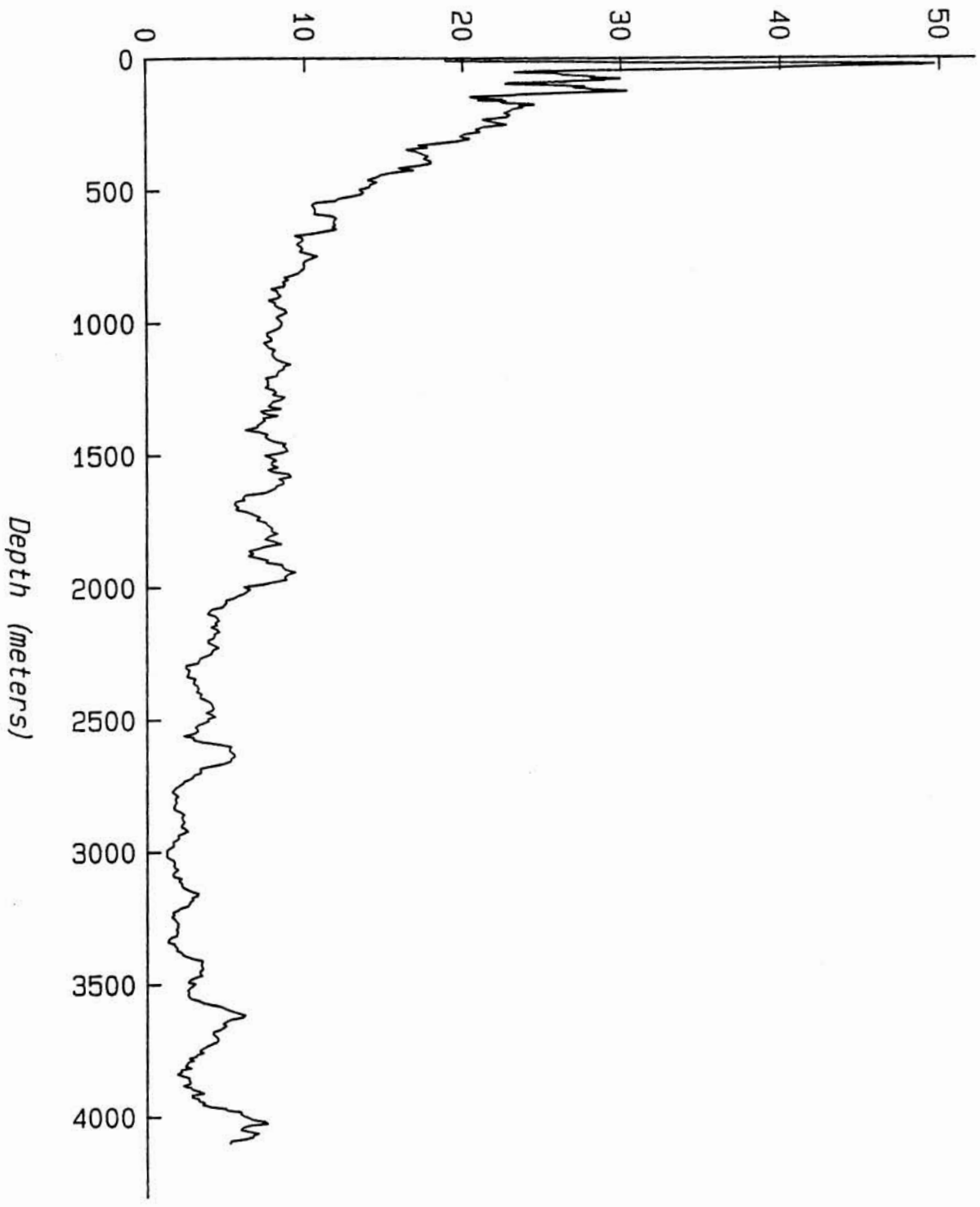

D

accepted with caution. Below the euphotic zone, most profiles show a decrease in number with depth to some minimum value. This mid-water minimum may be followed by an increase (to values often higher than surface values) near the sea floor, indicating resuspension. In several nearshore profiles, a midwater source is evidenced by a peak in abundance which occurs above the sea floor. In fact, some profiles show a shallow minimum followed by a continuous depthwise increase, indicating a combination of midwater and direct resuspension sources. Profiles taken near ocean margins tend to show greater influence of deep sources and therefore larger increases in aggregate abundance with depth.

Figures 2.8a-d show profiles taken along a transect from the Coiba Ridge southwest into the Panama Basin which illustrate the concept of multiple sources. Profile PBMS15 (fig. 2.8a) shows particularly significant deep sources of suspended aggregates with the large peaks in concentration at 500m and the sea floor. Farther offshore, profile PBMS14 (fig. 2.8b) contains generally lower abundances and only a small peak occurs at 500m. A more significant maximum appears at 1400m with continuing increase to the sea floor. This profile shape changes considerably at station PBMS13, which shows an increase only within 700m of the bottom and by station PBMS12 the entire profile shows decreasing abundances with increasing depth (surface source only). A similar onshore transect (figs. 2.9a,b, stations PBMS7 and PBMS11) shows the same pattern with abundances increasing with depth near the ocean margin but decreasing with depth offshore. Similar transport patterns also exist in the Atlantic data (figs. 2.10a-c) as seen in profiles A5 (shallow water Gulf Stream), A6

Figure 2.11 Machine produced contour plots of marine snow volume concentrations (abundance, $mm^3 liter^{-1}$). a) Stations A4-A7 in the Atlantic Ocean indicate horizontal transport of material resuspended from the shelf by the Gulf Stream. b) Stations PBMS15-PBMS12 in the Panama Basin. Several midwater sources of horizontally transported material are evident. c) Stations PBMS1-PBMS5 in the Panama Basin. In this case, the inferred current direction is into the page (to the north) so that little transport of material occurs in the East-West direction.

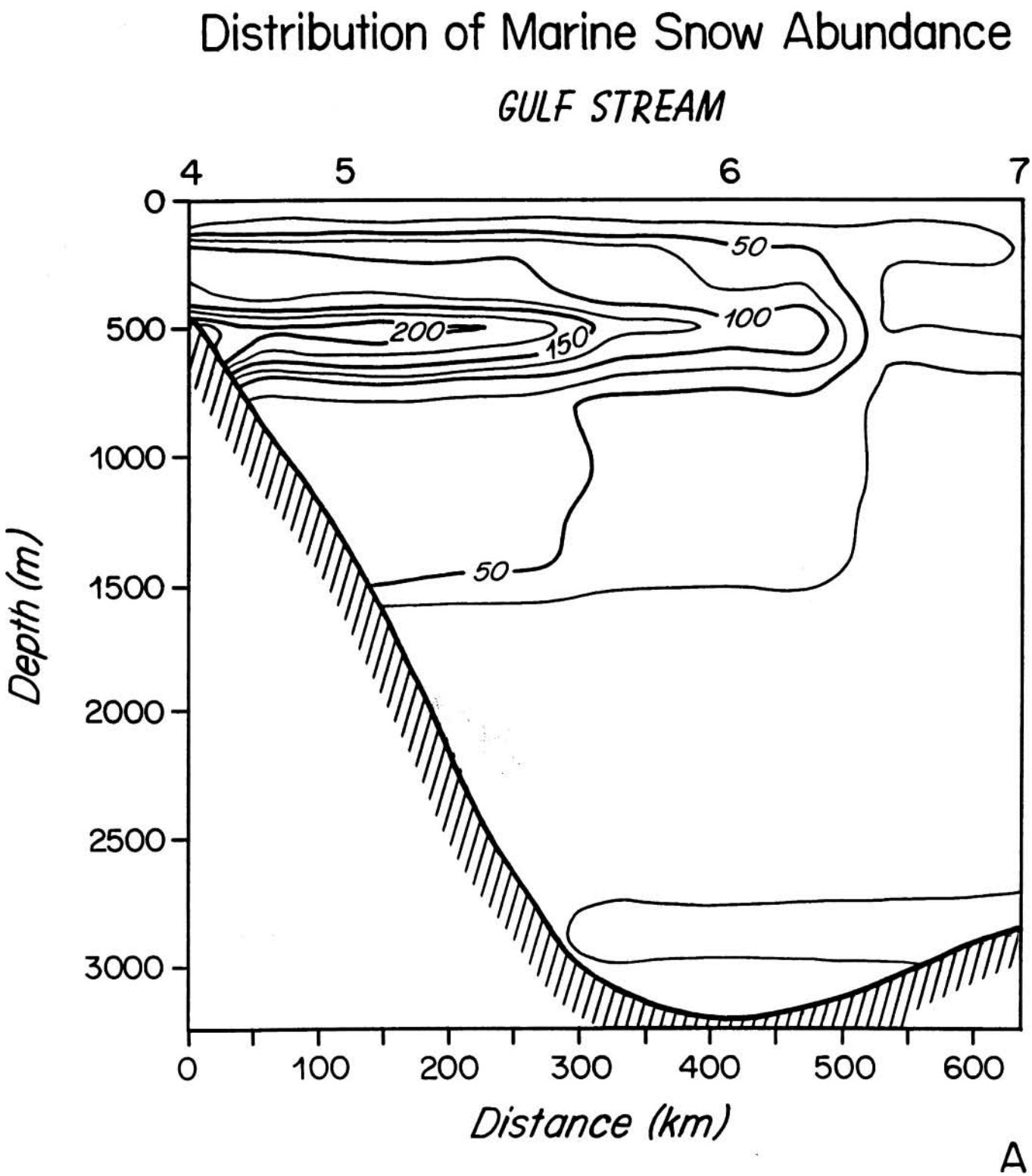
Distribution of Marine Snow Abundance
GULF STREAM
4
5
6
7
0
500
1000
1500
2000
2500
3000
50
100
200
150
50
Depth (m)
0
100
200
300
400
500
600
Distance (km)
A

Distribution of Marine Snow Abundance

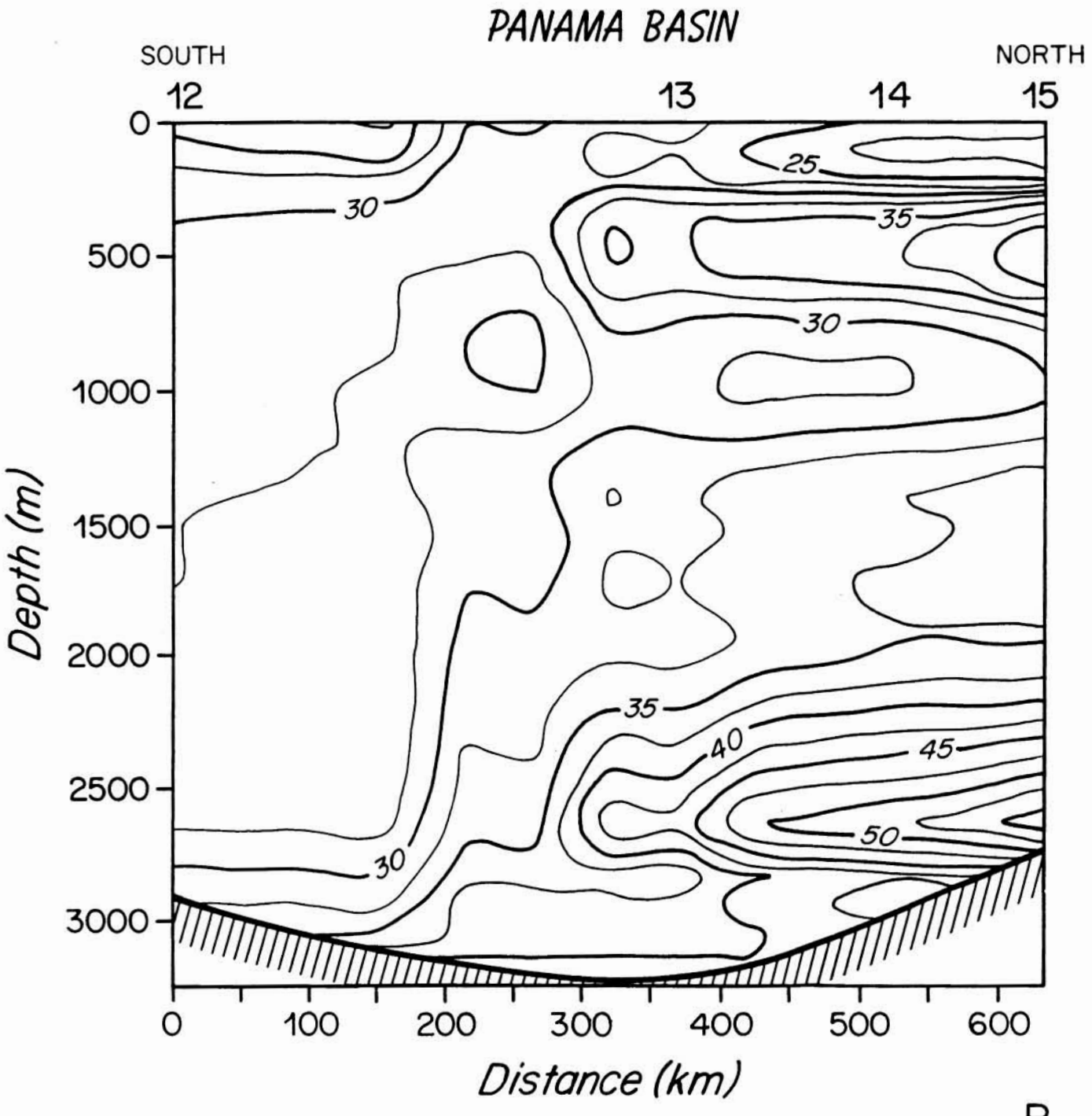

B

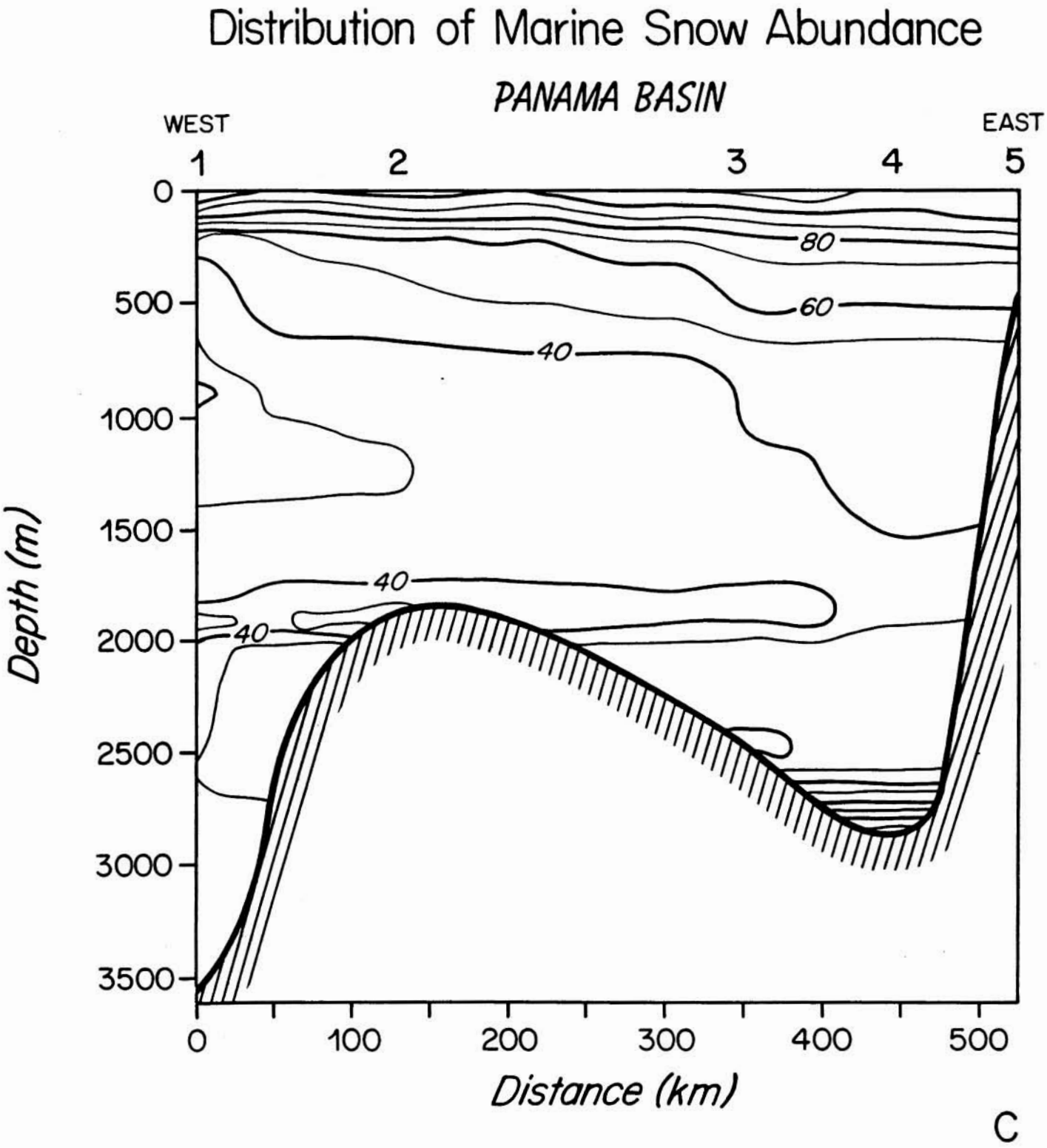
Distribution of Marine Snow Abundance
PANAMA BASIN
WEST
EAST
1
2
3
4
5
0
500
1000
1500
2000
2500
3000
3500
80
60
40
40
40
Depth (m)
0
100
200
300
400
500
Distance (km)
C

(deep water Gulf Stream), and A3 ("blue water" Sargasso Sea). In this case, the Gulf Stream resuspends material and transports it many kilometers downstream. A profile (fig. 9d) taken in a warm core ring 500 km from the source still contains evidence of resuspended material.

Distribution Patterns

Horizontal transport of marine snow is emphasized in contour plots of aggregate volume concentrations. Figure 2.11 shows machine produced contour plots for the profiles depicted on the location maps (figs. 2.2 and 2.3). Material suspended by the Gulf Stream (fig 2.11a) as it impinges on the continental shelf and slope, is clearly evident more than 400 km downstream. During this transit, insignificant settling has occurred, indicating that these resuspended aggregates sink slowly.

A contour plot of the Panama Basin profiles (fig. 2.11b) shows multiple midwater sources of aggregates. One source is located at ca. 500m below the surface and another, even larger source is located near the bottom. Material from both sources is carried by the inferred flow more than 300 km from the injection sites with little apparent sinking. These midwater concentration maxima correspond well with particle concentration maxima reported by Plank et al. (1973) along a similar sampling line. A similar contour plot (fig. 2.11c) taken normal to the inferred flow in the eastern Panama Basin indicates local resuspension; horizontal transport of the resuspended material would be into the page (to the north).

Temporal Variability

Profiles produced at the PB site (Honjo 1982) at intervals of 5 hours, one week, one month, and one year, indicate temporal stability of the processes which combine to produce the major features of these profiles. Profile E-5 (fig. 2.12e) was conducted as soon as possible after E-4 (fig.

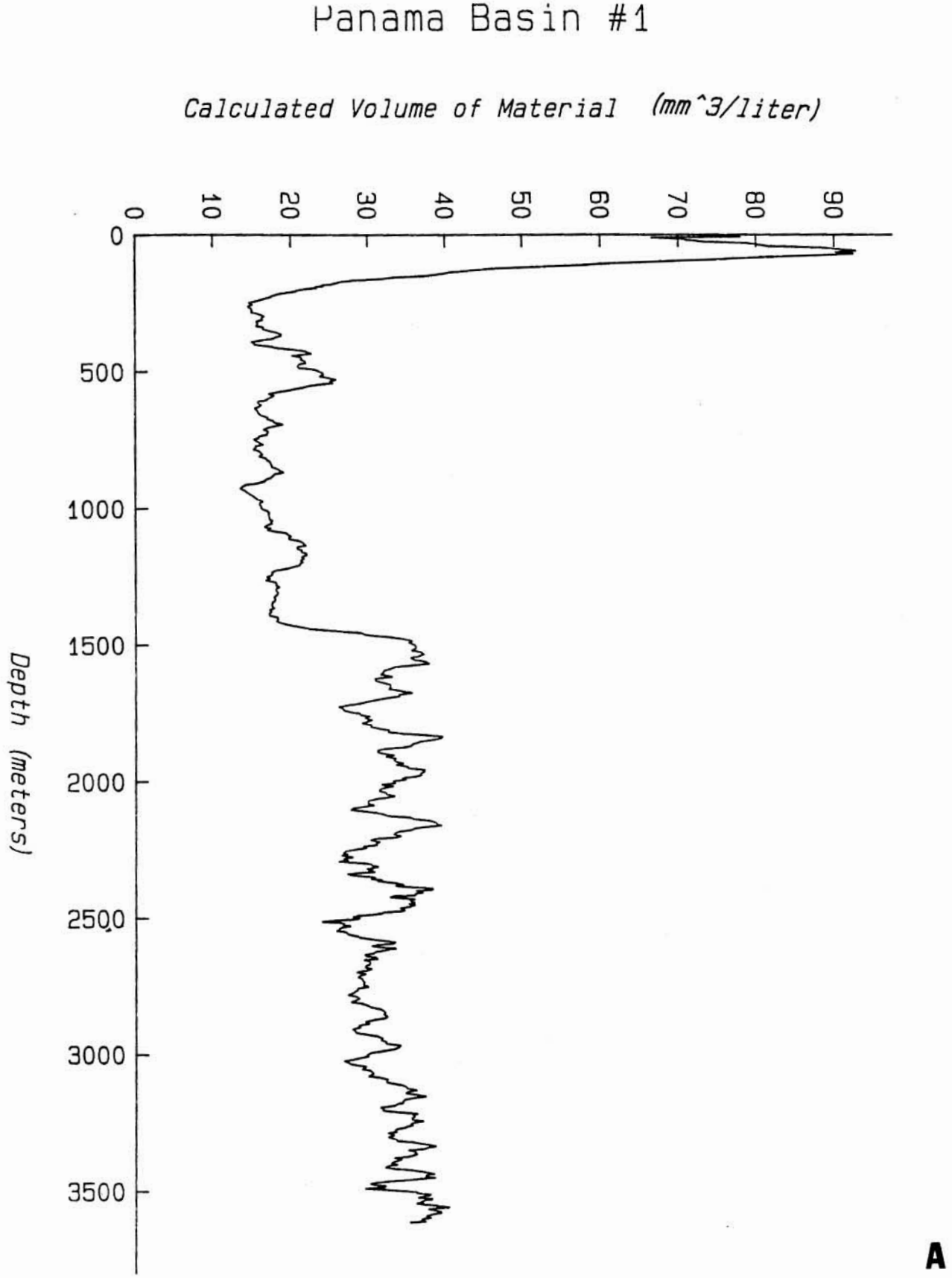
Panama Basin #1
Calculated Volume of Material (mm^3/liter)
0
10
20
30
40
50
60
70
80
90
0
500
1000
1500
2000
2500
3000
3500
Depth (meters)
A

Panama Basin #17

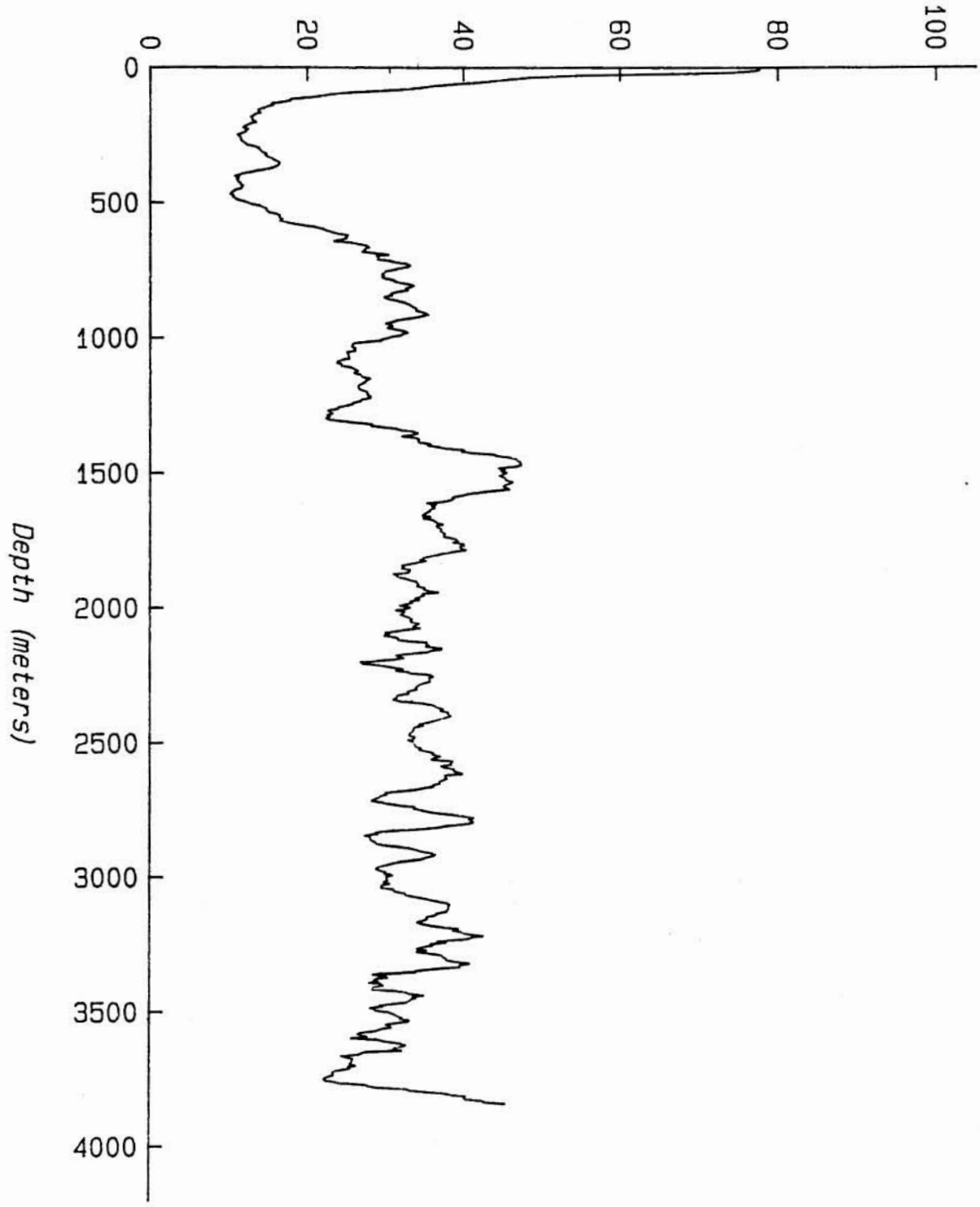

B

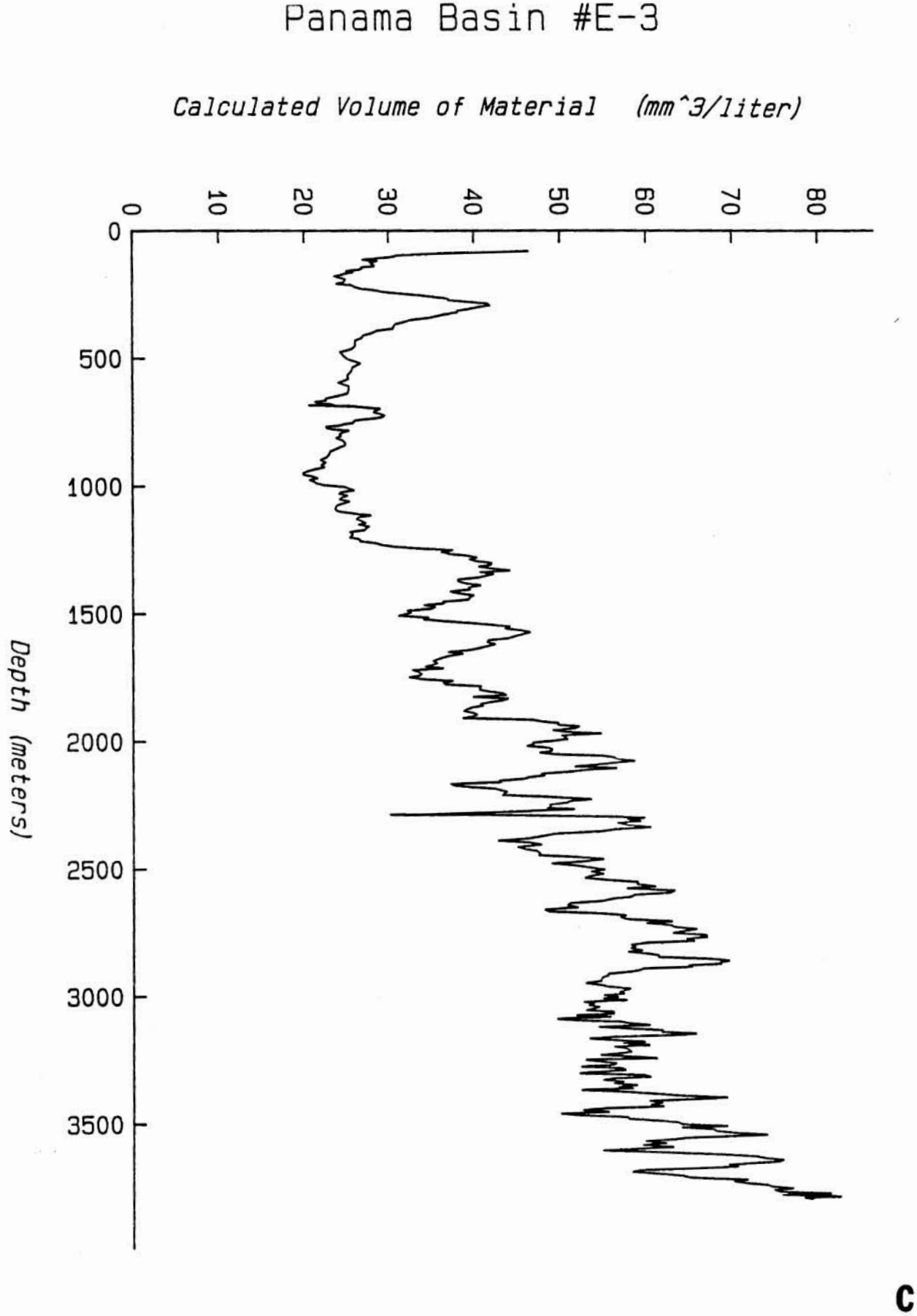
Panama Basin #E-3
Calculated Volume of Material (mm^3/liter)
0
10
20
30
40
50
60
70
80
0
500
1000
1500
2000
2500
3000
3500
Depth (meters)

C

Panama Basin #E-4

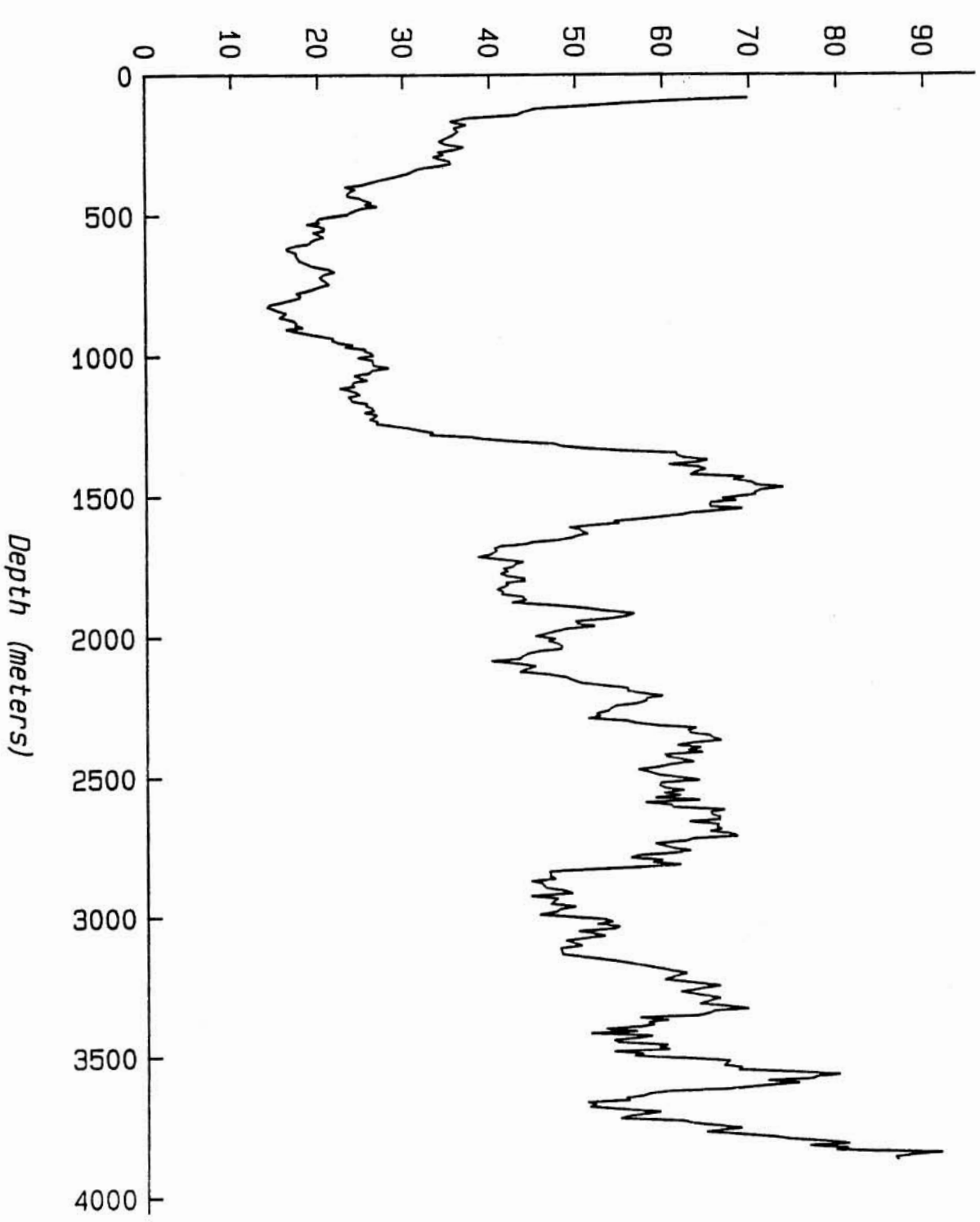

D

Panama Basin #E-5

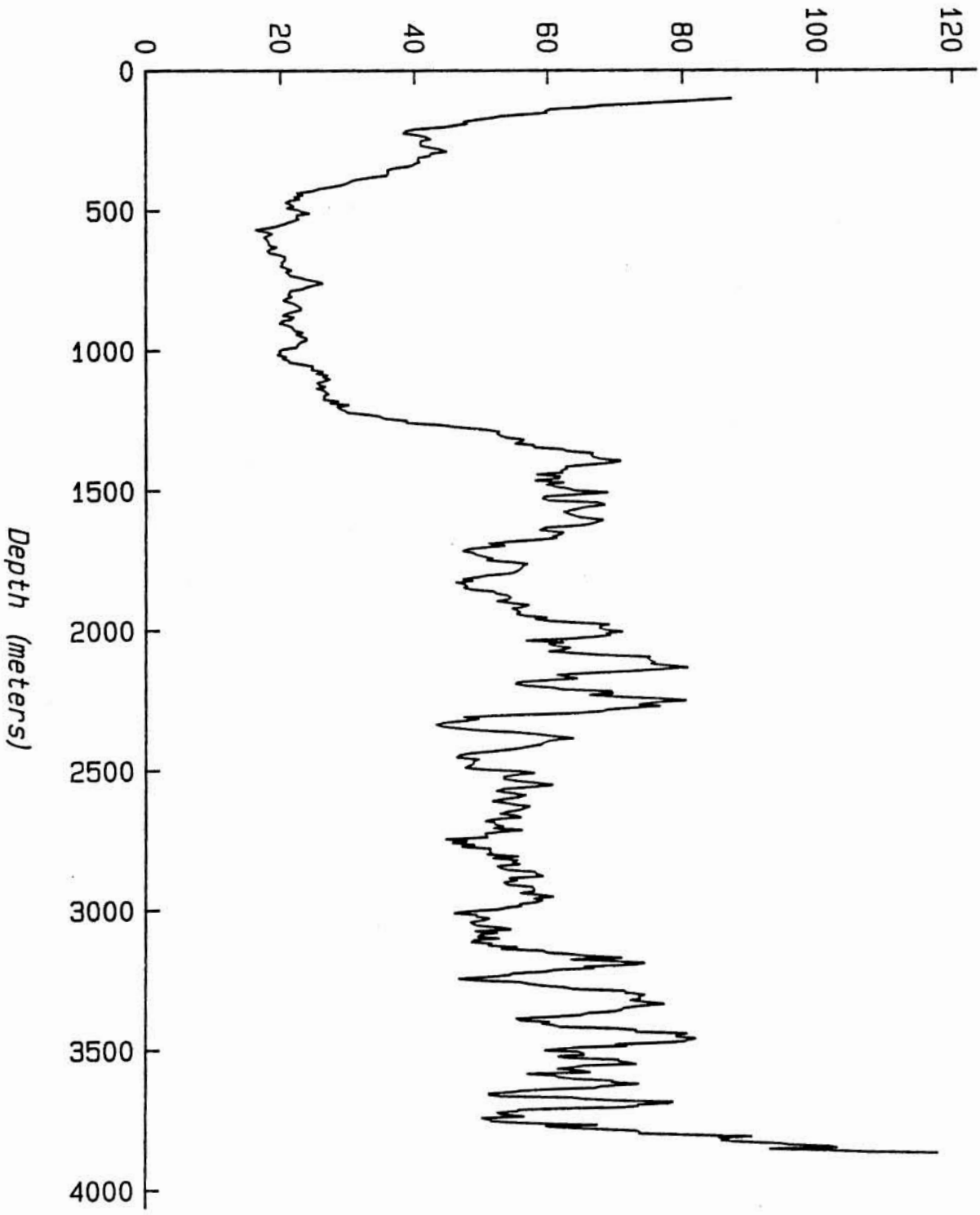

E

12d) was complete (2 hours). Comparison of these profiles shows that similar major features appear in both, although the smaller features were quite variable. This finding is consistent with the patchiness observed in a single profile and indicates horizontal patchiness on the order of hundreds of meters, the accuracy of the ship's navigation system. The large peak at 1500m in these profiles is not present in E-3 (fig. 2.12c) taken just 5 days earlier, indicating new input of material at this depth. Similar evidence of new input is seen in profiles PBMS1 (fig. 2.12a) and PBMS17 (fig. 2.12b) taken 20 days apart and one year earlier than the E series. These profiles, produced January 5 and 20 respectively, show lower abundances than the E series which were produced during the more productive March/April time period. The overall slopes of these profiles are quite similar except that a new maximum appears in the later (PBMS17) profile at ~800 meters.

Vertical particulate flux

If marine snow is important in vertical sedimentation processes, then the profiles of aggregate abundance described above should be directly related to sediment flux. Results of time series sediment traps deployed at the PB site are shown in figure 2.13. In both cases the deep traps collected only two usable samples. Deployment PB 3 occurred in the interval between marine snow profiles PBMS1 and PBMS17 while PB 4 began just after PBMS17. Using marine snow abundance values corresponding to depths and times of sediment trap flux measurements, a correlation coefficient of flux (mg m^{-2} day^{-1}) vs. marine snow abundance ($mm^3 liter^{-1}$) of 0.72 (n=4) is obtained (table 2.1). The fact that the

Table 2.1 Correlation of particle flux with marine snow aggregate abundance.

Depth (meters)	Particle Flux (mg $m^{-2}day^{-1}$)	Concentration of Marine Snow Aggregates (mm^3liter)
1935	97	34
2435	85	35
3035	77	30
3535	40	30

Correlation coefficient = 0.723; not significant at 95% confidence level.

Figure 2.13 Results of time series sediment traps deployed at the S.T.I.E. site in the Panama Basin; only the first two samples of the deep traps were usable. a) Deployment PB-3 lasted 20 days with each cup open for just 36 hours. During this time, flux varied by a factor of 6 in the shallow trap. b) Each cup in deployment PB-4 was open for 4.33 days. Initiation of the spring phytoplankton bloom is observed at the end of this deployment.

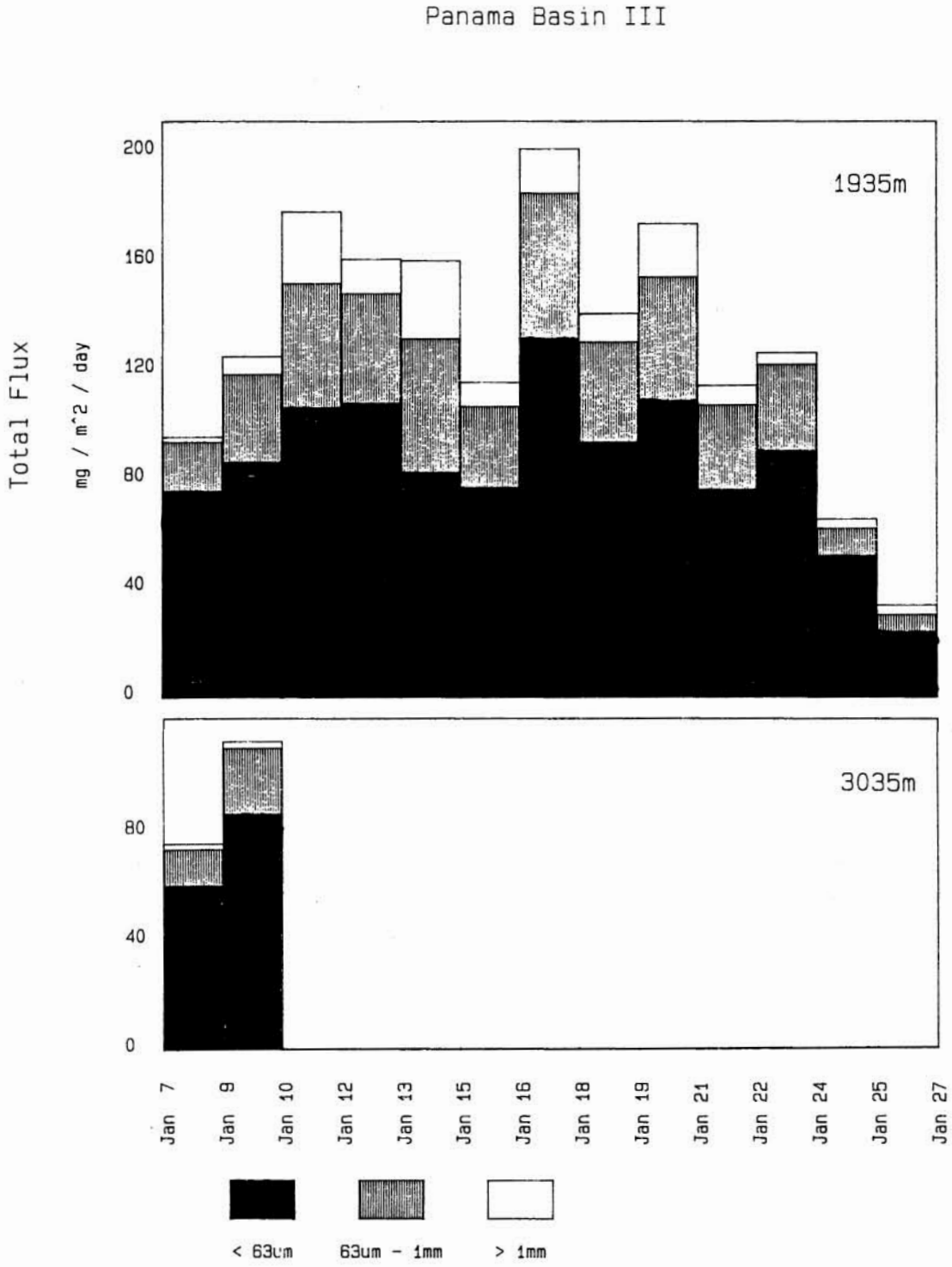
Panama Basin III
Total Flux
mg / m^2 / day
1935m
3035m
200
160
120
80
40
0
80
40
0
Jan 7
Jan 9
Jan 10
Jan 12
Jan 13
Jan 15
Jan 16
Jan 18
Jan 19
Jan 21
Jan 22
Jan 24
Jan 25
Jan 27
< 63um
63um - 1mm
> 1mm

A

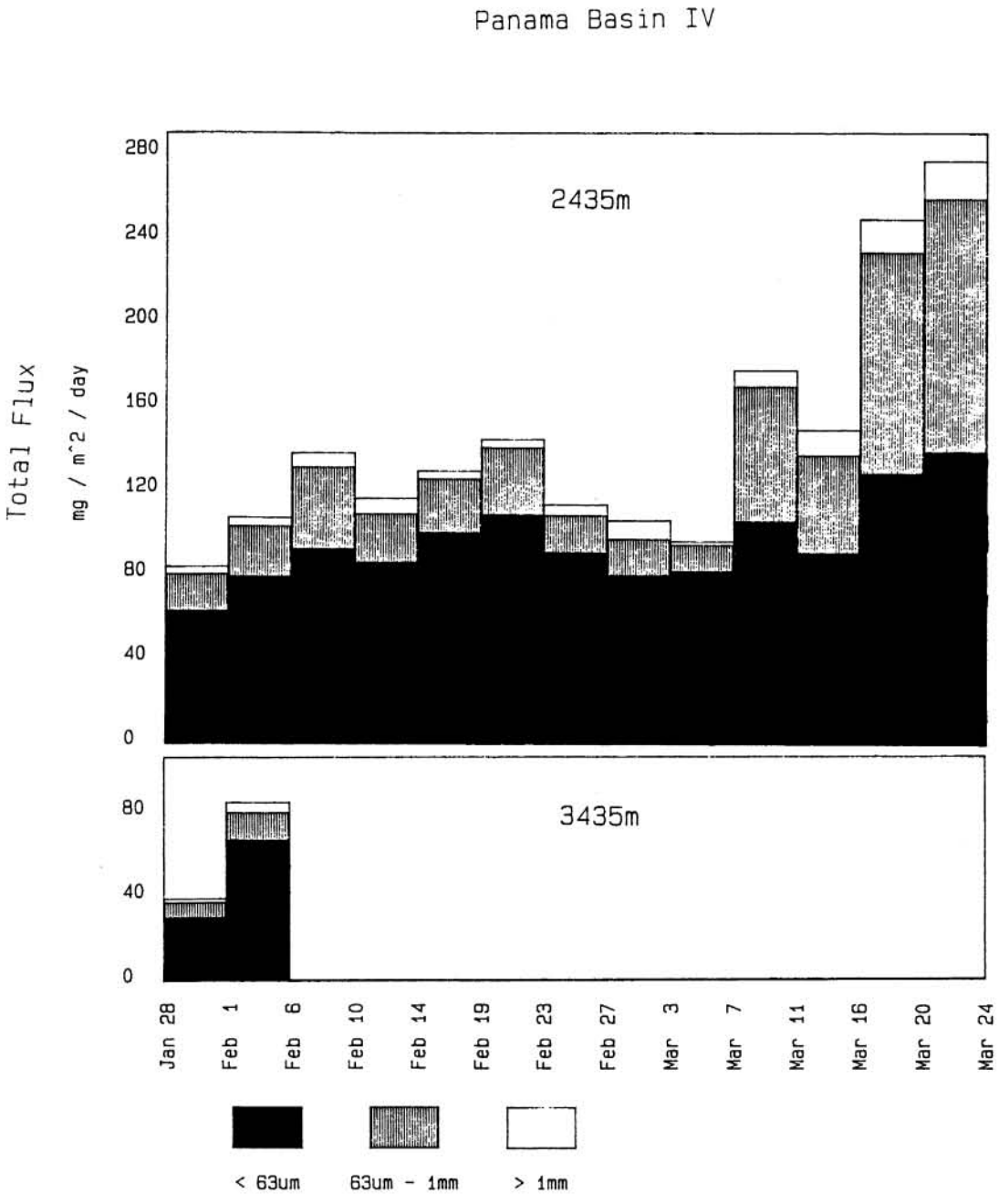
Panama Basin IV
Total Flux
mg / m^2 / day
2435m
3435m
280
240
200
160
120
80
40
0
80
40
0
Jan 28
Feb 1
Feb 6
Feb 10
Feb 14
Feb 19
Feb 23
Feb 27
Mar 3
Mar 7
Mar 11
Mar 16
Mar 20
Mar 24
< 63um
63um - 1mm
> 1mm

B

correlation is not significant at the 95% confidence level indicates that factors besides standing stock of marine snow aggregates are important in sediment flux. Assuming that this flux were due entirely to aggregates observed in the abundance profiles, and if all aggregates were sinking at 100m day^{-1} (Shanks and Trent 1980), then this time-flux signal should be reproduced in profile PBMS1 as a depth-abundance signal. Furthermore, PBMS17, taken 20 days later, should show a similar signal which has been phase shifted 2000m deeper (20 days x 100m day^{-1}) and should also contain the abundance-depth signal corresponding to the first 24 days of PB4 time-flux signal. Neither profile shows the predicted trend, however. In fact, during the 20 days that the PB3 traps were in place, flux varied from 34 to 203 mg m^{-2} day^{-1}, a factor of almost 6, while in the upper 2000m of PBMS1 the abundance of marine snow varies by a factor of only two. Also, as discussed below, profile PBMS17 is not significantly different from PBMS1. The temporal stability of the abundance profiles is not repeated in the vertical flux record. This evidence indicates that at this site, sediment flux is not uniquely controlled by the abundance of marine snow aggregates.

Sediment distribution patterns

The Panama Basin presents a particularly interesting location to investigate the apparent link between marine snow abundance and sediment flux. Sediment transport maps (Van Andel, 1973) indicate that observed sediment distributions are largely the result of resuspension and transport of sediment by deep currents. In fact, Van Andel's (1973) estimate of transport direction indicate that shallow ridges and the basin's margins are the primary sources of sediment. Also, sediment trap deployments

indicate significant deep input of resuspended material (Honjo 1982, Honjo et al. 1982b, Lee et al. 1983). Estimates of deep water flow velocities at the deployment site (Gardner et al., 1984; Honjo et al., 1981; Laird, 1971) are extremely low, however, so that local resuspension of individual clay particles is unlikely.

Particle Transport Model.

Honjo et al. (1982b) proposed the "amorphous aggregate hypothesis" to account for the observed vertical flux pattern and distinguished between suspended and settling particles. Gardner et al. (1984) applied this model to the specific Panama Basin environment and supplemented it with nephelometer and large volume pump sample profiles. An extension and refinement of the earlier hypothesis, the following model (fig. 2.14) proposes that much of the resuspension, transportation and redistribution of sediment occurs via marine snow aggregates and consequently evidence of these processes is observed in along-current transects of aggregate abundance.

According to the proposed model, surface produced (fresh) aggregates contain biogenic mineral hard parts from a variety of phyto- and zooplankton, causing them to sink quickly (100m day^{-1}) and reach the sea floor with minimal alteration. At the sediment/water interface (Benthic Transition Layer discussed by Honjo et al. 1982a), however, much of this solid material is remineralized (Cobler and Dymond, 1980; Baker et al., 1979) leaving a flocculent organic "fluff" which is easily resuspended. As a result of this process, turbulent mixing of stratified water types at ocean margins (Armi 1978, 1979) resuspends (Lampitt, in press) and entrains these altered aggregates, and transports them many kilometers from their

Figure 2.14 Schematic of proposed flux model. a) The euphotic zone is the primary source of most aggregates which sink quickly to the sea floor. This material is then resuspended and transported away from the margins. As it moves offshore, this material continues to settle, but at slower speeds than the fresh material falling directly from the surface. Fresh aggregates collide with the resuspended material, increasing its sinking speed, scavenging it from the water column and delivering it to the sea floor. b) Examples of hypothetical marine snow abundance profiles taken at various locations in (a) showing the influence of various sources of material.

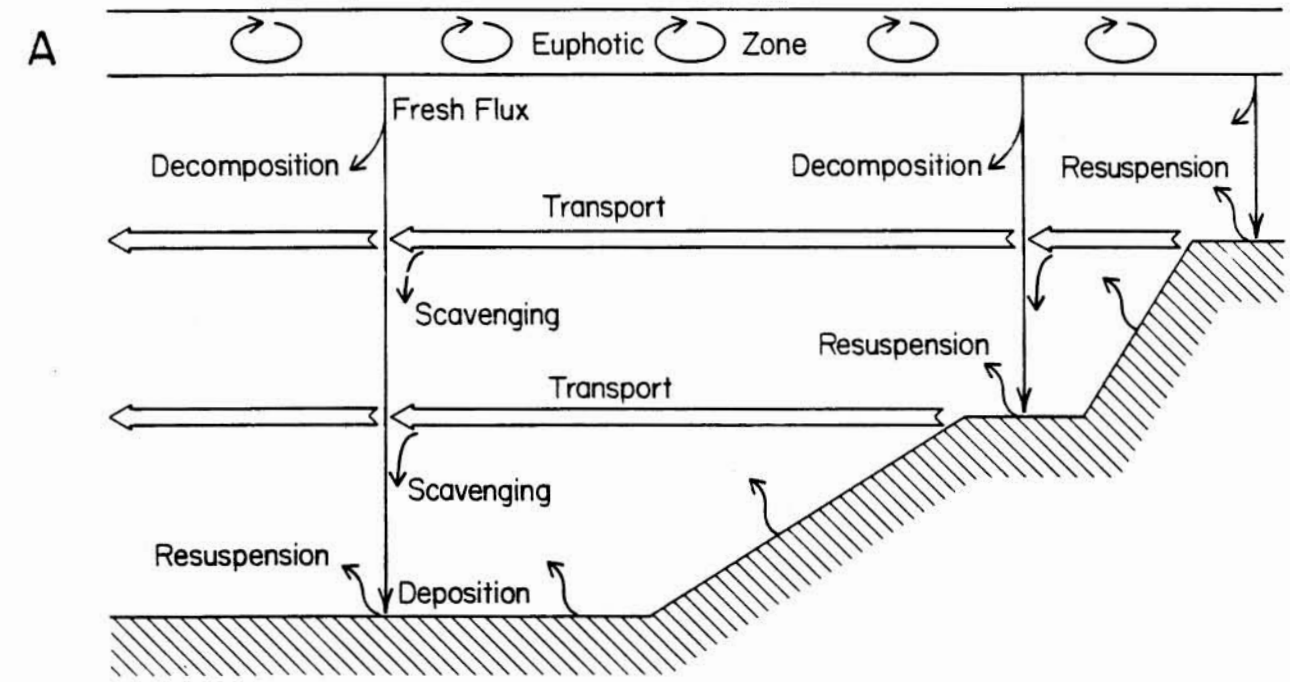
A
Euphotic Zone
Fresh Flux
Decomposition
Decomposition
Resuspension
Transport
Scavenging
Resuspension
Transport
Scavenging
Resuspension
Deposition

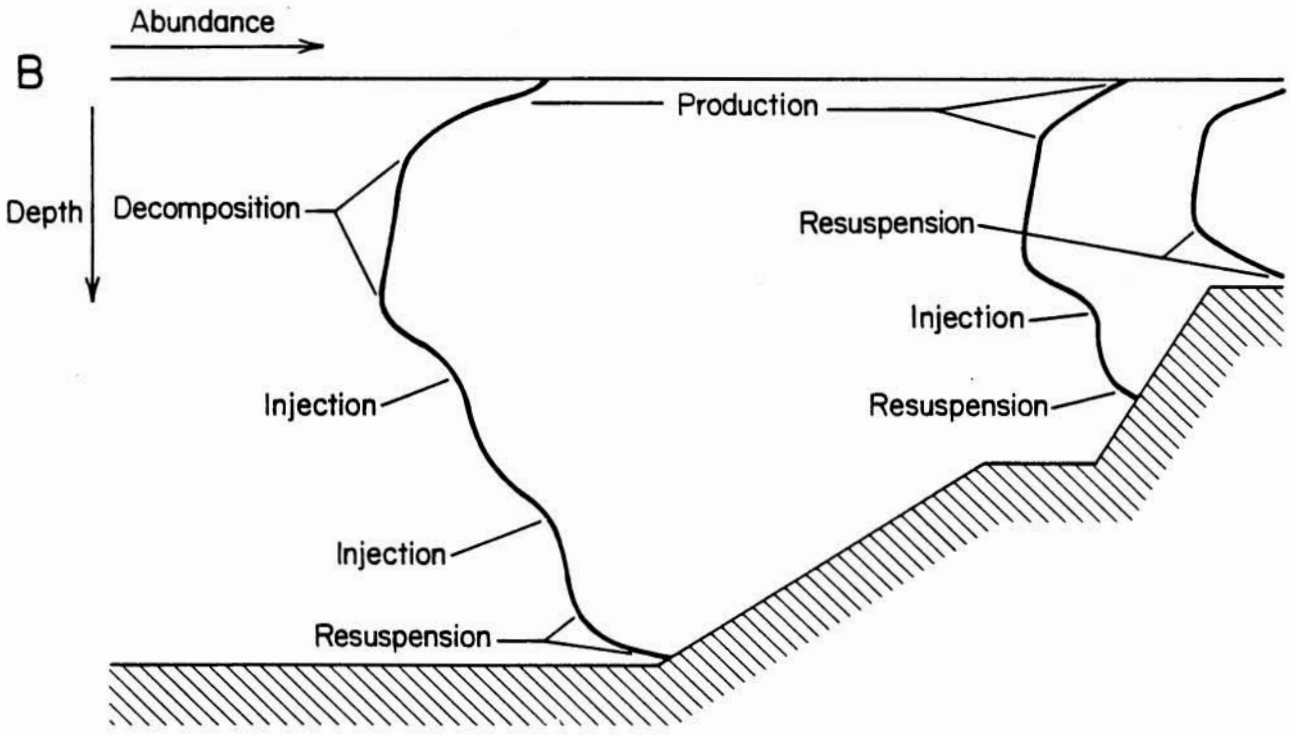
B
Abundance
Depth
Production
Decomposition
Resuspension
Injection
Injection
Resuspension
Injection
Resuspension

original deposition site. Thus it becomes necessary to distinguish between this older, lighter, resuspended material and the relatively heavier fresh material. This injection of material (and increase in aggregate abundance) at depth accounts for reported depthwise flux increases (Honjo, 1980; Honjo et al., 1982a, b).

In addition to the injection of aggregates at depth, surface production of fast-sinking particles throughout the basin must be invoked to account for the magnitude of the seasonality of flux observed here and described by Honjo (1982). Fast-sinking fresh material falls from the surface, collides with the altered aggregates, increases their sinking speed, and removes them from the water column. This scavenging process results in the overall lower abundances observed throughout the water column at greater distances from the margins. This model is compatible with the layered silicate flux values reported by Honjo et al. (1982b). These authors reported that while the flux of layered silicates increased with depth (except at the mid-gyre Hawaii site), the rate of increase was greater near a continental margin and decreased regularly with distance from shore.

Over the time scales investigated, the aggregate abundances were relatively stable and varied only over a factor of three with depth, whereas flux varied over a factor of 6 with time. Forsberg (1969) reports that for a station northeast of the PB site, monthly averages of diatom abundance (and by inference the potential for marine snow production) varied over a factor of 15 on an annual basis. Additionally, Deuser et al. (1981, 1983) and Honjo (1982) have shown that all components of flux vary

seasonally in response to primary production. This study indicates that this seasonal control of flux at all depths is the result of fast-sinking particles produced in surface water, whereas depthwise increase in flux is the result of resuspended, altered aggregates. The sinking speed of the resuspended aggregates are lower than those of fresh aggregates and are also too slow to account for the rapid vertical transfer of material from a coccolithophorid bloom described by Honjo (1982). Therefore, the proposed distinction between the resuspended and fresh material is necessary to allow for both rapid, seasonal sinking and also for lateral transport.

Preservation of Sediment Trap Material

As indicated by the biogenic calcium carbonate (calcite) samples pictured in figure 2.15, preservation of the collected particles is variable. The first micrographs (fig. 2.15a-b) show a tintinnid lorica composed of coccoliths which show no evidence of dissolution. In contrast, figure 2.15c-d shows a fragment of a foraminifera which has been severely eroded. The bacteria pictured in figure 2.15d appear to be in some way linked to this dissolution, as they are concentrated only on the more dissolved fragment and seem to collect in the corrosion pits.

Regardless of its cause, evidence of significant dissolution indicates that this fragment has spent some time on the sea floor and must therefore have been resuspended and delivered into the trap. Surface sediment collected by DSRV Alvin near the trap site indicate that settling particles are severely altered on or near the sea floor (fig. 2.16). These samples are composed primarily of benthic fecal pellets (benthic?) and large diatom and foraminifera fragments. The pellets contain numerous bacteria, small fragments of biogenic silica, and clay particles, but no recognizable

Figure 2.15 SEM images of samples of biogenic carbonate collected by a sediment trap at 3800m in the Panama Basin (water depth=3900m). a) Tintinnid lorica composed of several species of coccoliths. Scale bar is 20 μm. b) Enlargement of (a). The excellent preservation of the coccoliths indicates rapid vertical transport. Scale bar is 2μm. c) Fragment of planktonic foraminifera showing evidence of significant dissolution. Scale bar is 40μm. d) Close-up of (c) showing bacteria concentrated in dissolution pits. This dissolution indicates a relatively long residence time in undersaturated conditions. Scale bar is 2μm.

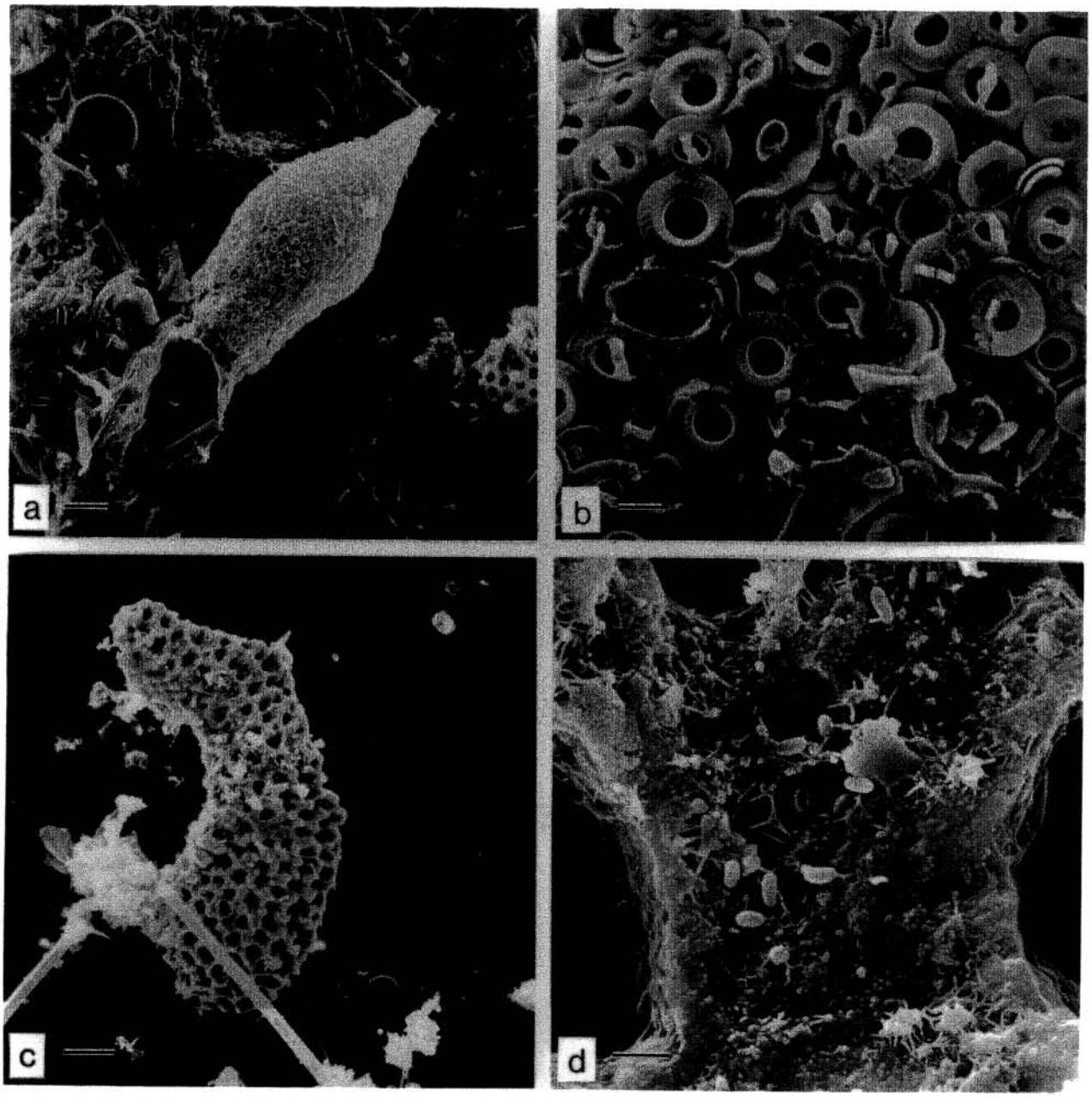
a
b
c
d

Figure 2.16 SEM images of sediment samples collected at sediment trap site. This material was taken from the upper 1mm of a DSRV Alvin tube core, preserved in glutaraldehyde, and critical point dried. a-b) Much of the sediment consists of rounded objects which are apparently benthic fecal pellets. Scale bars are 20μm and 10μm. c-d) Magnification of the surface of these pellets reveals that they contain small fragments of diatoms, clay particles, and numerous bacteria, but little organic matter and apparently no biogenic carbonate. Scale bars are 2μm.

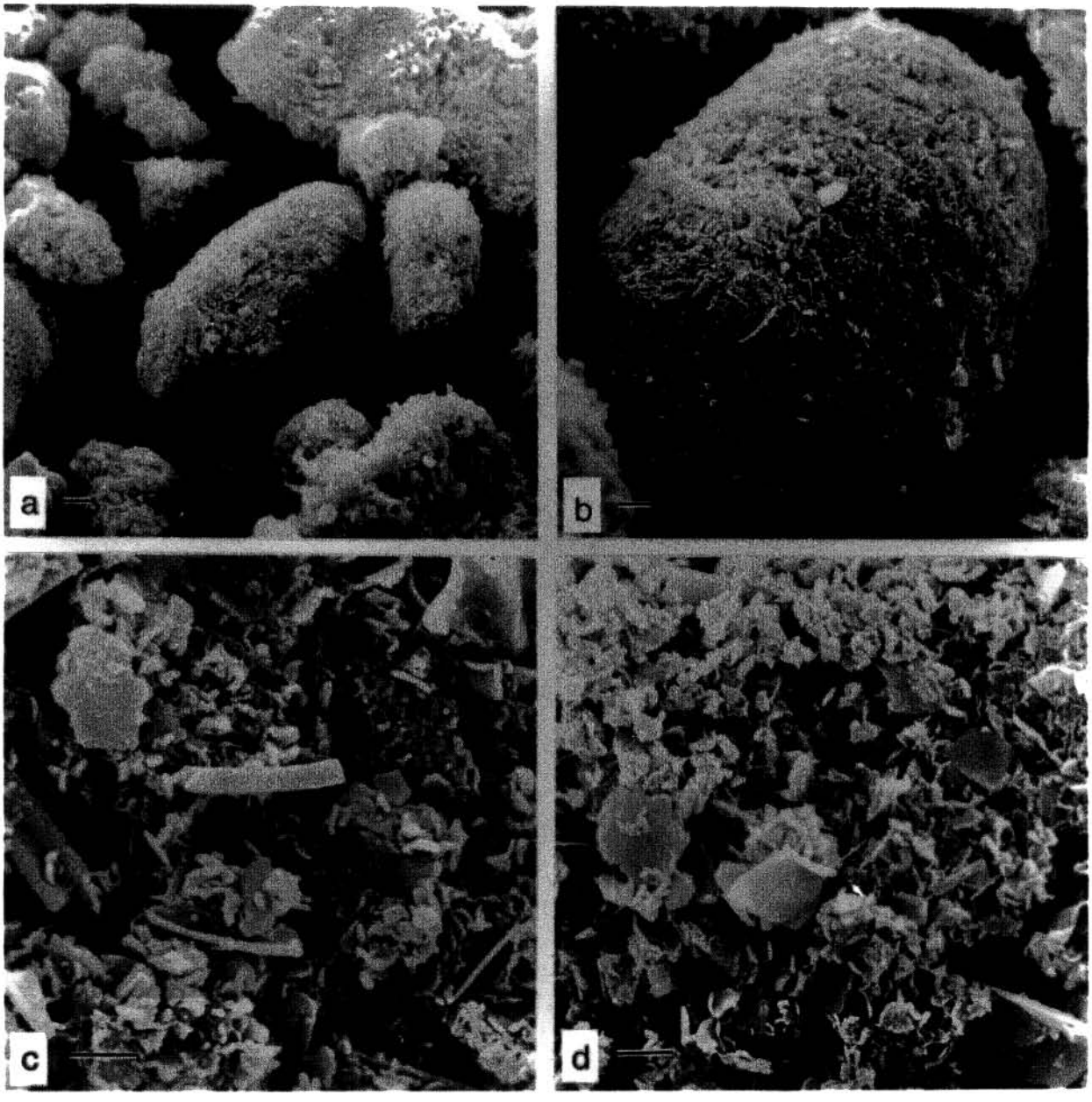
a
b
c
d

carbonate. This evidence supports the conclusion that the foraminifera fragment collected in the sediment trap was resuspended to the trap height, and therefore that not all of the trapped material arrived directly from the sea surface.

Calculated Proportion of Fresh and Resuspended Material in Flux Samples

Using flux data from Honjo et al. (1982) it is possible to calculate relative proportions of fresh and altered material in the total flux. This is accomplished by calculating the expected loss from surface derived material due to remineralization during settling. Decomposition and remineralization rates are calculated from changes in flux of material collected near Hawaii where no evidence of deep input was detected (trap depths from 670m to 3790m below the surface). Clay was assumed to be conservative and all other losses were calculated with respect to the clay flux. Remineralization rates (% km^{-1} settled through the water column) calculated from Hawaii station fluxes (Honjo et al., 1982a,b) are: biogenic opal = 6% km^{-1}, combustible material = 19% km^{-1}, clay = 0, and carbonate = 0 (no dissolution in the water column above the lysocline). These rate of loss estimates are applied to total flux values measured near the surface in the Panama Basin to arrive at the estimated surface derived flux arriving at any depth. Table 2.2 lists major elements of the surface and resuspended flux calculations. Horizontal injections of resuspended material are the difference between the observed total flux and the calculated flux from the surface. The resuspended material has been decomposed, and contains 2-3 times the lithogenic (refractory) material originally present in the surface derived flux. Also, deeper samples contain a higher proportion of resuspended material, indicating that several cycles of alteration and resuspension may have occurred.

Table 2.2 Calculations of surface and resuspended flux based on watter column decomposition rates from Honjo et al. (1982) for flux measurements reported in Honjo (1982). These decomposition rates are : biogenic opal = 6% km^{-1}, combustible material = 19% km^{-1}, clay = 0, and carbonate = 0, that is, no dissolution in the water column above the lysocline.

Depth	Total	Surface	Resuspended	% Resuspended	Percent (%) Lithogenic material in Flux		
(meters)	Flux	Flux	Flux	Flux	Surface	Resuspended	Total
670	111.9	111.9	0	0	19.2	0	19.2
1270	103.3	103.0	0	0	20.0	0	20.0
2270	120.8	98.2	22.6	18.7	21.1	45.1	25.5
2870	158.4	94.3	64.1	40.5	22.0	44.8	31.6
3770	178.8	90.6	88.2	49.3	22.8	61.6	41.9

The inference that material falling to the sea floor (and into sediment traps) derives from a combination of direct and indirect sources leads to several implications for marine sedimentation models. The apparent age of the material will reflect the proportions of material delivered from fresh and altered sources. Consequently, material collected within the influence of altered aggregate input will appear older than material without this influence. This could lead to the false conclusion that nearshore particles decompose more quickly (or settle more slowly) than particles produced offshore, or that sinking speed decreases with depth. Discrepancies between LVFS samples and sediment trap material are related to partitioning of material into settling and suspended classes; sediment traps collect settling particles while pumps and bottles collect mostly suspended particles. In regions beyond the influence of resuspended material, this distinction may disappear due to the removal of suspended particles due to scavenging by settling aggregates.

Recent investigations (Karl et al., 1984) have measured depthwise increases in flux and concluded that new material is forming within the water column and that flux is uncoupled from production. This may in fact be true for labile organic material; however it may also be possible that advected material (altered aggregates) is responsible in some cases. Input of material at discrete depths would influence not only the mass flux but the water chemistry and biology as well by supplying dissolved and particulate organic material for heterotrophs and a substrate for bacterial growth.

Clearly processes involved in marine sedimentation are not simple and more data are needed to further our understanding; information relating to aggregates and their formation and fate is especially desirable. One useful data set would consist of vertical and horizontal (shallow to deep) profiles of particle age (an indication of residence time), or better still, sinking speed. If the above model is correct, then the apparent age of material at a given depth should decrease with distance from a margin source. Another useful data set would include closely spaced transects of marine snow abundance in order to track populations of aggregates as they move offshore. Simultaneous deployments of time series sediment traps within such a transect would aid in determining the connection between flux and aggregate abundance.

Conclusions

1. Marine snow aggregates are an ubiquitous feature of the oceanic particulate matter population. They were found in significant quantities at all depths and locations surveyed. This material provides microhabitats and macro food particles in size classes which would otherwise be unavailable at these depths.

2. Aggregates observed in the water column derive from at least two distinct sources: direct production by phyto- and zooplankton, and resuspension of older, altered aggregates from the sea floor at the oceans' margins.

3. According to the proposed model, the resuspended particles control and dominate observed depthwise increases in flux whereas the fresh material falling from the surface controls seasonality in the flux.

4. Profiles of aggregate abundances appear to be relatively stable over a variety of time scales. However, small scale, low amplitude variations result from random three-dimensional patchiness of the suspended aggregates.

5. Shapes of profiles varied with location more than with time at a single location. The shape of the profiles reflects the vertical and horizontal processes which act together to supply the aggregate material at each depth.

References

Alldredge, A.L. (1972) Abandoned larvacean houses: a unique food source in the pelagic environment. Science vol. 177, 885-887.

Alldredge, A.L. (1976) Discarded appendicularian houses as sources of food, surface habitats and particulate organic matter in planktonic environments. Limnol. Oceanogr. vol. 21(1), 14-23.

Alldredge, A.L. (1979) The chemical composition of macroscopic aggregates in two neretic seas. Limnol. Oceanogr. vol. 24(5), 855-866.

Alldredge, A.L. (1984) Macroscopic organic aggregates (marine snow). In: Global Ocean Flux Study proceedings of a workshop. National Academy of Sciences, National Research Council, Washington, D.C. 167-179.

Alldredge, A.L. and J.L. Cox (1982) Primary productivity and chemical composition of marine snow in surface waters of the southern California Bight. in press, J. Mar. Res..

Alldredge, A.L. and M.W. Silver (1982) Abundance and production rates of floating diatom mats (Rhizoselenia castracanei and R. imbricata var. shrubsolei) in the Eastern Pacific. in prep.

Armi, L. (1979) Effects of variations in eddy diffusivity on property distributions in the oceans. J. Mar. Res. vol. 37, 515-530

Armi, L. (1978) Some Evidence for boundary mixing in the deep ocean. J. Geophys. Res. vol. 83(C4), 1971-1979.

Baker, E.T., R.A. Feely, and K. Takahashi (1979) Chemical composition, size distribution and particle morphology of suspended particulate matter at DOMES sites A,B, and C: relationships with local sediment composition. In: Marine Geology and Oceanography of the Pacific Manganese Nodule Province, J.L. Bischoff and D.Z. Piper, eds., 163-201.

Bacon, M.P., and R.F. Anderson (1982) Distribution of Thorium isotopes between dissolved and particulate forms in the deep sea. J. Geophys. Res. vol 87(c3), 2045-2056.

Barber, R.T. (1966) Interaction of bubbles and bacteria in the formation of organic aggregates in sea-water. Nature vol. 211, 257-258.

Baylor, E.R. and W.H. Sutcliffe Jr. (1963) Dissolved organic matter in seawater as a source of particulate food. Limnol. Oceanogr. vol. 8(4), 369-371.

Billet, D.S.M., R.S. Lampitt, A.L. Rice, and R.F.C. Mantoura (1983) Seasonal sedimentation of phytoplankton to the deep-sea benthos. Nature vol. 302(7), 520-522.

Bishop, J.K.B., J.M. Edmond, D.R. Keiten, M.P. Bacon, and W.B. Silker (1977) The chemistry biology, and vertical flux of particulate matter from the upper 400m of the equatorial Atlantic Ocean. Deep-Sea Res. vol. 24, 511-548.

Brewer, P.G., Y. Nozaki, D.W. Spencer and A.P. Fleer (1980) Sediment trap experiments in the deep North Atlantic: isotopic and elemental fluxes. J. Mar. Res. vol. 38, 703-708.

Caron, D.A., P.G. Davis, L.P. Madin, and J.McN. Sieburth (1982) Heterotrophic bacteria and bacterivorous protozoa in oceanic macroaggregates. Science vol. 218(19), 795-797.

Cobler, R., and J. Dymond (1980) Sediment trap experiment on the Galapagos Spreading Center, Equatorial Pacific. Science vol. 209(15) 208-209.

Deuser, W.G., P.G. Brewer, T.D. Jickells and R.F. Commeau (1983) Biological control of the removal of abiogenic particles from the surface ocean. Science vol. 219, 388-391.

Deuser, W.G., and E.H. Ross (1980) Seasonal change in the flux of organic carbon to the deep Sargasso Sea. Nature vol. 283, 364-365.

Deuser, W.G., E.H. Ross and R.F. Anderson (1981) Seasonality in the supply of sediment to the deep Sargasso Sea and implications for the rapid transfer of matter to the deep ocean. Deep-Sea Res. vol. 28A(5), 495-505.

Eppley, R.W., E.H. Renger, and P.R. Betzer (1983) The residence time of particulate organic carbon in the surface layer of the ocean. Deep-Sea Res. vol. 30(3A), 311-323.

Gardner, W.D., J.K.B. Bishop and P.E. Biscaye (1984) Nephelometer and current observations at the STIE site, Panama Basin. J. Mar. Res. vol. 42, 207-219.

Gilmer, R.W. (1972) Free-floating mucus webs: a novel feeding adaptation for the open ocean. Science vol. 176, 1239-1240.

Hamner, W.M., L.P. Madin, A.L. Alldredge, R.W. Gilmer, and P.P. Hamner (1975) Underwater observations of gelatinous zooplankton: sampling problems, feeding biology, and behavior. Limnol. Oceanogr. vol. 20(6), 907-917.

Heath, G.R., T.C. Moore and G.L. Roberts (1974) Mineralogy of surface sediments from the Panama Basin, eastern Equatorial Pacific. J. Geol. vol. 82, 145-160.

Honjo, S. (1976) Coccoliths: production, transportation and sedimentation. Mar. Micropaleo., vol. 1, 65-79.

Honjo, S. (1980) Material fluxes and modes of sedimentation in the mesopelagic and bathypelagic zones. J. Mar. Res. vol. 38, 53-97.

Honjo, S. (1982) Seasonality and interaction of biogenic and lithogenic particulate flux at the Panama Basin. Science vol. 218, 883-884.

Honjo, S., K.W. Doherty, Y.C. Agrawal and V.L. Asper (1984) Direct optical assessment of large amorphous aggregates (marine snow) in the deep ocean. Deep-Sea Res. vol. 31(1), 67-76.

Honjo, S., S.J. Manganini, and L.J. Poppe (1982a) Sedimentation of lithogenic particles in the deep ocean. Mar. Geol. vol. 50, 199-220.

Honjo, S., S.J. Manganini, and J.J. Cole (1982b) Sedimentation of biogenic matter in the deep ocean. Deep-Sea Res. vol. 29(9A), 609-625.

Honjo, S., D.W. Spencer, and J.W. Farrington (1982) Deep advective transport of lithogenic particles in Panama Basin. Science vol. 216, 516-518.

Jannasch, H.W. (1973) Bacterial content of particulate matter in offshore surface waters Limnol. Oceanogr. vol. 18(2), 340-342.

Johnson, B. (1976) Nonliving organic particle formation from bubble dissolution. Limnol. Oceanogr. vol. 21(3), 444-446.

Kajihara, M. (1971) Settling velocity and porosity of large suspended particle. J. Oceanogr. Soc. Jap. vol. 27(4), 158-162.

Kajihara, M., K. Matsunaga, and Y. Maita (1974) Anomalous distribution of suspended matter and some chemical compositions in seawater near the seabed: transport processes. J. Oceanogr. Soc. Jap. vol. 30(5), 24-32.

Kane, J.E. (1967) Organic aggregates in surface waters in the Ligurian Sea. Limnol. Oceanogr. vol. 12, 287-294.

Karl, D.M., G.A. Knauer, J.H, Martin and B.B. Ward (1984) Bacterial chemolithotrophy in the ocean is associated with sinking particles. Nature vol. 309, 54-56.

Knauer, G.A., D. Hebel and F. Cipriano (1982) Marine snow: major site of primary production in coastal waters. Nature vol. 300, 630-631.

Knauer, G.A., J.H. Martin, and K.W. Bruland (1979) Fluxes of particulate carbon, nitrogen, and phosphorus in the upper water column of the northeast Pacific. Deep-Sea Res. vol. 26A, 97-108.

Laird, N.P. (1971) Panama Basin deep water - properties and circulation. J. Mar. Res. vol. 29(3) 226-234.

Lal, D. (1977) The oceanic microcosm of particles. Science vol. 198(4321), 997-1009.

Lal, D. (1980) Comments on some aspects of particulate transport in the oceans. Earth Planet. Sci. Lett. vol. 49, 520-527.

Lampitt, R.S. (1985) Effects of the seasonal deposition of detritus to the deep-sea floor. (tentative title) submitted to Deep-Sea Res.

Lee, C., S.R. Wakeham and J.W. Farrington (1983) Variations in the composition of particulate organic matter in a time-series sediment trap. Mar. Chem. vol. 13, 181-194.

Lenz, J (1977) On detritus as a food source for pelagic filter-feeders. Mar. Biol. vol. 41, 39-48.

McCave, I.N. (1975) Vertical flux of particles in the ocean. Deep-Sea Res. vol. 22, 491-502.

Moore, T.C. Jr., G. R. Heath and R.O. Kowsmann (1973) Biogenic sediments of the Panama Basin. J. Geol. vol. 81, 458-472.

Osterberg, C., A.G. Carey, and H. Curl (1963) Acceleration of sinking rates of radionuclides in the ocean. Nature vol. 200, 1276-1277.

Paerl, H.W. (1975) Microbial attachment to particles in marine and freshwater ecosystems. Microb. Ecol. vol. 2, 73-83.

Plank, W.S., J.R.V. Zaneveld, and H. Pak (1973) Distribution of suspended matter in the Panama Basin. J. Geophys. Res. vol. 78(30), 7113-7121.

Pomeroy, L.R. and D. Deible (1980) Aggregation of organic matter by pelagic tunicates. Limnol. Oceanogr. vol. 25(4) 643-652.

Prezelin B.B. and A.L. Alldredge (1983) Primary production of marine snow during and after an upwelling event. Limnol. Oceanogr. vol. 28(6), 1156-1167.

Riley, G.A. (1963) Organic aggregates in seawater and the dynamics of their formation and utilization. Limnol. Oceanogr. vol. 8(4), 372-381.

Riley, G.A., D. Van Hemert, and P.J. Wangersky (1965) Organic aggregates in surface and deep waters of the sargasso sea. Limnol. Oceanogr. vol. 10, 354-363.

Shanks, A.L. and J.D. Trent (1980) Marine snow: sinking rates and potential role in vertical flux. Deep-Sea Res. vol. 27A, 137-143.

Silver, M.W., and A.L. Alldredge (1981) Bathypelagic marine snow: deep-sea algal and detrital community. J. Mar. Res. vol. 39(3), 501-530.

Silver, M.W., A.L. Shanks, and J.D. Trent (1978) Marine snow: microplankton habitat and source of small-scale patchiness in pelagic populations. Science vol 210, 371-373.

Spencer, D.W. (1980) Sediment trap intercomparison experiment. Woods Hole oceanographic Institution Technical memorandum. WHOI-1-81, 120pp.

Suess, E. (1980) Particulate organic carbon flux in the oceans-surface productivity and oxygen utilization. Nature vol. 288, 260-263.

Suzuki, N., and K. Kato (1953) Studies on suspended materials marine snow in the sea. Part I. Sources of marine snow. Bull. Fac. Fish. Hokkaido Univ. vol. 4, 132-137.

Tanoue, E., and N. Handa (1980) Vertical transport of organic materials in the northern North Pacific as determined by sediment trap experiment. J. Oceanogr. Soc. Japan vol. 36, 231-245.

Trent, J.D., A.L. Shanks, and M.W. Silver (1978) In situ and laboratory measurements on macroscopic aggregates in Monterey Bay, California. Limnol. Oceanogr. vol. 23(4), 625-635.

Tsunogai, S. and M. Minagawa (1978) Settling model for the removal of insoluble chemical elements in seawater. Geochem. J. vol. 12, 47-56.

Urrere, M.A. and G.A. Knauer (1981) Zooplankton fecal pellet fluxes and vertical transport of particulate organic material in the pelagic environment. J. Plankt. Res. vol. 3(3) 369-387.

Van Andel, T.H. (1973) Texture and dispersal of sediments in the Panama Basin. J. Geol. vol. 81, 434-457.

Wakeham, S.G., J.W. Farrington, R.B. Gagosian, C. Lee, H. DeBaar, G.E. Nigrelli, B.W. Tripp, S.O. Smith and N.M. Frew (1980) Organic matter fluxes from the sediment traps in the equatorial Atlantic Ocean. Nature vol. 286, 798-800.

Wheeler, J.R. (1975) Formation and collapse of surface films. Limnol. Oceanogr. vol. 20(3), 338-342.

Chapter 3

MEASURING THE FLUX AND SINKING SPEED OF MARINE SNOW AGGREGATES

ABSTRACT

The flux and concentration of large amorphous aggregates (marine snow) were measured at 3800m in the Panama Basin using new photographic techniques. Results at this site indicate that essentially all settling particles arrive as components of these large aggregates with insignificant contributions of solitary fecal pellets or fine particles. Flux of any particle divided by concentration gives an estimate of a model parameter which can be interpreted as particle settling speed. Application of this method to marine snow indicates that larger aggregates (4-5mm) settle more slowly (1m day^{-1}) than smaller aggregates (1-2.5mm, 36m day^{1-}). This result may be due to the input of large, flocculent aggregates which were resuspended from the sea floor at equivalent or shallower depths near the experimental location. Mass flux estimated from sinking speed and particle size is larger than the measured mass flux, suggesting loss of material to grazing activity.

Introduction

Marine snow has been shown to be a ubiquitous feature of the oceans' particulate population (Honjo et al., 1984; Silver and Alldredge, 1981). While this finding alone substantiates hypotheses regarding snow's importance in plankton interactions, it does little to prove the involvement of aggregates in the vertical transfer of material from the surface to the sea floor. In order to be important in sediment flux, aggregates must not only be found in significant concentrations, but must also settle through the water column.

The fragile nature of the aggregates makes accurately determining their sinking speeds difficult. Attempts to collect snow, return it to the laboratory, and time it's settling rate under controlled conditions usually result in broken, dis-aggregated or otherwise altered aggregates (Jannasch, 1973; Kajihara, 1971; Riley, 1963; Trent et al., 1978). Despite these difficulties, the sinking speed of marine snow aggregates has been estimated and measured using a variety of approaches.

Kajihara (1971) collected suspended material near the sea floor in shallow (30-42m) water, allowed this material to coagulate, and measured its settling velocity in a laboratory settling tower. These particles resembled the marine snow observed in situ and were easily disintegrated during attempts to transfer them from one container to another. Settling velocities varied with particle diameter from 17 to 260 m day^{-1}. The observed poor agreement with Stoke's law was attributed to variation of density with particle diameter.

Alldredge (1979) estimated the sinking speed of hand-collected aggregates using calculated density and drag coefficients. Her result of 91 m day^{-1} (maximum sinking rate of a 3mm diameter aggregate) was based on the assumptions of a porosity of 99.3%, a maximum dry weight of 38μgm, and a dry weight equaling 30% of the wet weight. Combining sinking speed with the observed abundance of aggregates resulted in a calculated flux which was an order of magnitude greater than the measured flux. This discrepancy was justified by allowing for variations in size, shape, and density of aggregates and by allowing for mixed layer circulation.

Stoke's law was also used by Bishop et al. (1977) to calculate the sinking speed and flux of 'fecal matter' collected by large volume filtration equipment. This fecal matter is most likely the fragments of marine snow which survive the pump filtration process (Honjo et al., 1982). Assuming a dry weight bulk density of 0.2gm cm^{-3} and a density contrast between the material and sea water of 0.05 gm cm^{3}, these authors arrive at sinking speeds of 3.6 m day^{-1} (47 μm particle) to 661 m day^{-1} (639 μm particle). These values are higher than other estimates for particles of similar size and density, and indicate the need for empirical measurements.

The only published in situ measurements of aggregate sinking speeds are those of Shanks and Trent (1980). Using open water SCUBA techniques, these authors measured sinking speeds by enclosing the aggregates in a clear tube and timing their fall through a measured distance. They reported that on several occasions the aggregates in the tubes either stopped sinking or actually began moving upward. This response was

attributed to turbulence in the settling tube and casts a degree of uncertainty on these measurements. Still, their values of 43-95 m day^{-1} represent the only direct measurements available.

Silver and Alldredge (1981) collected the first bathypelagic aggregates from 1000 and 1650m using DSRV Alvin. These samples were mechanically dispersed for light and electron microscopic examination so that no measurements of sinking speeds were obtained. Intact, apparently healthy phytoplankton were found on these aggregates, indicating a rapid transfer via marine snow from the euphotic zone to bathyl depths. Because many aggregates contained remains of larvacean houses, the authors measured the sinking speeds of these houses (57 - 65 m day^{-1}) and applied these rates to aggregate sinking.

An indirect estimate of aggregate sinking was obtained by Billett et al. (1983). These authors deployed a camera system on the sea floor in order to photograph the arrival and dispersal of aggregates over fairly long time periods (30-33 days). They observed large (2.5 mm in diameter) aggregates arriving on the sea floor, moving with tidal currents, and dis-aggregating into smaller components. In one case, material from a spring diatom bloom arrived at 2000 m just 2-3 weeks after the peak of the diatom bloom, indicating a sinking speed of 100-150 m day^{-1} for this non-fecal material. In a similar series of experiments, Lampitt (in press) observed detritus sinking at 100-150 m day^{-1} to 4000 m. Much of this material is held in suspension near the sea floor by weak currents and is quickly degraded.

While each of these studies contributes useful insight into the sinking speed problem, each has limitations. Only Silver and Alldredge (1981) used bathypelagic material and only Shanks and Trent (1980) measured sinking speeds directly in situ, and their technique is not readily extendable to measurements over long time periods and at great depths.

In an attempt to address these limitations, a new method is proposed here that will allow in situ determination of marine snow sinking speeds. Results of the first deployment indicate that essentially all settling particles arrive as components of these large aggregates. Within the range of aggregate sizes observed (1-5mm), the larger aggregates are more flocculent (higher porosity) and sink more slowly than the smaller ones. This method can be applied at any depth and is therefore capable of examining changes in sinking speed with depth below the surface, distance from a margin, or altitude above the bottom. Also, this method is capable of examining the temporal variability of sinking speeds in order to determine whether material sinks more (or less) quickly during times of high primary production, storm activity, or seasonal riverine input.

Materials and methods

Particulate flux can be thought of as the product of particulate concentration and sinking speed (eg. Berger, 1976; Bishop et al., 1977; Takahashi, 1983).

Concentration * Sinking Speed = flux

$$\frac{\#}{\text{volume}} * \frac{\text{distance}}{\text{time}} = \frac{\#}{\text{area} * \text{time}} \qquad 1.0$$

If any two of these parameters can be measured, then the other is easily estimated. In the case of marine snow, concentration can be measured using the non-destructive photographic method of Honjo et al. (1984), whereas measurement of in situ sinking speed is difficult.

In this study, flux of marine snow aggregates is measured using a combination sediment trap and photographic system referred to as the "marine snow flux camera." This system (fig. 3.1) consists of a polypropylene cylinder (0.069m^2 opening) which is open at the top and closed at the bottom by a clear plexiglass plate. Flash tubes from Vivitar® model 2800 strobe heads are attached to Impulse® connectors which are threaded into clear Plexiglass® rod. These pressure-tight strobe units are mounted just above the trap bottom and flush with the walls of the cylinder so as to illuminate any material lying on the clear plate. A Benthos® model 372 deep-sea camera is mounted one meter beneath this apparatus, so that the bottom of the trap is in focus and only material lying on the plate is photographed. Using a 100 ft. (30 meter) roll of film, 800 frames can be exposed, each showing successive additions of material to the trap. Kodak™ Panatomic-X film allows optical resolution on the order of 50μm.

Figure 3.1 a) Photograph of flux camera system as it is lowered into the water during deployment in the Panama Basin. b) Schematic showing principal components of the system. Particles lying on or just above the clear bottom are photographed.

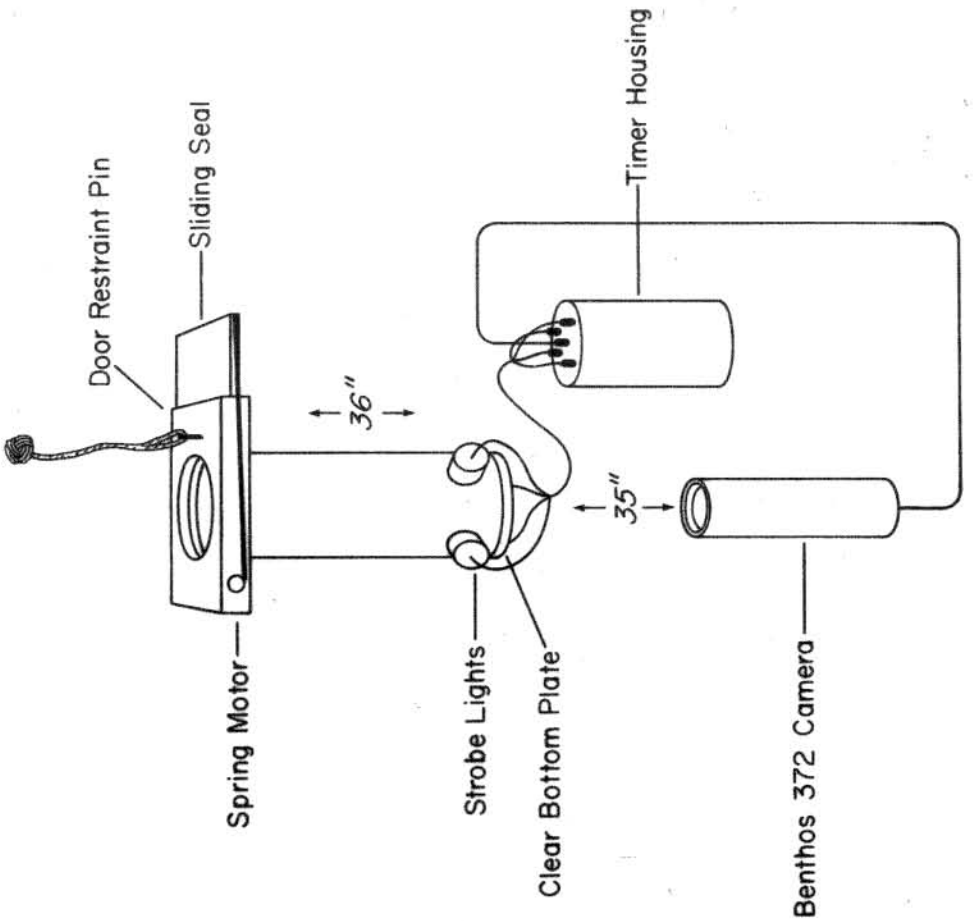
Door Restraint Pin
Sliding Seal
Timer Housing
36"
35"
Spring Motor
Strobe Lights
Clear Bottom Plate
Benthos 372 Camera

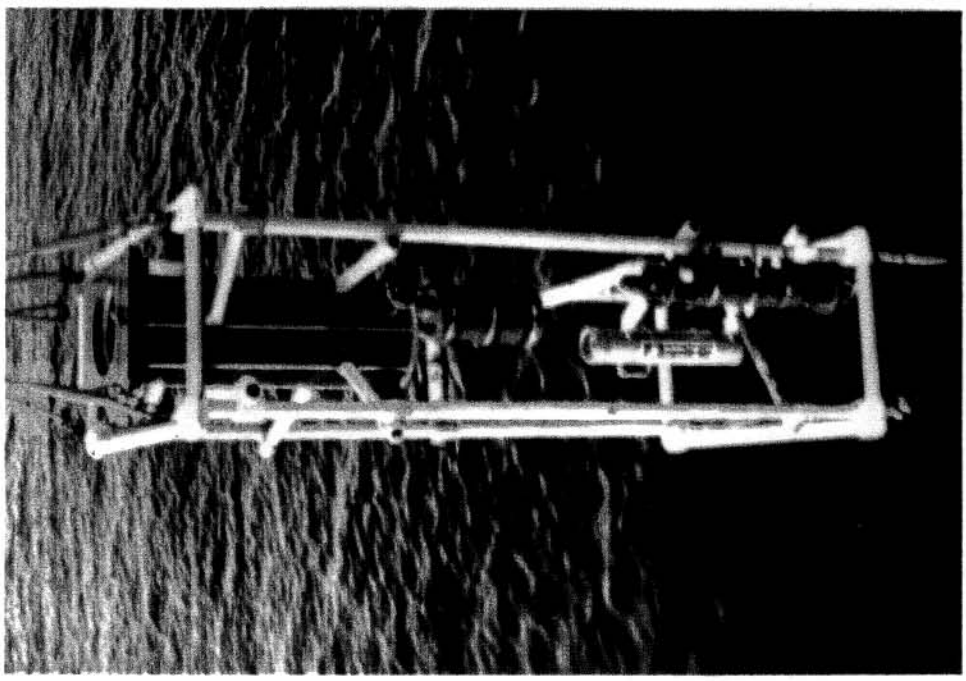

The amount of new material added per time interval between frames per area in the photograph is flux of that material. When this flux value is divided by a concentration value obtained by lowering the marine snow survey camera (Honjo et al., 1984, this thesis chapter 2), an effective aggregate sinking speed is can be calculated from equation 1.0. This procedure can be carried out over any practical time scale; temporal resolution is determined by the time interval between photographs. Also, both flux and abundance numbers can be obtained for several size classes of aggregates, allowing the determination of a sinking speed estimate for each size aggregate. The top of the trap is fitted with a sliding-door seal allowing retrieval of the material and determination of the composition of the settling aggregates.

Several assumptions are inherent in the above mentioned method of determining particle sinking speeds. First, the material falling into the flux camera and photographed by it must represent the same material as that photographed by the marine snow camera for each size class. Second, all material of a given size is assumed to be sinking at the same speed. Third, material photographed by the flux camera is assumed to have fallen into the trap in the form (shape and size) in which it is photographed, with insignificant alteration or deformation between the times of deposition and imaging. Finally, material collected by the trap is assumed to accurately represent particulate flux and not an artifact of trap design or over/under trapment of settling particles.

The initial deployment of this system was conducted in a manner designed to minimize the potential for error introduced independent of these assumptions. Figure 3.2 shows the mooring configuration with the flux camera

GLASS FLOATATION SPHERES

(150M ABOVE BOTTOM)

"FLUX CAMERA"
(100M ABOVE BOTTOM)

ACOUSTIC RELEASE

PULL-PIN RELEASE

ANCHOR

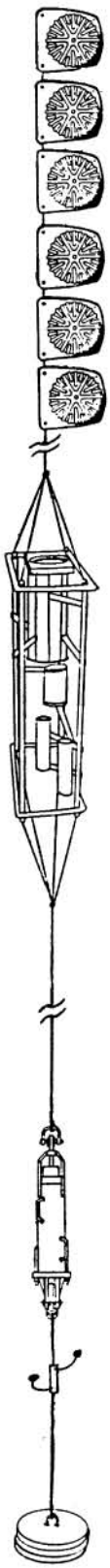

positioned 100m above the sea floor. This system was deployed in the Panama Basin at 5° 21' N, 81° 56' W (PB site, Honjo 1982) as a free falling vehicle on March 30 with the frame interval timer set for 9 minutes. The sliding door seal was held open by a stainless steel pin attached to a short length of polypropylene line, allowing the trap to flush as it fell through the water column; no poisons were used. Daily dives were conducted using DSRV Alvin in the area and neither currents nor evidence of recent current activity were detected during the deployment period. The trap was inspected and the restraining pin was pulled by Alvin on April 4 (5 day deployment) allowing the door to slide shut, sealing the contents. Immediately thereafter, the acoustic release was triggered, sending the mooring to the surface where it was recovered aboard R/V Atlantis II. The sample was allowed to settle and then siphoned, concentrated, and refrigerated for return to the laboratory.

Water column profiles of marine snow abundance were also acquired using the photographic method (marine snow camera) of Honjo et al. (1984). A vertical profile of marine snow abundance was obtained just before deployment of the flux camera to obtain concentration numbers for sinking speed estimation.

Data Analysis

The film (Kodak® Panatomic-X for the flux camera and Kodak® Tri-X for the marine snow camera) was returned to shore for professional development. Negative images were digitized using a Luzex® 450 particle analyzer and Hewlett Packard® 87XM microcomputer similar to the method

described in chapter 2 of this thesis. Parameters evaluated included total image area occupied by aggregates, total number of aggregates, and the number of aggregates in a given size class. The minimum size particle counted (0.5mm) was determined by the enlargement factors in the image analyzer and not by resolution of the negatives.

A portion of the sample was either air-dried or fixed in 3% glutaraldehyde, dehydrated in ethanol and critical point dried from Freon™ 113 for scanning electron microscopic (SEM) examination (Honjo, 1980). Samples of the "fluff" from the sediment-water interface were also collected and preserved for SEM in order to compare contents of the two samples. After coating with gold/palladium, samples were examined with a JEOL JSM-U3 SEM.

Results

Although the timer was initially configured to expose frames of film at nine minute intervals, a partial failure of the timing circuit caused this interval to decrease to smaller values after 12 hours. The correct time was printed on each film negative, so that even though the frames were exposed more rapidly than planned (resulting in only 25 hours of usable film data), timing information was not compromised.

Flux camera images

Examples of flux camera images are shown in figures 3.3-3.4. Resolution is estimated to be on the order of 50μm for particles laying on the bottom plate and less for those situated just above it due to poorer focus. The four light sources produced a 70cm^2 area which is evenly illuminated. In spite of the flushing which occurred as the trap settled through 3800m of water to the sea floor, a small amount of material accumulated in the trap during transit (fig. 3.3a). Without photographic documentation of this occurrence, this material would have been included in the flux estimate. This error could be especially important in short deployments where this input might be a large portion of the total flux.

Figure 3.3 shows the accumulation of material as time progressed. The background is entirely black with only the aggregates scattering light into the camera. This series of pictures shows that essentially all of the sedimenting material arrives in the form of aggregates and not as individual sediment grains. Several individual aggregates can be traced through the deployment (25 hours) with little apparent morphological alteration during this short period. Others appear to enlarge as new

Figure 3.3 Flux camera photographs showing the accumulation of material in the sediment trap. Times since arrival on the bottom are: a) 0 hours, b) 2.3 hours, c) 6.1 hours, d) 12 hours, e) 18 hours, f) 27 hours.

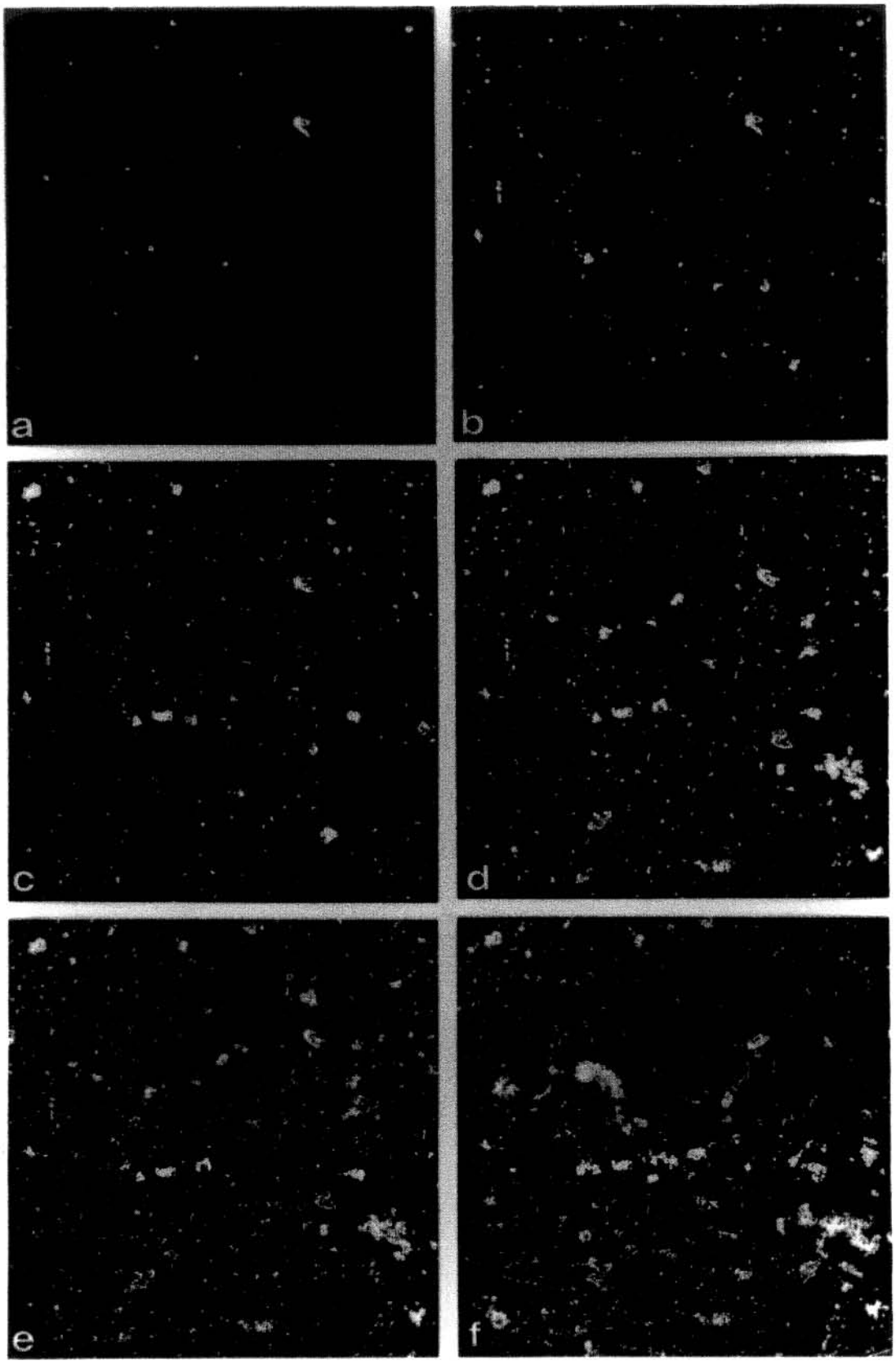
a
b
c
d
e
f
2cm

Figure 3.4 Flux camera photographs showing resuspension events. a-d) Small event at 10.1-10.7 hours. e-f) A more dramatic event at 25.8-26 hours shows significant motion of aggregates. One large aggregate (arrow) appears to roll over and move 7 cm from its original position.

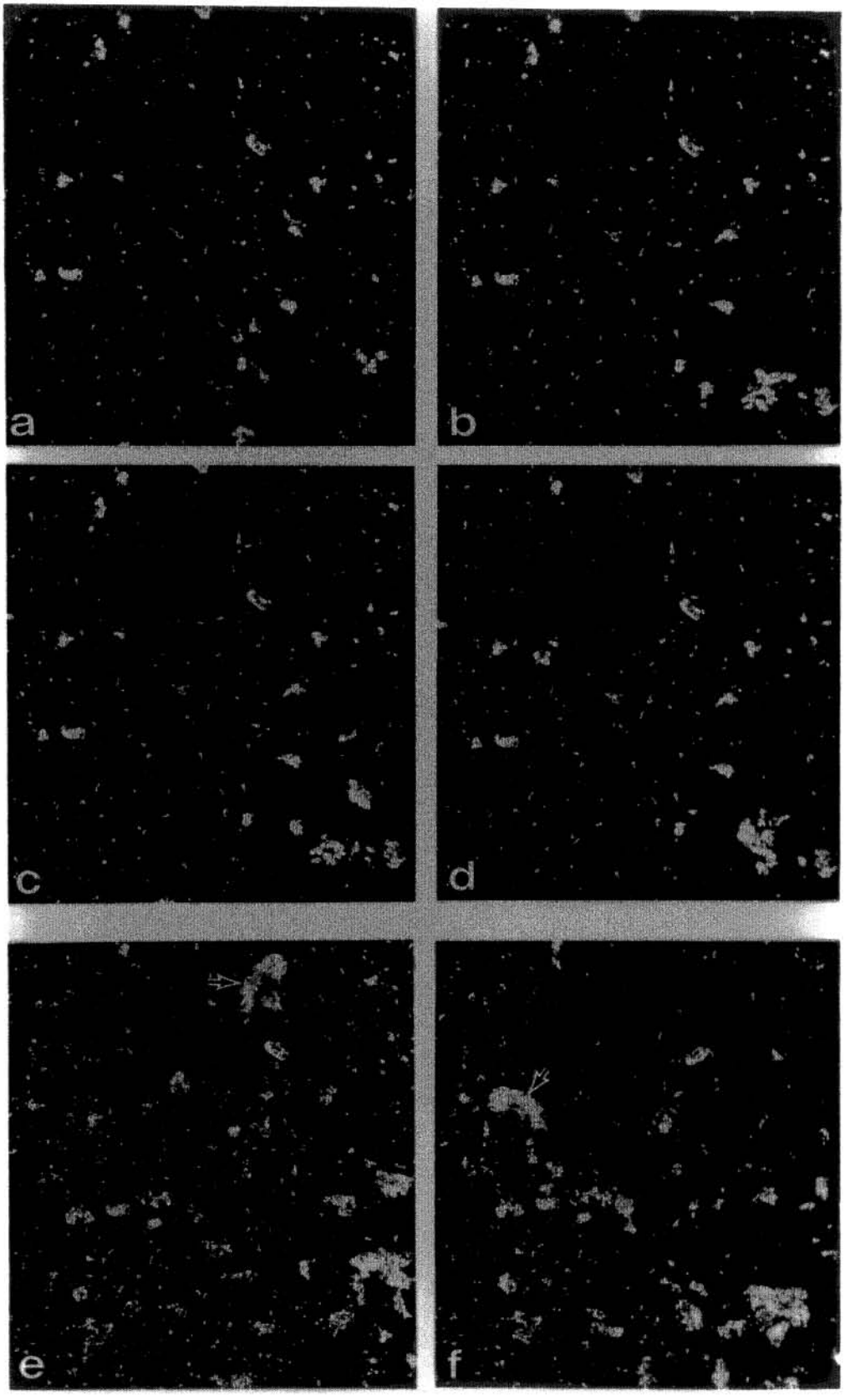
a
b
c
d
e
f
2cm

material falls into adjacent areas, suggesting that aggregate sizes measured in sediment trap material after trap recovery may be artificialy biased to larger sizes.

Feeding events

Several times during the deployment, apparent resuspension of the sediment occurred. Figure 3.4 shows frames from two such events. Although observations from DSRV Alvin dives indicate that no currents were active during the deployment period, several aggregates disappear and others move across the bottom of the trap. This movement of the trapped material is interpreted as an indication of foraging by zooplankton or nekton.

The resuspension event pictured in figure 3.4a-d is relatively minor with only the larger aggregates in the lower right corner of the image showing significant movement over the 35 minute interval. Figure 3.4e-f depicts a later, more dramatic event with most of the aggregates moving within 12 minutes. One large aggregate (arrow) appears to overturn and move several cm from its original location. These observations support concerns that non-poisoned sediment traps may not accurately measure total sediment flux due to losses from grazing, particularly in an area where large populations of zooplankton are found. This activity also appears to result in dis-aggregation and re-aggregation of the material, further complicating aggregate size measurements.

Sediment Preservation

Electron microscopic observation reveals that, in spite of the inferred grazing, the sediment trap sample appears to be well preserved. Figure 5 shows SEM images of the trap collected material. Most of this material appears as collections of intact diatoms entangled in mucous

Figure 3.5 Scanning electron micrographs (SEM) of material from the flux camera trap. All material was critical point dried from Freon® except c and d which were air dried. a-b) Aggregates showing typical contents and morphology. Note the intact diatom cells and abundant mucous. Scale bar is 100μm. c) Well preserved diatom and dinoflagellate specimens. Compare with sediment samples in figure 7. Scale bar is 10μm. d) Diatom spines entangled in the remains of a feeding web. Scale bar is 20μm. e-f) This well preserved feeding web and diatom indicate that these structures may be involved in the vertical transport of particulate matter. Scale bar is 10μm.

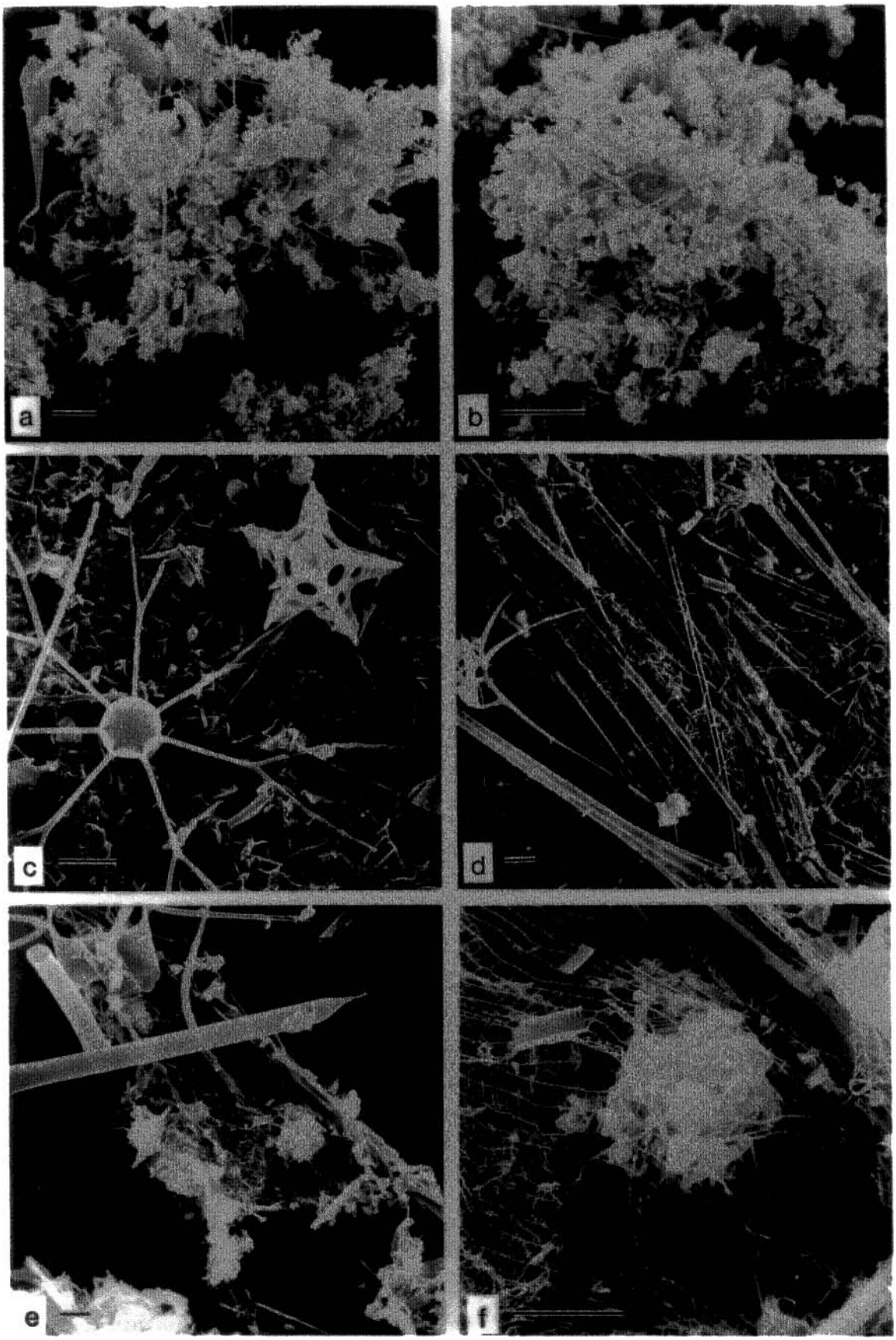
a
b
c
d
e
f

strands and amorphous organic matter (fig. 3.5a-c); few fecal pellets are present. The morphology and overall condition of this material is nearly indistinguishable from that of marine snow aggregates collected in surface water. Mucous strands are often organized into regular lattice patterns resembling the feeding webs used by some gelatinous zooplankton (Gilmer, 1972). These feeding structures have also been observed in marine snow aggregates in surface (Caron et al., 1982) and deep (Silver and Alldredge, 1981) water. Their collection in such a deep sediment trap implies that they may be an important mechanism of accelerated vertical transport of fine material.

Time series record of sediment arrival.

The total number of particles in the images is plotted vs. time since arrival at 3800m in figure 3.6. Twelve hours into the deployment, the sampling interval changed unexpectedly from nine minutes to ca. two minutes, resulting in more closely spaced samples after that time. The resulting accelerated battery drain caused the strobe lights to begin to fail at 27 hours. The drop in light intensity is partly responsible for the lower numbers after this time, but particle consumption by grazers is also involved. Much of the scatter of the points on the curve is caused by small imperfections on some of the frames due to the developing process. Frames with obvious scratches or other marks in the field of interest were not included in the analyses.

The slope of this curve is a measure of the flux of particles (number meter^{-2} day^{-1}). The slope is initially quite steep but levels off to a relatively constant level after ten hours. This flattening is caused by

Figure 3.6 The total number of aggregates arriving in the trap as a function of time is determined by digitizing the flux camera images. The slope of this line is flux of aggregates (# $m^{-2}day^{-1}$). Resuspensions of material are evident as local minima in the plot at 10.5 and 23 hours. The higher sampling rate after 11 hours is due to a partial malfunction of the timing circuit.

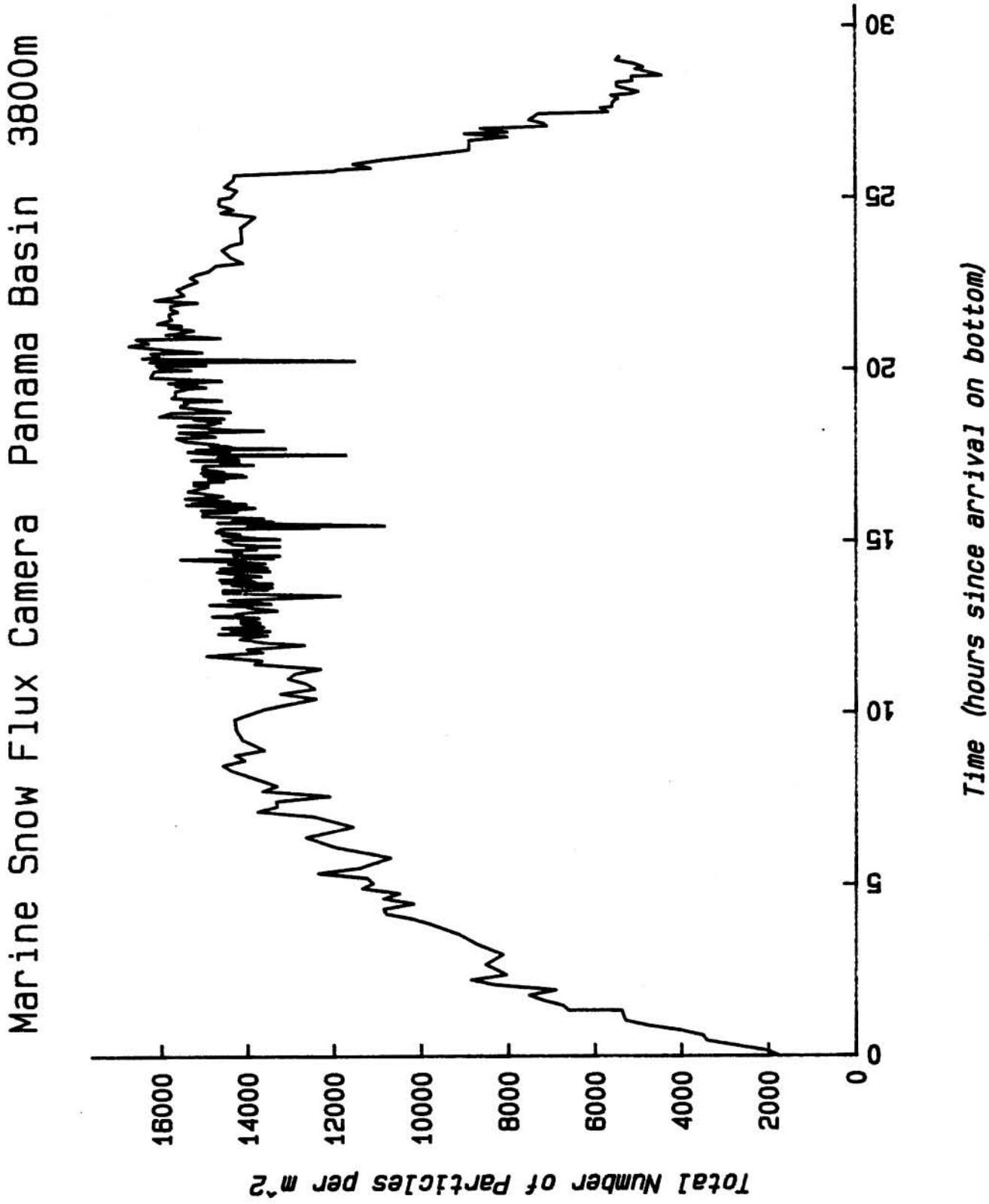
Marine Snow Flux Camera Panama Basin 3800m
Total Number of Particles per m^2
2000
4000
6000
8000
10000
12000
14000
16000
0
5
10
15
20
25
30
Time (hours since arrival on bottom)

Figure 3.7 Image area occupied by aggregates provides a useful representation of the quantity of material arriving in the trap. Whereas the plot of number of aggregates leveled off due to saturation of the trap surface, image area continues to increase, indicating a relatively constant flux of material.

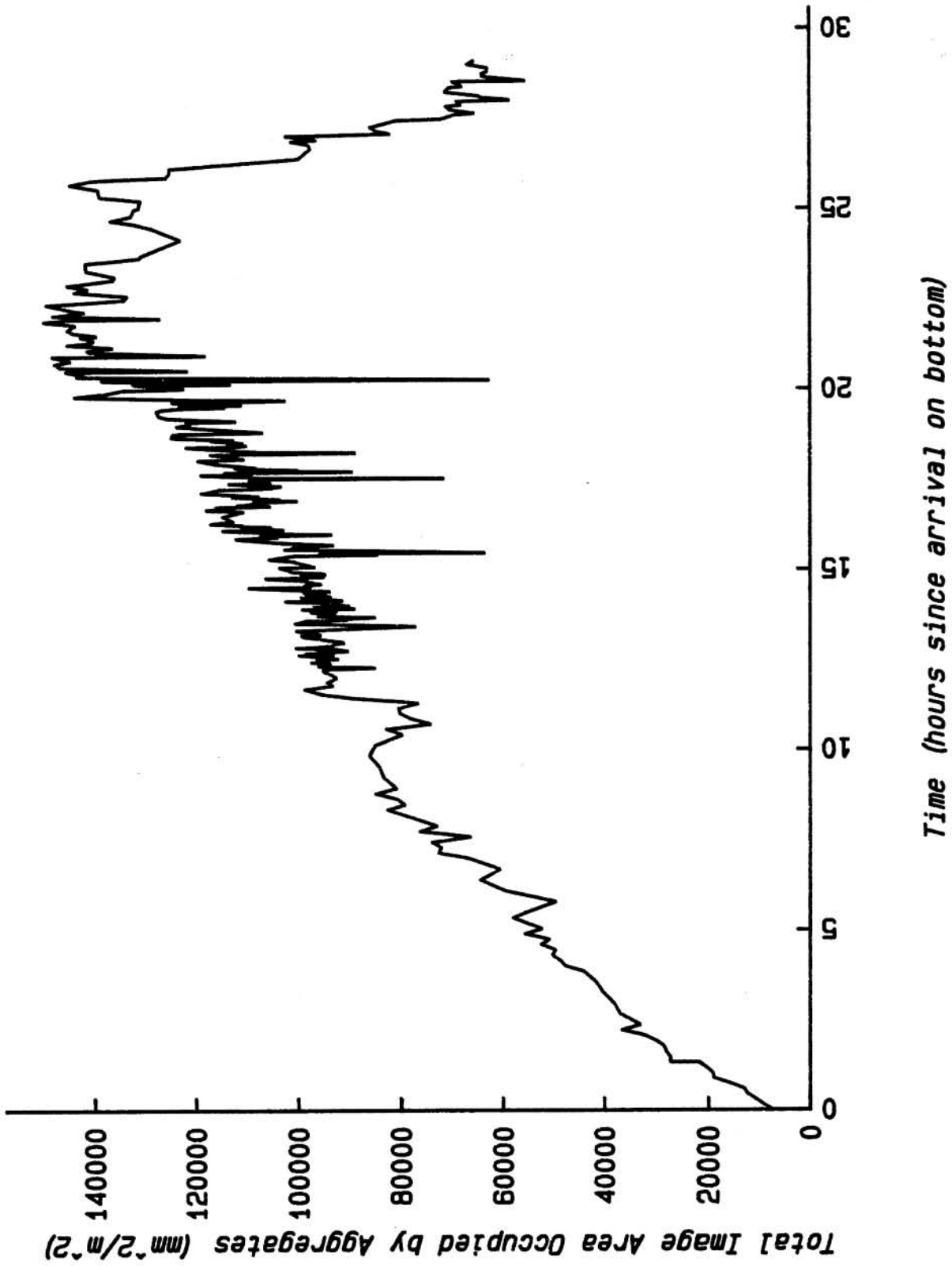
Marine Snow Flux Camera Panama Basin 3800m
Total Image Area Occupied by Aggregates (mm^2/m^2)
0
20000
40000
60000
80000
100000
120000
140000
0
5
10
15
20
25
30
Time (hours since arrival on bottom)

overlapping or contacting of adjoining particles. This interpretation is supported by a plot of total image area occupied by aggregates (fig. 3.7). In this case, the slope of the curve is more nearly constant, as would be expected for a uniform sedimentation rate.

Resuspension and feeding events

The episodes of particle redistribution described from the photographic images are also apparent in the time series plots of aggregate abundance vs. time. These events are expressed as sharp decreases in numbers followed by return to initial values. Events occur at 12 and 25 hours and correspond to particle movements pictured in figure 3.4. Another event is seen in the time series plot at 23-24 hours and in the photographs in figure 3.8. After 25 hours, the amount of detected material decreases rapidly (fig. 3.9). This reduction is due partly to intermittent strobe light failures which began at 27 hours, but, as can be seen in figure 3.4, particle loss is also occurring.

Figure 3.8 Flux camera photographs of particle motions associated with the resuspension event at 23 hours. Times since arrival on the bottom are: a) 22.80 hours, b) 22.90 hours, c) 22.95 hours d) 23.06 hours, e) 23.15 hours, and f) 24.45 hours.

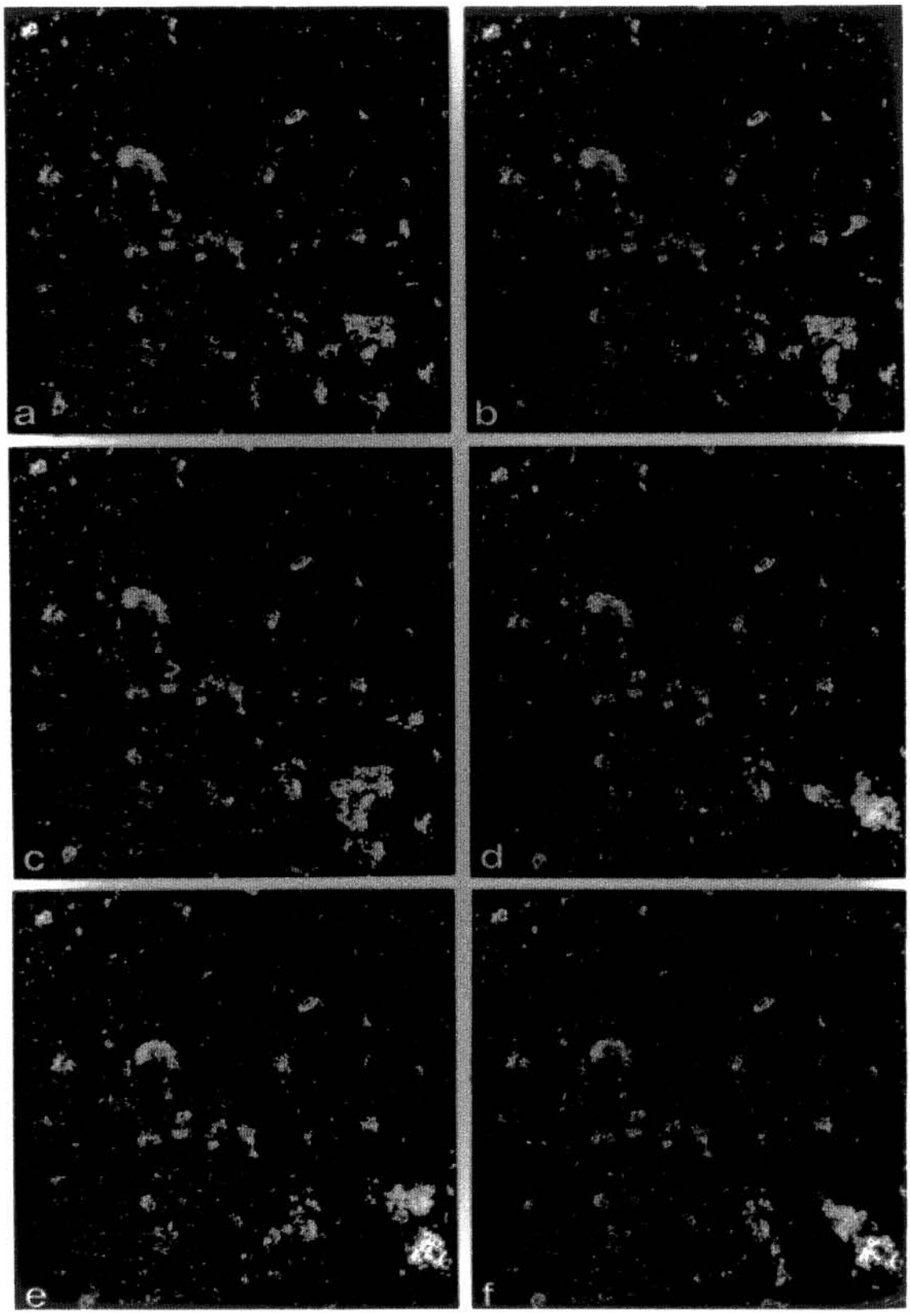
a
b
c
d
e
f
2cm

Figure 3.9 Flux camera images of resuspension event corresponding to the minimum in the flux plot at 26 hours. Times since arrival on the bottom are: a) 26.01, b) 26.03, c) 26.13, d) 26.15, e) 26.24, and f) 26.26 hours.

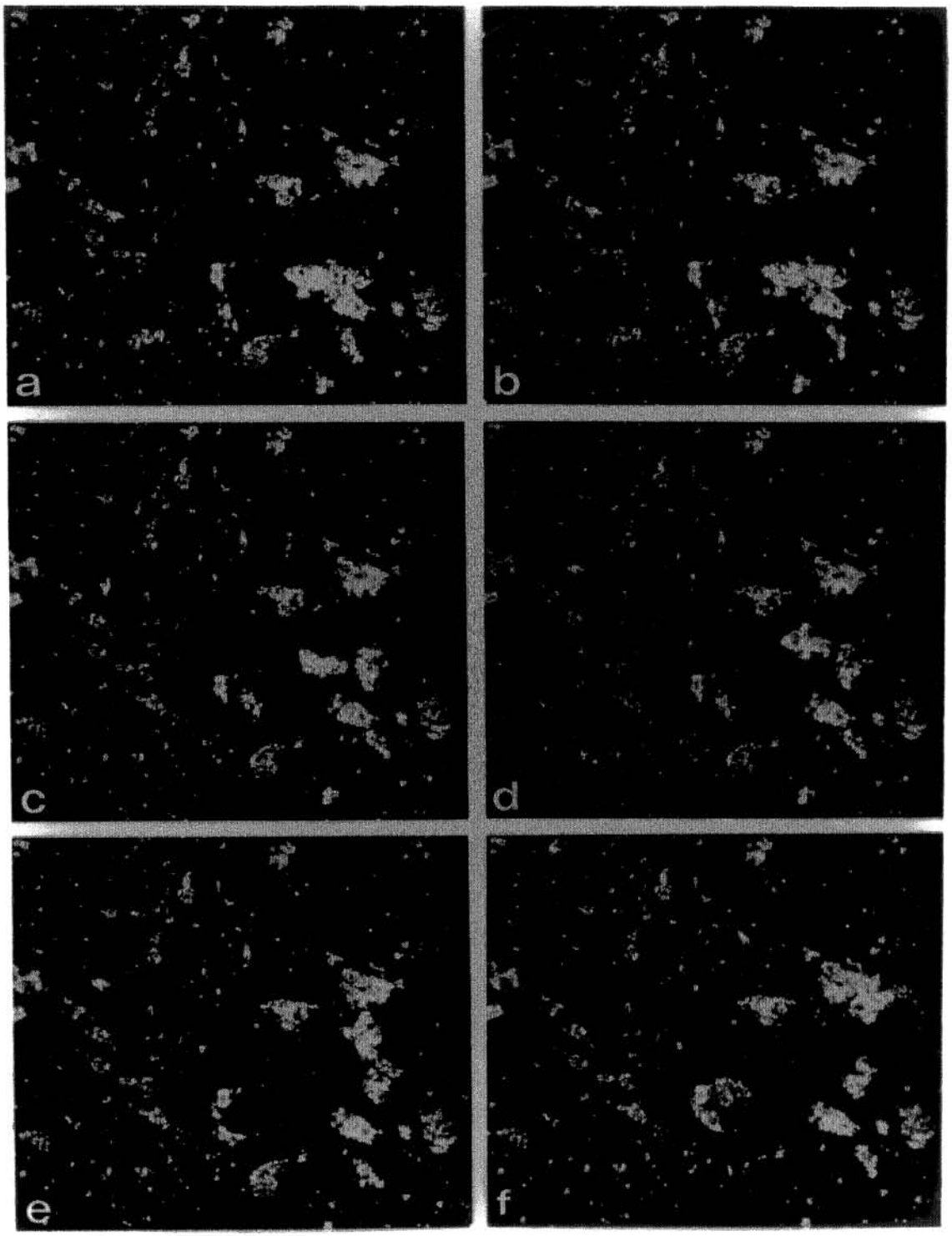
a
b
c
d
e
f
2cm

Discussion

The data produced by this experiment strongly implicate marine snow aggregates in the vertical sedimentation of marine particulate matter. In fact at this location, time and depth, essentially all particles which contribute to the flux of sediment arrive as aggregates. Measured during the initial stage of the deployment, the most abundant size class of aggregates is 1.4mm to 1.9mm, but aggregation within the trap increased the average size of aggregates as the deployment progressed.

Evidence for post-deposition aggregation

The observation that the material is aggregated in the trap is supported by examining changes in the number of particles of a given size; figures 3.10-3.12 show time series plots of the flux of aggregates in three of the size classes counted (0.5-1.0mm, 1.4-1.9mm, and 3.3-3.8mm). The number of small particles increases sharply and then decreases gradually while the number of medium sized particles (1.4-3.8mm) rises to a constant value. Only the larger (3.3-3.8) particles continue to increase in number. This is clear evidence of aggregation of material within the trap. Small particles continue falling into the trap but as the surface area becomes increasingly occupied, the new arrivals begin overlapping existing ones, reducing their numbers and increasing the number of larger particles. In the case of 1.4-1.9mm particles, a balance is reached at ca. 8 hours between addition by aggregation of smaller particles and loss by aggregation into larger particles. The average particle size (fig. 3.13) thus continues to increase throughout the deployment due to aggregation.

Figure 3.10-3.12. Plots of the arrival of aggregates in three size classes. 3.10) The number of small particles (0.5-1.0mm) increases to a maximum and then decreases due to saturation of the bottom plate area and aggregation into larger particles. Material no longer counted in this class will be counted in the larger size classes. 3.11) Medium (1.4-1.9mm) particles reach a balance between addition of material and removal by aggregation into larger particles. 3.12) Large aggregates (3.3-3.4mm) continue to increase due to arrival of large particles and aggregation of smaller ones.

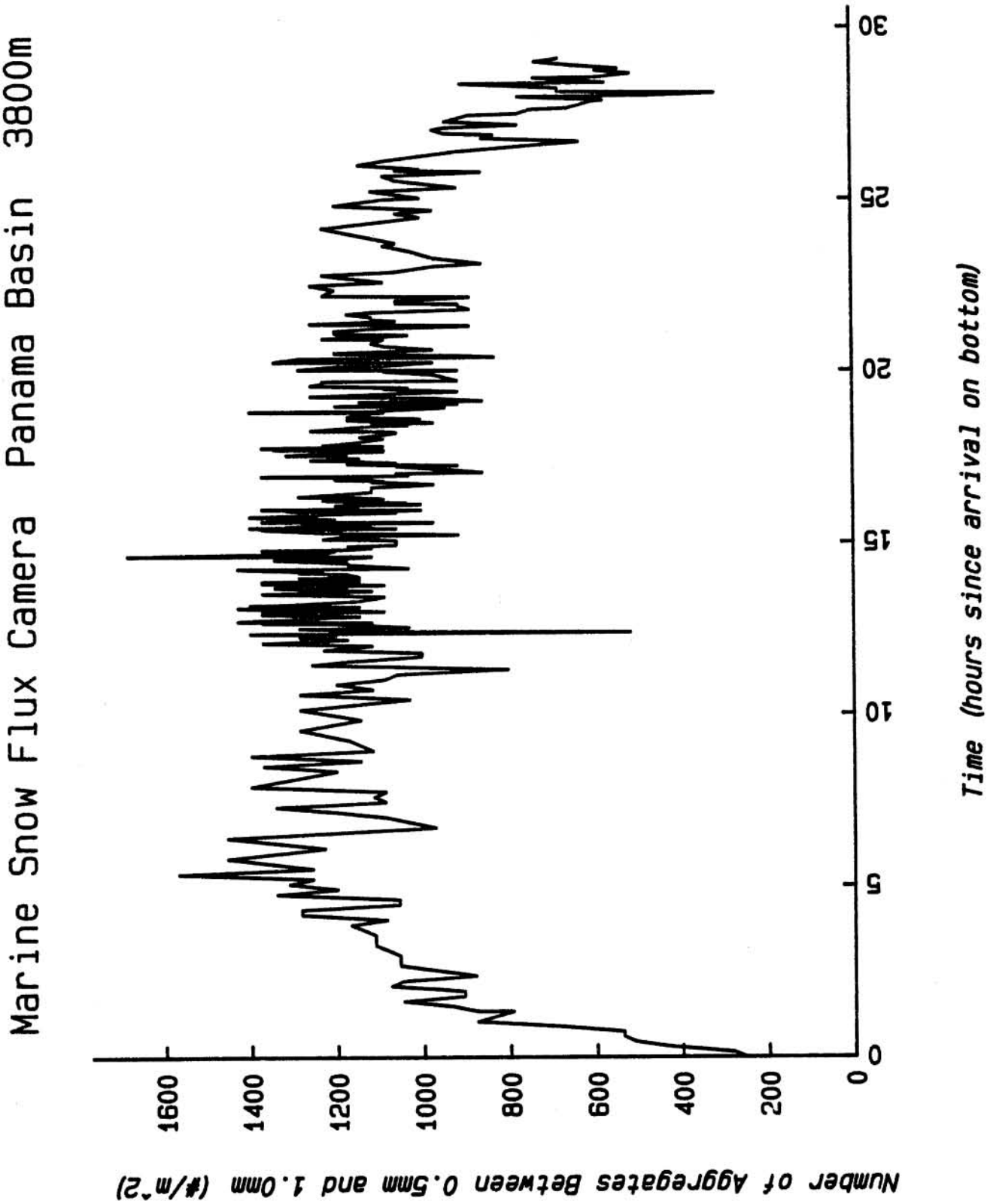
Marine Snow Flux Camera Panama Basin 3800m
Number of Aggregates Between 0.5mm and 1.0mm (#/m^2)
0
200
400
600
800
1000
1200
1400
1600
0
5
10
15
20
25
30
Time (hours since arrival on bottom)

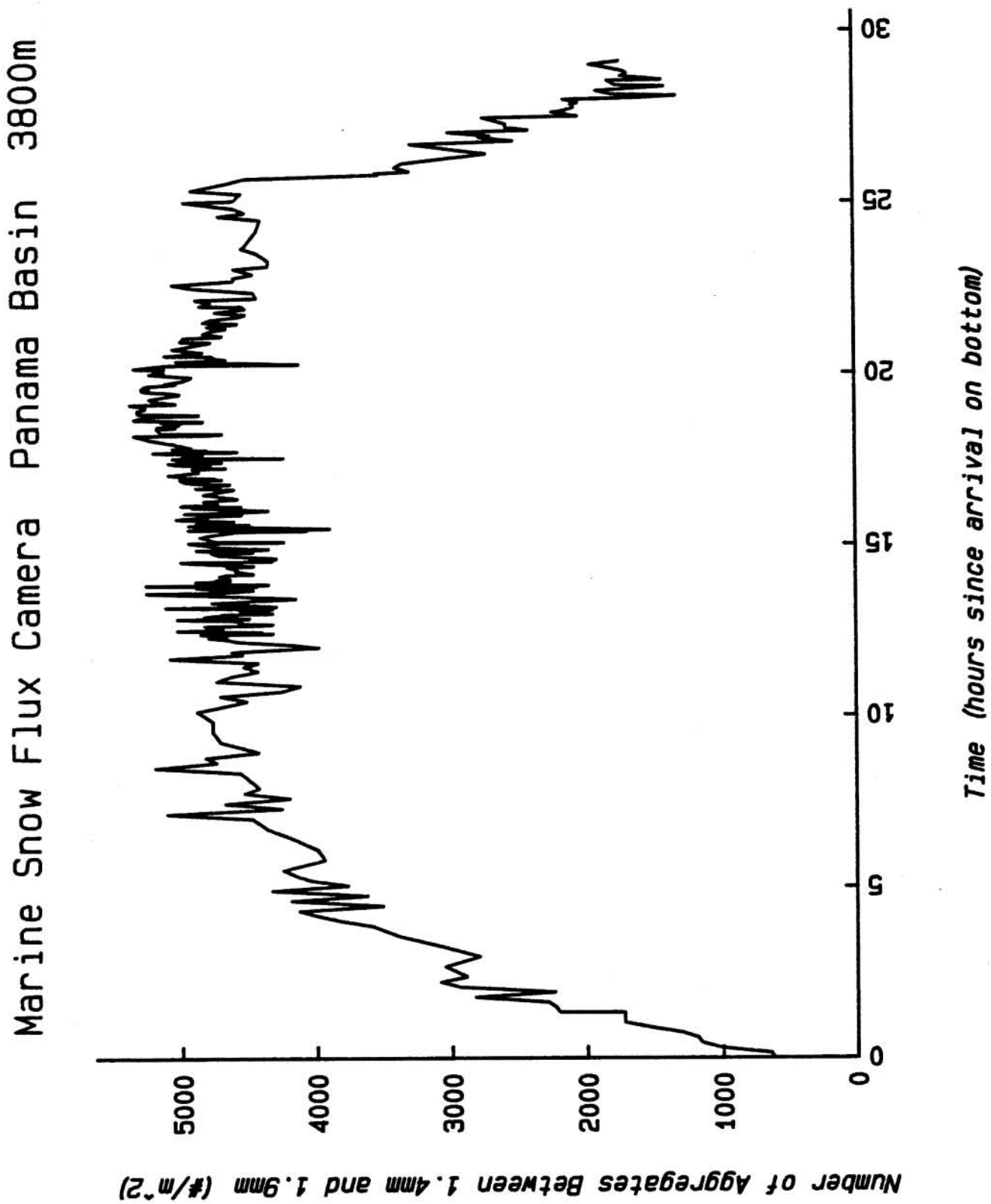
Marine Snow Flux Camera Panama Basin 3800m
Number of Aggregates Between 1.4mm and 1.9mm (#/m^2)
5000
4000
3000
2000
1000
0
0
5
10
15
20
25
30
Time (hours since arrival on bottom)

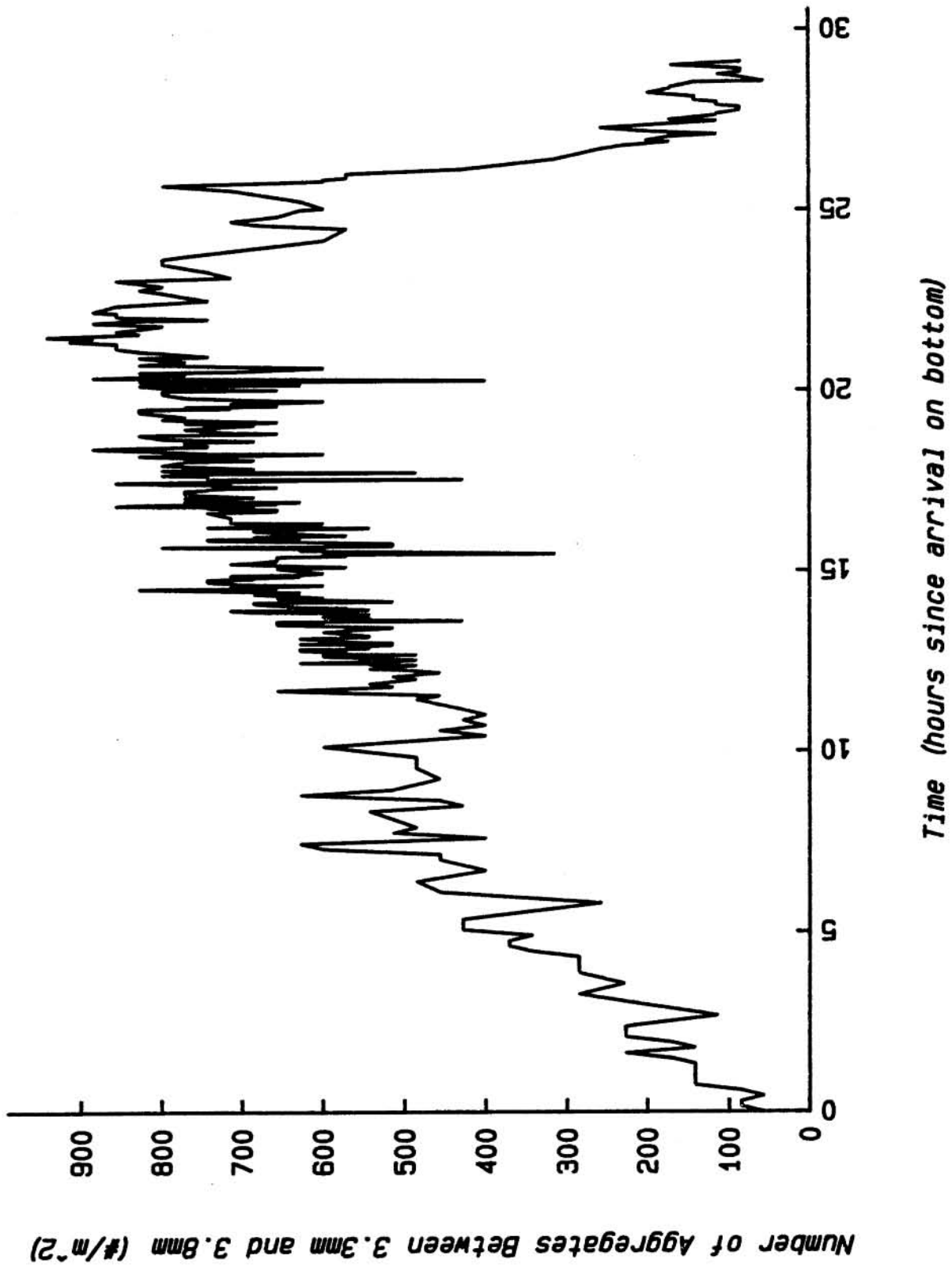
Marine Snow Flux Camera Panama Basin 3800m
Number of Aggregates Between 3.3mm and 3.8mm (#/m^2)
0
100
200
300
400
500
600
700
800
900
0
5
10
15
20
25
30
Time (hours since arrival on bottom)

Figure 3.13 The average size of aggregates in he trap continues to increase due to aggregation of material.

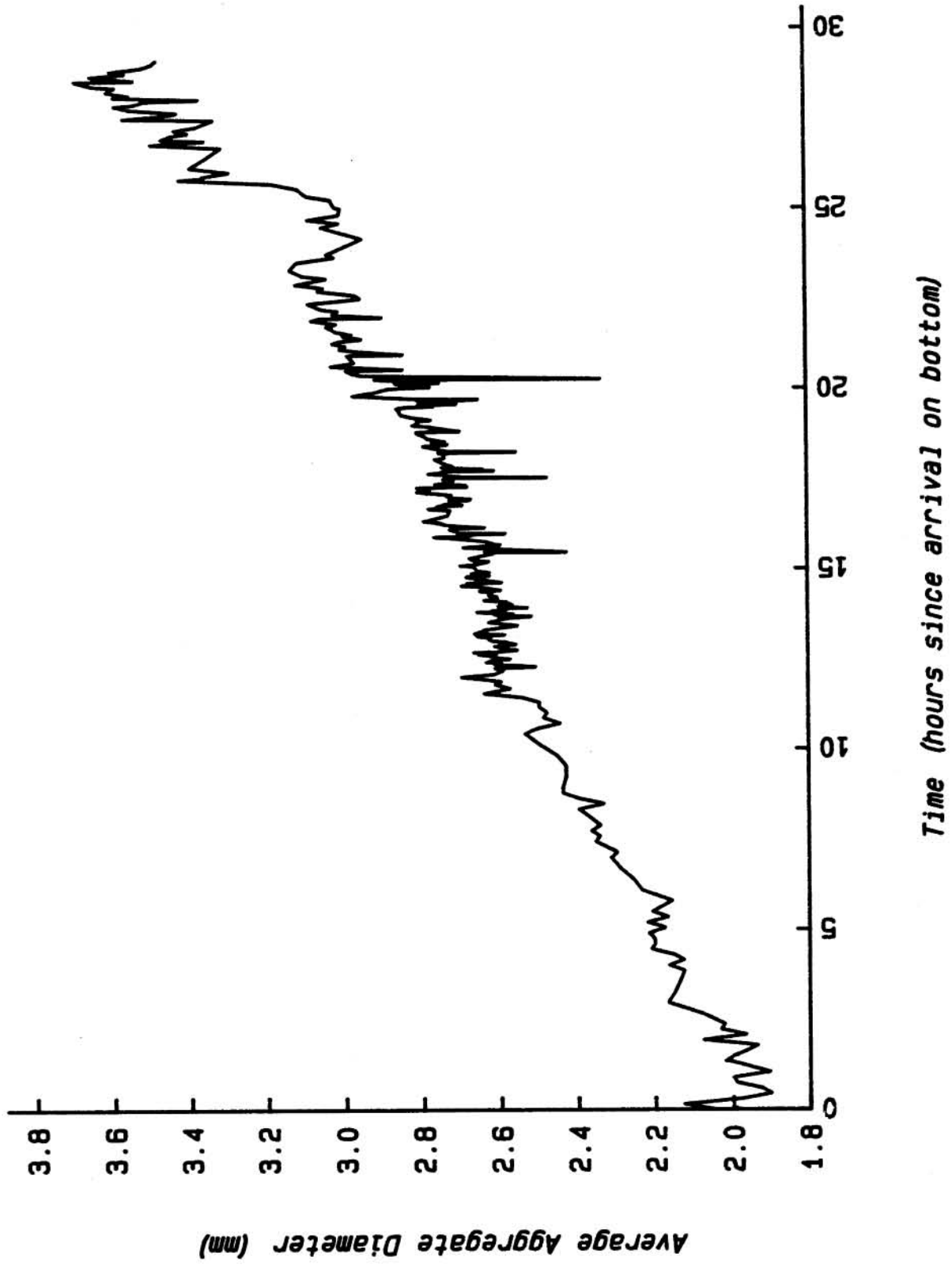
Marine Snow Flux Camera Panama Basin 3800m
Average Aggregate Diameter (mm)
3.8
3.6
3.4
3.2
3.0
2.8
2.6
2.4
2.2
2.0
1.8
0
5
10
15
20
25
30
Time (hours since arrival on bottom)

Sinking speed estimates

As outlined above, particulate sinking speeds can be obtained by dividing aggregate abundance values into measured aggregate flux values. Profiles of the abundance of marine snow in the three smallest size classes at the flux camera deployment site are shown in figure 3.14a-c. Values of 1.4, 0.58. and 0.70 aggregates per liter are obtained for the 3800m deployment depth of the flux camera for 1.0-2.5mm, 2.5-4mm and 4-5mm size classes respectively. Aggregate flux estimates are obtained by determining the slope of flux camera records. In order to avoid the effects of aggregation of the material in the trap (flux camera), flux estimates were obtained by linear regression of the first two hours of data (N=15, table 3.1).

The calculated sinking speeds are 36, 26, and 1 m day^{-1} for the 1.0-2.5mm, 2.5-4mm and 4-5mm size classes respectively. These speeds are lower than previous estimates and indicate that larger aggregates sink more slowly than smaller ones. This result supports the model proposed in chapter two of this thesis; large porous aggregates are easily resuspended from the sea-floor and sink more slowly than smaller, fresh aggregates. Because of their larger size, however, the contribution of these large aggregates to the flux of material may be similar to the contribution of the more abundant but smaller aggregates. The volume of material contributed by each class of aggregate is the product of the flux of aggregates (# m^{-2} day^{-1}) and the geometric mean volume (assuming spheres) of aggregates in a size class (Table 1). The two smaller sizes appear to contribute similar volumes of material, while the largest

Figure 3.14 Plots of the vertical distribution of marine snow aggregates at the flux camera site in three size classes. A nine point running mean filter has been passed over this data in order to enhance the lower frequency signal. a) 1.0-2.5mm. b) 2.5-4mm. c) 4-5mm.

Marine Snow Camera Panama Basin #E3

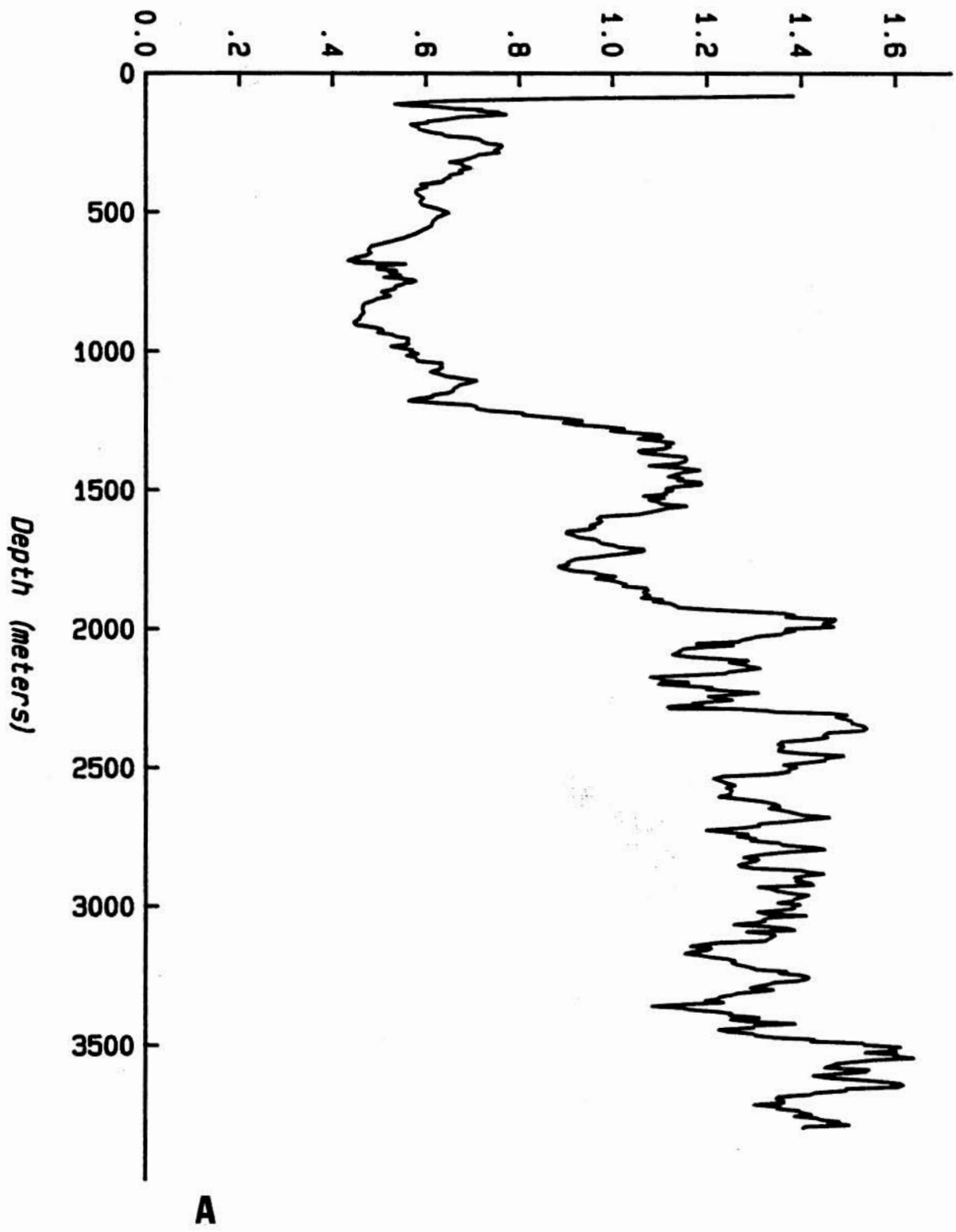

A

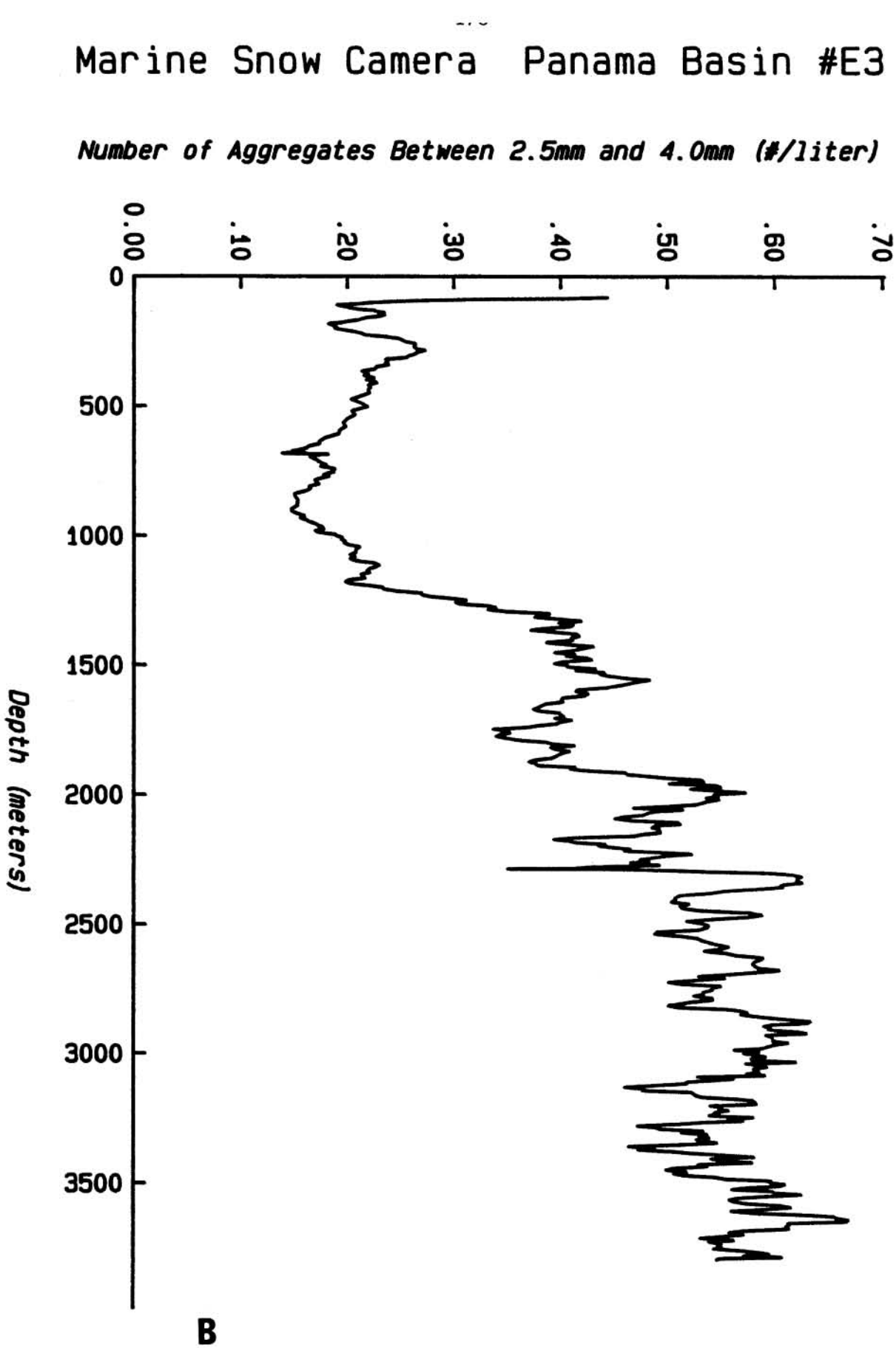
Marine Snow Camera Panama Basin #E3
Number of Aggregates Between 2.5mm and 4.0mm (#/liter)
0.00
.10
.20
.30
.40
.50
.60
.70
0
500
1000
1500
2000
2500
3000
3500
Depth (meters)
B

Marine Snow Camera Panama Basin #E3

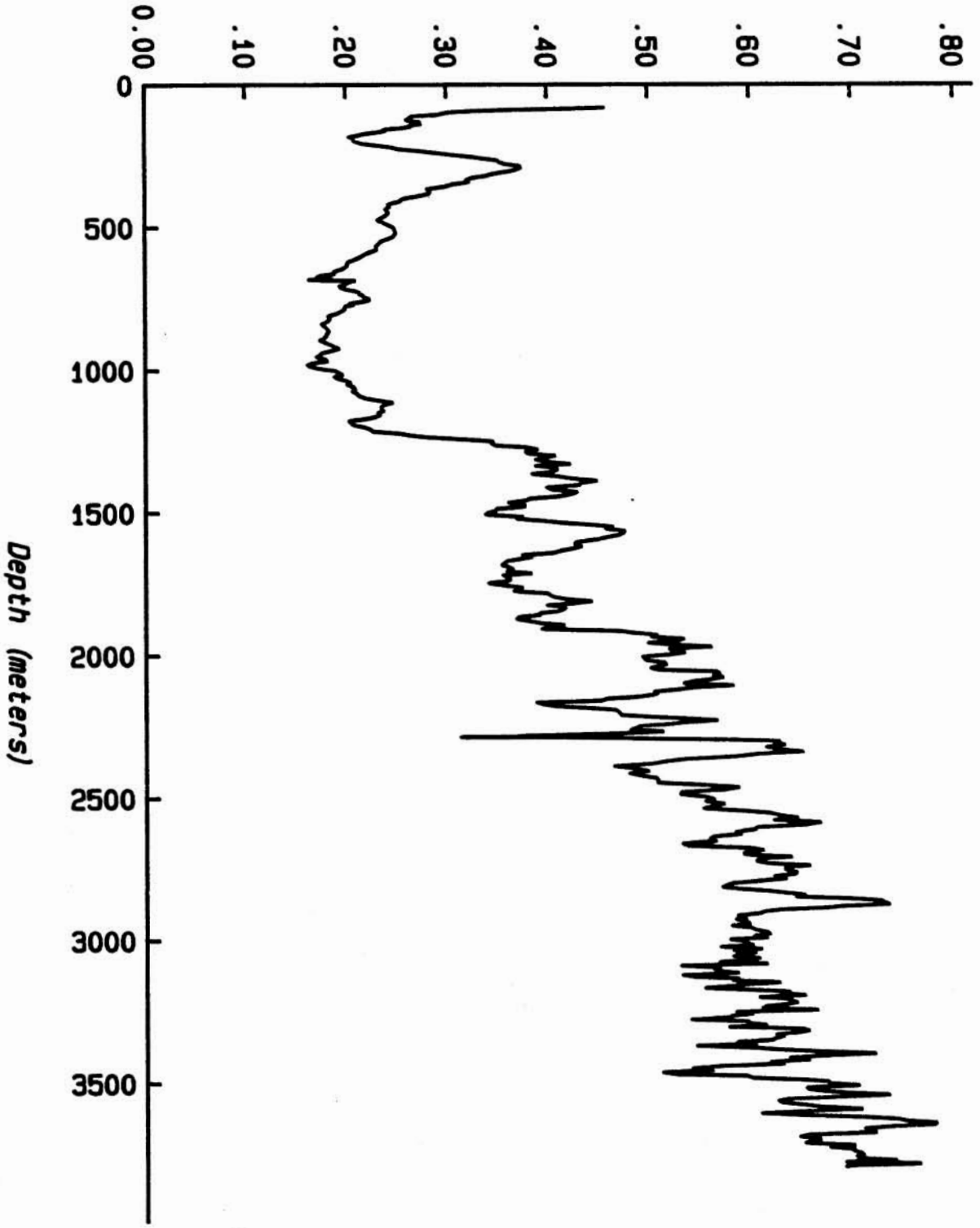

C

aggregates contribute somewhat less. These trends may be due to the small sample sizes in the larger size classes and this factor should be considered throughout the following calculations.

Mass flux can also be estimated, although this calculation depends on a particle density value arrived at by assuming the aggregates sink according to Stokes' equation. Although this assumption may not be entirely valid (eg. the aggregates are not rigid spheres), the calculations used here are patterned after those described by Alldredge (1979), Kajihara (1971), and Bishop et al. (1977). Particle Reynold's numbers are calculated from the equation

$$R_e = DW\rho_f\mu^{-1} \qquad 2.0$$

where D is the particle diameter in cm, W is the sinking speed in cm sec^{-1} determined above, ρ_f is the density of seawater (1.02475gm cm^3 at 1.75°C, 34.7°/$_{oo}$ salinity), and μ is the seawater viscosity ($1.79x10^{-2}$gm $cm^{-1}sec^{-1}$, Sverdrup et al. 1941). The Reynolds numbers range from 0.0296 to 0.577 so the particles are marginally within the range of Stoke's settling (R_e < ~0.5-1.0).

Aggregate bulk densities (ρ_a) are calculated using

$$\rho_a = 18W\mu D^{-2}g^{-1} \qquad 3.0$$

where g is the gravitational acceleration (981cm sec^{-1}). These densities are quite low, ranging from 1.024752 to 1.02516gm cm^{-3}. Most of the aggregate volume is occupied by seawater so that a value for aggregate porosity must be estimated. Kajihara (1971) found that re-aggregated marine snow (D=1mm) aggregates were 99.3% porous and Alldredge (1979) used this value for 3mm diameter aggregates. The wet density of the particulate

component (ρ_p) is a function of the assumed porosity (P) and bulk density (ρ_a).

$$P\rho_f + (1-P)\rho_p = \rho_a \qquad 4.0$$

This equation is then re-arranged to solve for ρ_p.

$$\rho_p = (\rho_a - P\rho_f)(1-P)^{-1} \qquad 5.0$$

For the 2.5-4mm size class, which corresponds most closely to Alldredge's 3mm aggregates (1979), the calculated wet density (ρ_p) is 1.03732gm cm^3. This value is then applied to the other two sizes of aggregates to obtain their estimated porosities using a re-arrangement of equation 4.

$$P = (\rho_a - \rho_p)(\rho_f - \rho_a)^{-1} \qquad 6.0$$

These estimated porosities (96.6%, 99.3%, and 99.9% for 1-2.5mm, 2.5-4mm and 4-5mm aggregates respectively) support the hypothesis that the larger aggregates are more flocculent and thus may be composed of re-suspended material. The calculated residence time of the large aggregates (4,000 days in 4,000m if they were surface derived) also tends to preclude a direct surface origin.

Mass flux is calculated as the product of the estimated mass of particulate matter per aggregate (M_a) and the number of aggregates observed in the flux (F_n). M_a is calculated from the estimated values of porosity (P), aggregate volume (V_a) and wet density of the particulate component (ρ_p).

$$M_a = (1-P)\rho_p V_a \qquad 7.0$$

The resulting values are listed in table 1. Due to the differences in porosity, the smaller aggregates contain a greater mass of solid matter than the largest aggregates. This low mass leads to a correspondingly low

Table 3.1 Application of Stoke's law settling to marine snow aggregates allows calculation of their bulk densities. These values are used with flux measurements and assumed porosities and solid densities to arrive at mass flux estimates.

	Size class (cm)	0.1-0.25	0.25-0.4	0.4-0.5	Total
D	Geometric mean diameter (cm)	0.18	0.36	0.45	-
F_N	Initial flux (# $m^{-2}day^{-1}x10^{-4}$)	5.0	1.5	0.8	7.3
	Concentration (# $cm^{-3}x10^{3}$)	1.4	0.58	0.7	2.68
W	Sinking speed (cm $sec^{-1}x10^{2}$)	4.2	3.0	0.12	-
	Individual aggregate volume ($cm^{3}x10^{3}$)	3.2	20	47	-
	Volume flux (cm^{3} $m^{-2}day^{-1}x10^{-2}$)	1.4	1.7	0.36	3.46
R_e	Reynold's number	0.44	0.58	0.030	-
ρ_a	Bulk aggregate density (gm cm^{-3})	1.0252	1.0248	1.0247	-
P	Porosity (%)	96.6	99.3	99.99	-
M_a	Individual aggregate mass ($gmx10^{6}$)	108	143	7.3	-
F_M	Wet mass flux (gm $m^{-2}day^{-1}$)	5.4	2.2	0.058	7.7
	Dry mass flux (gm $m^{-2}day^{-1}$)	1.6	0.66	0.017	2.3

contribution to mass flux (F_m).

$$F_m = M_a F_n \qquad 8.0$$

Total mass flux (for the three size classes studied) is 7.81gm m^2 day^{-1}. Alldredge (1979) assumed that only 30% of this mass would be preserved as dry weight. Application of this drying loss estimate reduces the calculated flux to 2.34gm m^{-2} day^{-1} which is an order of magnitude greater than the measured total mass flux of 0.21gm $m^{-2}day^{-1}$. Although the calculated mass flux value relies on several assumptions, the large (order of magnitude) difference between calculated and measured mass flux is most likely due to loss of material to grazing activities. The crustacean carapace observed in all of the photographs was not found in the recovered sample, confirming sample loss. Proximity to the sea floor may be a factor in this grazing activity, but this finding suggests that care should be taken in all sediment trap deployments to prevent sample loss to grazers.

Effect of Oceanographic Setting

All of the estimates of aggregate flux, sinking speed, and mass flux are affected by the proximity of the station to sources of resuspended material on the continental shelf and slope. This partially remineralized material is input at varying depths below the surface and arrives as flocculent, slowly settling aggregates (see chapter 2 of this thesis). Fresher, faster-sinking material from the surface collides with this older material and adheres to it. The new multi-source aggregates sink at speeds which are proportional to the relative amounts of old and new material and their sinking speed is expected to decrease with depth due to the deep

input of flocculent material. It is expected, therefore, that the sinking speeds determined by this method would most likely be higher in environments free of this allochthonous input.

Conclusions and proposal for future studies

The results obtained by this experiment strongly implicate marine snow in the process of marine particle sedimentation. The following conclusions were derived from the experimental results and discussion:

1. Essentially all of the material in the photographs arrives in the form of aggregates with only minor amounts of fine debris and fecal pellets.

2. Sediment flux (2.34 gm $m^{-2}day^{-1}$) estimated from the size and sinking speed of the aggregates is sufficient to produce the measured flux (0.21 gm $m^{-2}day^{-1}$), confirming the conclusion that marine snow may be a viable mechanism of sedimentation.

3. In this specific oceanographic setting, the larger aggregates are more flocculent, sink more slowly, and contribute less to the total mass flux, indicating a secondary (resuspended) source for these aggregates.

4. Grazing of the trap material may be a significant problem in unpoisoned traps.

The results of this preliminary deployment demonstrate the value of this type of experiment and indicate a need for extension of the technique. The following are suggestions for improvement and further application of the method:

1. Because the smallest particles studied appear to settle more quickly than the larger ones, the optical resolution of both the marine snow camera and flux camera should be improved. This would allow inclusion of still smaller aggregates which may settle even faster. Also, the size

classes studied by both systems should be forced into agreement to avoid the existing slight offsets.

2. The devices should be deployed in an area removed from deep sources of resuspended material in order to obtain sinking speeds more representative of typical water column values.

3. Deployment in low flux areas would reduce the problem of particle overlap and therefore allow better estimation of aggregate flux as well as estimation of the temporal variability over longer time periods.

4. The addition of a poison or preservative should eliminate the grazing problem (although the potential grazers may die and become part of the flux) and provide a better sample for mass flux estimation.

5. Ideally, marine snow flux cameras could be deployed at several depths along a taunt-line mooring to examine changes in sinking speed as aggregates settle (and possibly decompose). In addition, if marine snow cameras and time series pumping systems were deployed on the same mooring and near the flux camera depths, directly comparable samples of suspended (concentration) and settling (flux) aggregates could be obtained.

REFERENCES

Alldredge, A.L. (1979) The chemical composition of macroscopic aggregates in two neretic seas. Limnol. Oceanogr. vol. 24(5), p 855-866.

Berger, W.H. (1976) Biogenous deep sea sediments: production, preservation and interpretation. In: J.P. Riley and R. Chester (eds.) Chemical Oceanography. vol. 5, 2nd ed. Acad. Press, London.

Billet, D.S.M., R.S. Lampitt, A.L. Rice, and R.F.C. Mantoura (1983) Seasonal sedimentation of phytoplankton to the deep-sea benthos. Nature vol. 302(7), 520-522.

Bishop, J.K.B., J.M. Edmond, D.R. Ketten, M.P. Bacon, and W.B. Silker (1977) The chemistry biology, and vertical flux of particulate matter from the upper 400m of the equatorial Atlantic Ocean. Deep-Sea Res. vol. 24, 511-548.

Caron, D.A., P.G. Davis, L.P. Madin, and J.McN. Sieburth (1982) Heterotrophic bacteria and bacterivorous protozoa in oceanic macroaggregates. Science vol. 218(19), 795-797.

Gilmer, R.W. (1972) Free-floating mucus webs: a novel feeding adaptation for the open ocean. Science vol. 176, 1239-1240.

Honjo, S. (1982) Seasonality and interaction of biogenic and lithogenic particulate flux at the Panama Basin. Science vol. 218, 883-884.

Honjo, S., K.W. Doherty, Y.C. Agrawal and V.L. Asper (1984) Direct optical assessment of large amorphous aggregates (marine snow) in the deep ocean. Deep-Sea Res. vol. 31(1), 67-76.

Jannasch, H.W. (1973) Bacterial content of particulate matter in offshore surface waters Limnol. Oceanogr. vol. 18(2), 340-342.

Kajihara, M. (1971) Settling velocity and porosity of large suspended particle. J. Oceanogr. Soc. Jap. vol. 27(4), 158-162.

Lampitt, R.S. (1985) Effects of the seasonal deposition of detritus to the deep-sea floor. (tentative title) submitted to Deep-Sea Res.

Riley, G.A. (1963) Organic aggregates in seawater and the dynamics of their formation and utilization. Limnol. Oceanogr. vol. 8(4), 372-381.

Shanks, A.L. and J.D. Trent (1980) Marine snow: sinking rates and potential role in vertical flux. Deep-Sea Res. vol. 27A, 137-143.

Silver, M.W., and A.L. Alldredge (1981) Bathypelagic marine snow: deep-sea algal and detrital community. J. Mar. Res. vol. 39(3), 501-530.

Stokes, G.G. (1851) On the effect of internal friction of fluids on the motion of pendulums. Trans. Cambridge Phil. Soc. vol. 9, 8-106. (reprinted in Stokes, G.G. (1901) Mathematical and Physical Papers. vol. 3, 1-141.

Sverdrup, H.U., M.W. Johnson, and R.H. Fleming (1942) The oceans. Prentice-Hall. 502

Trent, J.D., A.L. Shanks, and M.W. Silver (1978) In situ and laboratory measurements on macroscopic aggregates in Monterey Bay, California. Limnol. Oceanogr. vol. 23(4), 625-635.